RESUMEN

En el presente informe se realiza un estudio de transitorios de pérdida de control del plasma en ITER. Para la realización del estudio se ha utilizado AINA 3.0, un código de seguridad desarrollado por *Fusion Energy Engineering Laboratory* (FEEL-UPC) de la *Universitat Politécnica de Catalunya*.

En primer lugar se realiza una pequeña introducción al mundo de la fusión nuclear: sus principios físicos, el estado del arte de la investigación en fusión, así como una descripción del proyecto ITER y del código AINA.

Finalmente se presentan y analizan los resultados de las simulaciones. Primero se seleccionan los casos más críticos de pérdida de control del plasma a partir del comportamiento del plasma frente a distintos tipos de perturbaciones, entre las que destacan:

- fallo en el sistema de inyección de combustible dando lugar a un evento de sobrealimentación,
- mejora del tiempo de confinamiento del plasma,
- incremento súbito de potencia externa dando lugar a un evento de sobrecalentamiento del plasma,
- terminación súbita de potencia externa y/o inyección de combustible.

También se estudia la combinación de distintas perturbaciones, tanto simultáneas como consecutivas.

Por último, para los casos seleccionados como más peligrosos para la integridad del reactor, se realiza un estudio completo de la paredes y del plasma para ver si existe riesgo de fusión o carga excesiva sobre los componentes de la pared.

Además, este informe se complementa con *AINA safety code* [1], un documento donde se describen los modelos físicos y el código (ver *ANNEX B*).

[1] JOSÉ CARLOS RIVAS, JAVIER DIES: *AINA safety code: User's Manual and Code Description (Release 3.0)*. FEEL-UPC, 2013.

CONTENTS

FIGURE LIST

TABLE LIST

1 GLOSSARY

AINA 1.0: Safety code developed by FEEL-UPC from SAFALY code, by contrast with SAFALY, AINA 1.0 included graphic interface and complete code models documentation. Although in the same manner that SAFALY, it is programmed in *Fortran*. AINA 1.0 was the code used to perform *Review of Loss of Plasma Control Transients in ITER* (2007).

AINA 3.0*: AINA version developed during 2012. It is a similar version to the used in this report (AINA 3.0). However, since 2012, there have been introduced some changes that improve the code.

AINA 3.0: Later version of AINA code used to develop this document.

Alpha particle (α): It is the nucleus of the helium atom, consisting of two protons and two neutrons. It is one of the products of the deuterium-tritium reaction (see Eq. 1.1). In a fusion reactor it is the major source of plasma heating by the interaction with the particles of fuel.

$$D + T \rightarrow He^4(3.5\,MeV) + n\,(14.1\,MeV) \qquad \textbf{\textit{Eq. 1.1}}$$

Beta (β): Ratio of the plasma pressure to the magnetic pressure. It is given by Eq. 1.2, where p is the pressure, B the magnetic field and μ_0 the magnetic permeability.

$$\beta = \frac{p}{B^2/2\mu_0} \qquad \textbf{\textit{Eq. 1.2}}$$

β_P: Ratio of the plasma pressure to the poloidal magnetic pressure.

β_T: Ratio of the plasma pressure to the toroidal magnetic pressure.

Beta limit (β_{LIM}): It is an upper limit for the beta parameter; above this limit disruption due to MHD instabilities appears.

Breeding: Ability of the wall modules to produce tritium within the fusion power plant when neutrons escaping the plasma interact with lithium contained in the blanket. This ability will be tested in ITER from TBM, within these test blankets modules, viable techniques for ensuring tritium breeding self-sufficiency for DEMO will be explored.

Blanket: Set of modules that forms the inner wall of the reactor, capable of supporting high thermal loads and intense neutron fluxes. Its main mission in ITER is to stop the neutrons and transfer heat to the cooling system of the reactor.

Blanket first wall: Each blanket has a detachable first wall which directly faces the plasma and removes the plasma heat load.

Bootstrap current ($I_{bootstrap}$): In a tokamak, it is a self-generated current by plasma that produces an important part of the magnetic field.

Breakeven point: The plasma energy breakeven point describes the moment when plasmas in a fusion device release at least as much energy as is required to produce them. Fusion performance is measured by Q. Plasma energy breakeven, or Q=1, has never been achieved. ITER has been designed to produce more power than it consumes: for 50 MW of input power, 500 MW of output power will be produced (Q=10)

Bremsstrahlung radiation (P_{BRM}): It is electromagnetic radiation produced by the deceleration of a charged particle when deflected by another charged particle.

Cassette: Divertor module.

Confinement: Restriction of hot plasma to a given volume as long as possible by Magnets and pinch effects.

Confinement mode: When magnetically confined plasma is heated strongly and a threshold heating power level is exceeded, it may spontaneously transition from a low confinement (or L-mode) state to a high confinement (or H-mode) state.

H-mode: High confinement mode that occurs above a threshold power which is characterized by a high pressure gradient and a high confinement time.

L-mode: Low confinement mode in which the pressure gradient is low.

Confinement time: The length of time for which particles are confined within the plasma.

Decommissioning: The process by which the facility is permanently taken out of operation at the end of the plant lifecycle with adequate regard for the health and safety of workers and the public, and protection of the environment.

DEMO: Acronym of DEMOnstration Power Plant. It is a proposed experimental-commercial nuclear fusion power plant that is intended to build upon the expected success of the ITER experimental nuclear fusion reactor. The main objective of DEMO it to demonstrate the viability of the commercialization of fusion energy.

Deuterium (D): One of the two isotopes of hydrogen that will be used to fuel the fusion reaction in ITER.

Disruption: Phenomenon related to plasma instabilities, causing a rapid loss of confinement and consequent termination of the plasma. The lost energy is dissipated in a small area of the wall and can cause serious damage.

External heating: The application of neutral particle beams and/or high-frequency microwave radiation to the plasma from external sources in order to provide the input heating power necessary to reach the temperatures required for fusion. Additional heating bridges the gap between resistive,

or ohmic heating due to plasma toroidal current (which gets weaker with increased temperature) and alpha-particle heating due to the slowing down of the helium reaction product in the plasma (which gets stronger with higher temperature).

Fission: The process by which a neutron strikes a nucleus and splits it into fragments; during the process of nuclear fission, neutrons are released at high speed, and heat and radiation are released.

Fuel cycle system: The system which extracts deuterium, tritium and impurities from the plasma exhaust stream and prepares deuterium and tritium for re-injection into the plasma.

Fusion: The merging of two light atomic nuclei into a heavier nucleus, with a resultant loss in the combined mass and a massive release of energy.

Hot cells: A concrete-shielded chamber with a controlled atmosphere that can be used to work on radioactive materials and components with a view to repairing them and refurbishing them for future re-use, or dismantling them for disposal. The chamber is equipped with remote manipulators or robotic devices for this purpose. No human access is foreseen.

Ignition: The point at which a fusion reaction becomes self-sustaining. At ignition, fusion self-heating is sufficient to compensate for all energy losses, external sources of heating power are no longer necessary to sustain the reaction.

ITER: Originally an acronym of International Thermonuclear Experimental Reactor and Latin for "the way" or "the road". It is an international nuclear fusion research and engineering project, which is currently building the world's largest experimental tokamak nuclear fusion reactor.

Impurities: One of the most severe problems for a reactor is the presence of impurities in the plasma. The impurities are of two types. Firstly there are impurity ions, which come from solid surfaces, and secondly there are the α-particles resulting from the fusion process which is an intrinsic impurity. The requirement for the “helium ash” is that it should not have too long a confinement time in the plasma. Impurities from the wall produce partially stripped ions which the give rise to the plasma energy loss through radiation.

Magnetic confinement: The containment of a plasma during fusion experiments by applying a specific pattern of magnetic fields. Also referred to as a Magnetic Bottle.

Plasma: It is one of the four fundamental states of matter (the others being solid, liquid, and gas) and it is the state in which the fuel is in the reactor. Plasma is an ionized gas. When fully ionized it is composed entirely of ions and electrons, being all neutral and electricity conductor. Plasma forms with similar conductive proprieties to that of metals.

Plasma impurities: Atoms or particles which fall within the confinement, they interact with plasma and magnetic field causing energy losses of the plasma.

Plasma radiation losses (P_{RAD}): In a tokamak there is a continuous loss of energy from the plasma which has to be replenished by plasma heating. Plasma energy losses in the form of radiation is given by Eq. 1.3.

$$P_{RAD} = P_{BRM} + P_{SYN} + P_{LIN} \qquad Eq.\ 1.3$$

Poloidal: Direction along the smaller circumference of the torus.

Q: Plasma power amplification; the ratio of fusion power input to the plasma divided by external power supplied to the plasma. In ITER, the programmatic goal - Q≥10 - signifies delivering ten times more power it consumes.

Scrape-off layer (SOL): Narrow region outside the border of the confined region known as the separatrix. The SOL may be imagined as the region where the plasma is essentially scraped off from the core plasma. There is a way by which the last closed field line can be delimited: using a modification of the magnetic field lines at the plasma edge, the field lines of the SOL are diverted into a dedicated region, the divertor.

Separatrix: Border of the confined region of the plasma. It is the last closed line of the confinement.

Sputtering: It is the process by which atoms are ripped from a solid surface by bombarding particles. It is the erosion process of the reactor walls.

Superconductivity: The flow of electric current without resistance in certain metals and alloys at temperatures near absolute zero.

Steady state: A tokamak in which conditions such as temperature, reaction rate, and neutron flux do not change appreciably with time.

Synchrotron radiation (P_{SYN}): Synchroton radiation is electromagnetic radiation emitted by moving charged particles deflected by a magnetic field.

Tokamak: The word tokamak is a transliteration of the Russian word токамак, an acronym of either "тороидальная камера с магнитными катушками" (*toroidal'naya kamera s magnitnymi katushkami*), that is toroidal chamber with magnetic coils. Tokamaks are based on the concept of magnetic confinement, in which the plasma is contained in a doughnut-shaped vacuum vessel.

Toroidal: Direction along the axis of the torus.

Torus: A surface of revolution generated by revolving a circle in three-dimensional space about an axis coplanar with and not touching the circle. Examples of tori include the surfaces of doughnuts and inner tubes. The solid contained by the surface is known as a toroid.

Tritium: One of the two isotopes of hydrogen that will be used to fuel the fusion reaction in ITER.

2 INTRODUCTION

2.1 OBJECTIVES

AINA is a code in development so improvements must be continuously validated. Thus, one of the main objective of this project is to test the introduced modifications. This involves performing various simulations to evaluate different scenarios to detect and correct any anomaly.

The project also aims to determine the behaviour of the plasma and the walls of the reactor in the face of unexpected situations, ie, situations in which failure of any of the systems that forms the ITER machine lead to a loss of plasma control; to detect those cases that can be more dangerous and harmful and make an in-depth analysis of both plasma physics and walls heat transfer of these critic cases is intended.

2.2 SCOPE

Within the scope of this project are the following points:

- detecting bugs of the current version of AINA code, that is, AINA 3.0, so they can be corrected in later versions;
- study of the plasma behaviour in front of perturbations that lead to a loss of plasma control situation;
- analysis of the behaviour of the plasma and reactor wall in those cases that are considered more critical or interesting.

3 FUSION ENERGY

Energy supply has become one of the major challenges faced by humanity. Fossil fuels were the energy source that shaped 19th and 20th century civilization. But burning coal, oil and gas has been proved highly damaging to our environment. Carbon dioxide emissions, greenhouse effect gases, and fumes all contribute to the disruption in the balance of our planet's climate. Global energy consumption is set to triple by the end of the century, and yet supplies of fossil fuels are depleting and the environmental consequences of their exploitation are serious.

Nuclear fission, another of the major energy sources used nowadays, implies also some problems that have been created much controversy and discussion. On one side it is the difficulty of treatment and storage of radioactive waste product of nuclear fission, and secondly, it is the serious environmental implications of a possible accident at a nuclear power plant.

So the question loom over humanity today is how to supply energy demand, which increases every day, without compromising the environment. In the last years there has been a growing awareness of the whole population on the need to respect the environment and it has been understood that the current energy model is not the way to follow. Every day there are more countries that are committed to renewable and clean energy research. In this context fusion energy has become one of the energy alternatives for the future.

3.1 PHYSICAL PRINCIPLES

Fusion is the process that powers the sun and the stars. It is called *fusion* because the energy is produced by fusing together light atoms, such as hydrogen, at the extremely high pressures and temperatures that exist at the centre of the sun (15 million ºC). At this high temperatures experienced in the sun any gas becomes plasma, the fourth state of matter. Atoms never rest, the hotter they are, the faster they move. In the core of the Sun hydrogen atoms are in a constant state of agitation, colliding at very great speeds. The natural electrostatic repulsion that exists between the positive charges of their nuclei is overcome, and the atoms fuse. The fusion of light hydrogen atoms (H-H) produces a heavier element, helium. The mass of the resulting helium atom is not the exact sum of the two initial atoms, however some mass has been lost and great amounts of energy have been gained. This is what Einstein's formula describes (see Eq. 3.1).

$$E = m \cdot c^2 \qquad \textbf{\textit{Eq. 3.1}}$$

The tiny bit of lost mass (m) multiplied by the square of the speed of light (c^2), results in the amount of energy created by a fusion reaction (E).

As can be seen in Figure 3.1.1, the atom of hydrogen and its isotopes deuterium (H^2) and tritium (H^3), are the most feasible to carry out a fusion reaction, since they require low energy to overcome the natural electrostatic repulsion existing between nucleons.

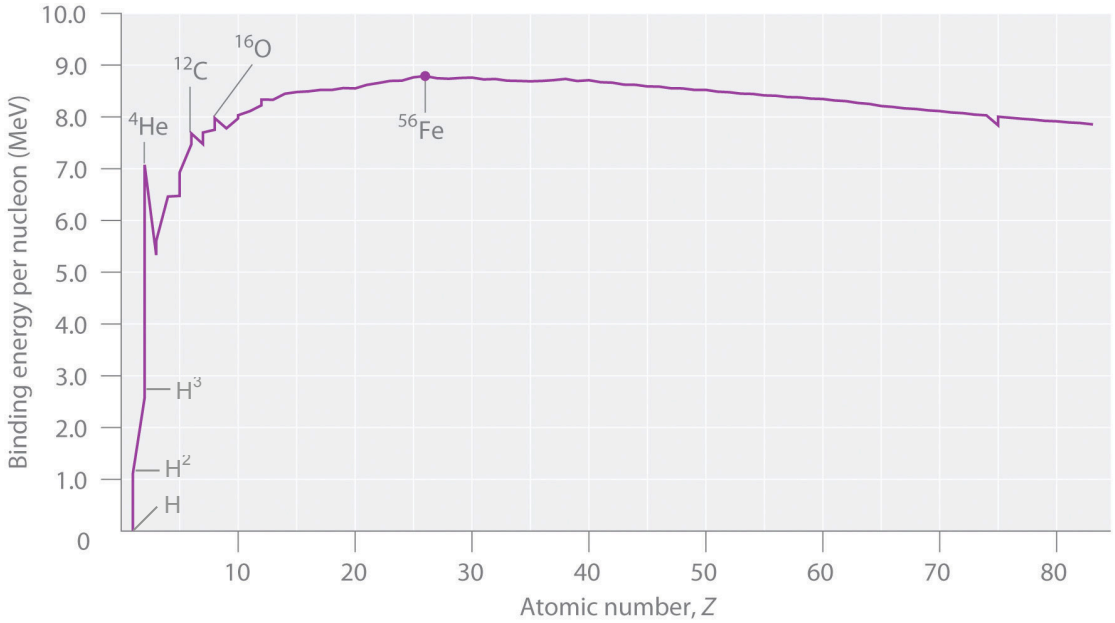

Figure 3.1.1. *Binding energy per nucleon function of atomic number*

Next, the most important fusion reactions of the deuterium and tritium within a fusion reactor are shown:

$$D + D \rightarrow T\ (1.01\ MeV) + p\ (3.02\ MeV)$$

$$D + D \rightarrow He^3\ (0.82\ MeV) + n\ (2.45\ MeV)$$

$$D + He^3 \rightarrow He^4\ (3.6\ MeV) + p\ (14.7\ MeV)$$

$$D + T \rightarrow He^4\ (3.5\ MeV) + n\ (14.1\ MeV)$$

$$T + T \rightarrow He^4 + 2n + 11.3\ MeV$$

$$He^3 + T \rightarrow He^4 + p + n + 12.1\ MeV$$

$$He^3 + T \rightarrow He^4\ (4.8\ MeV) + D\ (9.5\ MeV)$$

$$He^3 + T \rightarrow He^5\ (11.9\ MeV) + p\ (2.4\ MeV)$$

All this reactions happen simultaneously at the core of a fusion reactor, but the probabilistic distribution for each is different in function of the energy of the system. For this reason there are reactions more important than others since they require less input energy to be carried out.

The fusion science has identified the reaction between deuterium (H^2) and tritium (H^3) as the most efficient fusion reaction to reproduce in the laboratory setting. The D-T fusion reaction produces the highest energy gain at the lowest temperatures. In Figure 3.1.2 fusion cross-section for different reactions are shown, the concept of cross section is used to express the likelihood of interaction between particles, so from the graph it can be concluded that for the same kinetic energy of the particles, the combination of deuterium and tritium is the one most likely to result in a fusion reaction.

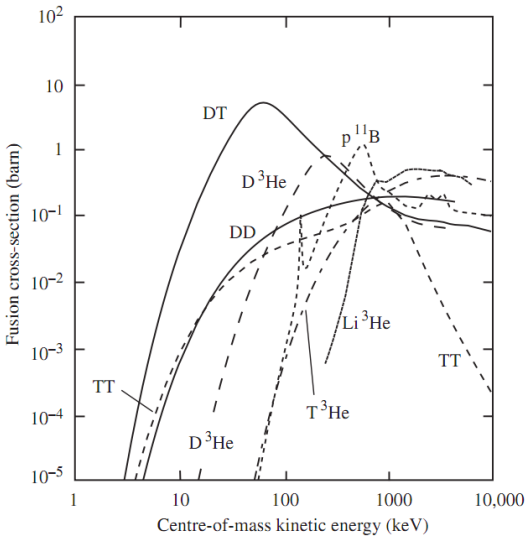

Figure 3.1.2. *Fusion cross-section*

At extreme temperatures, electrons are separated from nuclei, that is, gas is ionized and it becomes plasma. When fully ionized it is composed entirely of ions and electrons, being all neutral and electricity conductor. It forms with similar conductive proprieties to that of metals. Plasma is susceptible to magnetic fields, which is the way to get it confined in a fusion reactor. For obtaining high energy values it is required that fusion reactors are able to heat plasma to high temperatures, since temperature is a determining factor of the number of fusion reactions produced.

3.2 Fusion Science History

Following the first fusion experiments in the 1930s, fusion physics laboratories were established in many of industrialized nation. By the mid-1950s fusion machines were operating in the Soviet Union, the United Kingdom, the United States, France, Germany and Japan.

A major breakthrough occurred in 1968 in the Soviet Union. Researchers were able to achieve temperature levels and plasma confinement times that had never been attained before. The Soviet machine was a doughnut-shaped magnetic confinement device called a tokamak. From this time on, the tokamak was to become the dominant concept in fusion research. Tokamak devices multiplied across the globe and a steady progress has been made in fusion devices since then.

The Joint European Torus (JET) in United Kingdom, in operation since 1983, was a first step in the international research and financial resources collaboration. JET is collectively used by the EURATOM (European Atomic Energy Community) Associations from more than 20 European countries. In 1991, the JET tokamak achieved the world's first controlled release of fusion power. The Tore Supra Tokamak that is part of the Cadarache nuclear research centre holds the record for the longest plasma duration time of any tokamak: six minutes and 30 seconds. The Japanese JT-60

achieved the highest value of fusion triple product –density, temperature and confinement time– of any device to date. US fusion installations have reached temperatures of several hundred million degrees Celsius.

All these achievements turned fusion energy in one of the possible energy alternatives for the future. The next goal that was imposed by fusion science is to get the long sought-after plasma energy breakeven point. Breakeven describes the moment when plasmas in a fusion device release at least as much energy as is required to produce them. Plasma energy breakeven has never been achieved: the current record for energy release is held by JET, which succeeded in generating 70% of input power.

In this context ITER project was born: in 1985, a group of industrial nations agreed on a project to develop a new, cleaner, sustainable source of energy. ITER is an experimental reactor that will produce more power than it consumes: for 50 MW of input power, 500 MW of output power will be produced. So ITER is an important step on the road to fusion power plants.

3.3 ITER [2]

3.3.1 ITER project

ITER (*International Thermonuclear Experimental Reactor*) is a large-scale scientific experiment that aims to demonstrate that it is possible to produce commercial energy from fusion. Seven nations are participating: European Union, United Estates of America, Republic of China, Japan, Republic of Korea, Russia and India. It is located adjacent to the CEA Cadarache research centre where an outstanding scientific environment and technical infrastructure is already in place.

The objective of the ITER project is to gain the knowledge necessary for the design of the next-step device: a demonstration fusion power plant (DEMO). In ITER, scientists will study plasmas under conditions similar to those expected in a future power plant. ITER will be the first fusion experiment to produce net power; it will also test key technologies, including heating, control, diagnostics, and remote maintenance. The principal goals of ITER are:

- ITER should produce more power than it consumes. This is expressed in the value of Q, which represents the amount of thermal energy that is generated by the fusion reactions, divided by the amount of external heating. ITER has to be able to momentarily produce Q=10, and Q larger then 5 during a longer period.

[2] Most of the information in this section has been extracted from the official website of ITER www.iter.org. It is a divulgative website which is very adequate to enlarge the knowledge on fusion energy and more specifically on ITER project and technology.

- ITER should maintain a fusion plasma up to 8 minutes, and to sustain a "burning plasma", which means that most of the heating from the plasma comes from the fusion reactions themselves.
- ITER should implement and test technologies and processes needed for future fusion power plants, including superconducting magnets and remote handling (maintenance by robots).

The construction work on ITER began in 2010 and is expected to be finished in 2019. A commissioning phase will follow that will ensure all systems operate together and prepare the machine for the achievement of First Plasma in November 2020. ITER's operational phase is expected to last for 20 years. First, a several-year "shakedown" period of operation in pure hydrogen is planned during which the machine will remain accessible for repairs and the most promising physics regimes will be tested. This phase will be followed by operation in deuterium with a small amount of tritium to test wall-shielding provisions. Finally, scientists will launch a third phase with increasingly frequent operation with an equal mixture of deuterium and tritium, at full fusion power. If all goes well, DEMO will lead fusion into its industrial era, beginning operations in the early 2030s, and putting fusion power into the grid as early as 2040.

3.3.2 ITER power plant

A fusion power plant is based on the same principle as other power plants. There is a heat source that gives power to the primary circuit, and a heat exchanger to produce steam in the secondary circuit. This last converts thermal energy into electrical energy through a turbine and an alternator. In the case of a Tokamak the heat source are the neutrons produced on the D-T reaction, the plasma is surrounded by blankets which one of them roles is absorb the 14 MeV neutrons, transforming their energy into heat which is then carried away by a suitable coolant to provide most of the reactor power output. In Figure 3.3.2.1 a scheme of a commercial fusion power plant is shown.

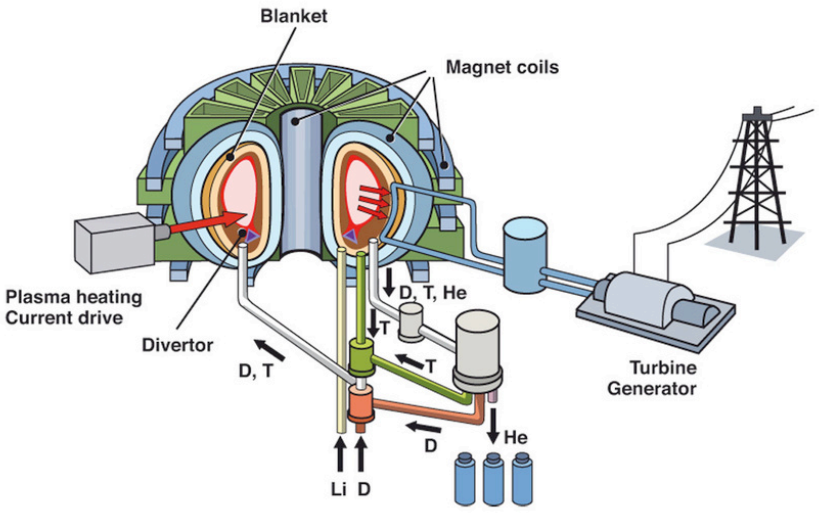

Figure 3.3.2.1. *Scheme of how would be a commercial fusion power plant*

However, as ITER is an experimental facility and it is not designed to produce electricity, the heat produced by the fusion reaction will be evacuated, cooling water will pass through primary and secondary heat exchangers that lower its temperature before it is stored in cooling towers where most of the water will evaporate. So ITER do not exactly fit with the scheme showed in Figure 3.3.2.1 since it has not a turbine-generator system to transform heat into electricity.

The helium produced by the fusion reaction forms part of a gaseous exhaust that also contains unburned fuel and impurities. This exhaust is extracted continuously from the fusion chamber in order to keep the fusion plasma clean and at temperature. A sophisticated gas processing system in ITER will separate the different components of the exhaust gas and recover the fusion fuels in order to reinject them back into the fuel cycle. This closed loop fuel cycle minimizes effluents. Detritiation systems in ITER have been designed to remove tritium from liquids and gases for reinjection into the fuel cycle.

3.3.3 ITER reactor

ITER is based on the Tokamak concept of magnetic confinement, in which the plasma is contained in a doughnut-shaped vacuum vessel. The fuel (a mixture of deuterium and tritium) is heated to temperatures in excess of 150 million°C, forming a hot plasma. Strong magnetic fields are used to keep the plasma away from the walls; these are produced by superconducting coils surrounding the vessel, and by an electrical current driven through the plasma.

- **Cryostat**

The cryostat is a large, stainless steel structure surrounding the vacuum vessel and superconducting magnets, providing a super-cool, vacuum environment. It has several openings, which provide access to the vacuum vessel for cooling systems, magnet feeders, auxiliary heating, diagnostics, and the removal of blanket and divertor parts.

- **Vacuum Vessel**

The vacuum vessel is a hermetically-sealed steel container inside the cryostat that houses the fusion reaction and acts as a first safety containment barrier. In its torus chamber the plasma particles spiral around continuously without touching the walls.

The vacuum vessel will have double steel walls, with passages for cooling water to circulate between them. The inner surfaces of the vessel will be covered with blanket modules that will provide shielding from the high-energy neutrons produced by the fusion reactions.

Forty-four ports will provide access to the vacuum vessel for remote handling operations, diagnostic systems, heating, and vacuum systems.

- **Blanket**

The blanket covers the interior surfaces of the vacuum vessel, providing shielding to the vessel and the superconducting magnets from the heat and neutron fluxes of the fusion reaction. The neutrons are slowed down in the blanket where their kinetic energy is transformed into heat energy and collected by the coolant circuit. In a fusion power plant, this energy will be used for electrical power production.

For purposes of maintenance on the interior of the vacuum vessel, the blanket wall is modular. It consists of 440 individual segments, each segment has four detachable first walls which directly faces the plasma and removes the plasma heat load, and a blanket shield dedicated to the neutron shielding.

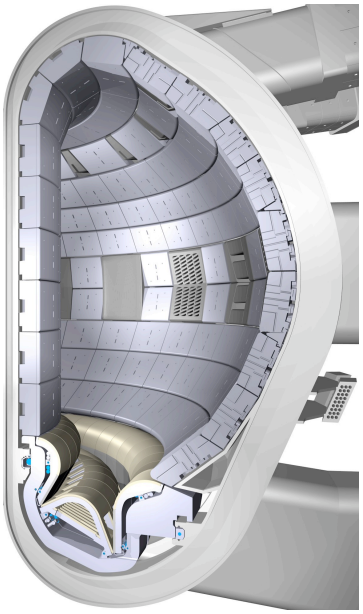

Figure 3.3.3.1. A cut-away of the ITER vacuum vessel showing the blanket modules attached to its inner wall and the divertor at the bottom

The ITER blanket is one of the most critical and technically challenging components in ITER because, together with the divertor, it directly faces the hot plasma. Because of its unique physical properties, beryllium has been chosen as the element to cover the first wall. The rest of the blanket shield will be made of high-strength copper and stainless steel.

Tritium and deuterium are two isotopes of hydrogen that will be used to fuel the fusion reaction in ITER. While deuterium can be extracted from seawater in boundless quantities, the supply of tritium is limited. But fortunately a second source of tritium exists: tritium can be produced within the tokamak when neutrons escaping the plasma interact with the lithium contained in the blanket. This concept of breeding tritium during the fusion reaction is an important one for the future needs of a large-scale fusion power plant. ITER will procure the tritium necessary for its expected 20-year lifetime from the global inventory. But for DEMO, the next step on the way to commercial fusion power, about 300 g of tritium will be required per day to produce 800 MW of electrical power. No sufficient external source of tritium exists for fusion energy development beyond ITER, making the successful development of tritium breeding essential for the future of fusion energy. ITER will provide a unique opportunity to test breeding blankets in a real fusion environment. Within these test blankets, viable techniques for ensuring tritium breeding self-sufficiency will be explored.

- **Divertor**

Plasma particles are confined to a certain degree within the volume composed of closed magnetic field lines. Those that escape this region are called plasma exhaust. The border of the confined region is known as the Last Closed Flux Surface (LCFS) or separatrix, while the term Scrape-Off Layer (SOL) designates a narrow region (usually only a few centimetres wide) outside this border. The SOL may be imagined as the region where the plasma is essentially scraped off from the core plasma. There is a way by which the last closed field line can be delimited: using a modification of the magnetic field lines at the plasma edge, the field lines of the SOL are diverted into a dedicated region, the divertor, located at the very bottom of the vacuum vessel.

The ITER divertor is made up of 54 remotely-removable cassettes, each holding three plasma-facing components, or targets. These are the inner and the outer vertical targets, and the dome. The targets are situated at the intersection of magnetic field lines where the high-energy plasma particles strike the components. Their kinetic energy is transformed into heat; the heat flux received by these components is extremely intense and requires active water cooling.

The choice of the surface material for the divertor is an important one. Only very few materials are able to withstand temperatures of up to 3,000°C for the projected 20-year lifetime of the ITER machine; these will be tested in ITER. ITER planned to begin operations with a divertor target made of carbon fibre-reinforced carbon composite (CFC), a material that presents the advantage of high thermal conductivity, to be followed by a second divertor with tungsten targets which offer the advantage of a lower rate of erosion and longer lifetime. Currently, due to cost cutting considerations, the ITER management is investigating the feasibility of implementing tungsten right from the beginning of operations.

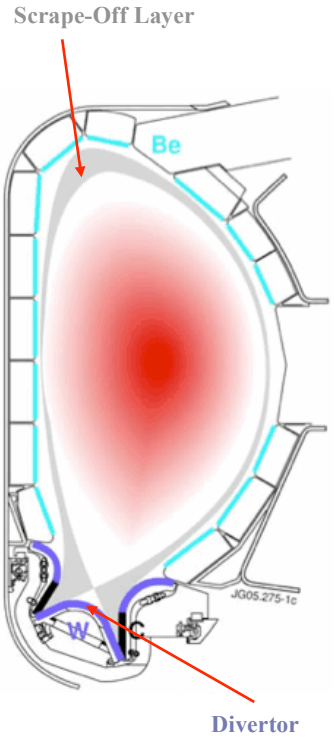

Figure 3.3.3.2. A cut-away of the ITER vacuum vessel showing the Scrape-Off Layer and the divertor

- **Magnets**

The ITER magnet system comprises 18 superconducting toroidal field and 6 poloidal field coils, a central solenoid, and a set of correction coils that magnetically confine, shape and control the plasma inside the vacuum vessel.

The power of the magnetic fields required to confine the plasma in the ITER vacuum vessel is extreme. For maximum efficiency and to limit energy consumption, ITER uses superconducting magnets that lose their resistance when cooled down to very low temperatures.

The toroidal and poloidal field coils lie between the vacuum vessel and the cryostat, where they are cooled and shielded from the heat generating neutrons of the fusion reaction.

- **Diagnostics**

An extensive diagnostic system will be installed on the ITER machine to provide the measurements necessary to control, evaluate and optimize plasma performance in ITER and to further the understanding of plasma physics. These include measurements of temperature, density, impurity concentration, and particle and energy confinement times.

The system will comprise about 50 individual measuring systems drawn from the full range of modern plasma diagnostic techniques, including lasers, X-rays, neutron cameras, impurity monitors, particle spectrometers, radiation bolometers, pressure and gas analysis, and optical fibres.

Because of the harsh environment inside the vacuum vessel, these systems will have to cope with a range of phenomena not previously encountered in diagnostic implementation, as high levels of neutral particle flux or long pulse length of the fusion reaction, while all the while performing with great accuracy and precision.

- **External Heating**

The temperatures inside the ITER Tokamak must reach 150 million° Celsius in order for the gas in the vacuum chamber to reach the plasma state and for the fusion reaction to occur. The hot plasma must then be sustained at these extreme temperatures in a controlled way in order to extract energy.

The ITER Tokamak will rely on three sources of external heating that work in concert to provide the input heating power of 50 MW required to bring the plasma to the temperature necessary for fusion. These are neutral beam injection and two sources of high-frequency electromagnetic waves.

3.3.4 ITER environmental and social impact

- **Fuel resources**

The nucleus of deuterium contains one proton and one neutron and it has a natural abundance in Earth's ocean of about one part in 6700. The mass of water in the oceans is $1.4 \cdot 10^{21}$ kg and the mass of deuterium is therefore $4 \cdot 10^{16}$ kg. In D-T reactors with a thermal efficiency of 1/3 this would allow the production of 10^{22} GJ (el). This is about $3 \cdot 10^{11}$ times the world's annual electrical energy consumption. Clearly there is no problem with deuterium resources. The cost of deuterium is of the order 0.72 € per gram. One gram of deuterium allows the production of 300 GJ (el). The cost

contribution of the deuterium fuel is therefore 0.002 € per GJ (el), which is negligible compared to the cost of electricity.

The supply of tritium is limited, estimated currently at twenty kilos. ITER will procure the tritium necessary for its expected 20-year lifetime from the global inventory. However, tritium can be bred from lithium using the neutron induced fission reactions (see Eq. 3.2 and Eq. 3.3). Breeding will be tested in ITER from test blanket modules (TBM), within these test blankets, viable techniques for ensuring tritium breeding self-sufficiency for DEMO will be explored.

$$Li^6 + n \rightarrow T + He^4 + 4.8\ MeV \qquad \textbf{Eq. 3.2}$$

$$Li^7 + n \rightarrow T + He^4 + n - 2.5\ MeV \qquad \textbf{Eq. 3.3}$$

With the breeding system that would be implemented in DEMO, the basic fuels are deuterium and lithium. The natural abundances of lithium are 7.4% Li^6 and 92.6% Li^7. The cost of lithium is of order of 28.91 € per kg and so the contribution of the lithium fuel to the cost is less than 0.0007 €, which is a very small cost compared to the cost of electricity. In Table 3.3.4.1 a summary of estimated fusion energy fuel resources is done. The values are only indicatives, since it being dependent on prices and subject to uncertainty because of incomplete exploration.

		Total GJ (el)	Years
Lithium	Land	10^{16}	30000
	Oceans	10^{19}	$30 \cdot 10^6$
Deuterium		10^{22}	$3 \cdot 10^{10}$

Table 3.3.4.1. *Estimated fusion energy fuel resources* [3]

- **Location**

The site chosen for the ITER project is a parcel of about 180 hectares located within a forested zone that covers 1,600 hectares. Studies were carried out to identify the biodiversity on the ITER parcel and to recommend measures to limit the environmental impact of construction.

Two areas have been fenced off permanently as "protected zones" where protected or rare species will benefit from preservation measures on the ITER site.

About half of the 180-hectare ITER site was preserved in its wooded state. Trees cleared from the other half were re-employed for millwork or for heating. Of the 2.5 million cubic metres of earth and rock moved to excavate the ITER platform, over two-thirds were re-employed on site. The remaining material has been stored on site, and will be replanted at the end of construction.

[3] JOHN WESSON: *Tokamaks*. Oxford, Third Edition, 2004, pg. 24-25.

- **Water and electricity consumption**

Approximately 3 million cubic meters of water will be necessary per year during the operational phase of ITER to evacuate the heat generated by the fusion reaction inside the ITER machine. This water will be supplied by the nearby Canal de Provence, and transported by gravity through underground tunnels to the fusion installation. The volume of water needed for ITER represents 2% of the total water transported by the Canal de Provence.

ITER is an experimental facility and is not designed to produce electricity; the heat produced will be evacuated by cooling water system, which in two independent circuits will pass through primary and secondary heat exchangers that lower its temperature before it is stored in cooling towers where most of the water will evaporate. What remains will pass through cooling basins on the ITER site and be tested for parameters such as temperature (maximum 30°C), pH, hydrocarbons, chlorides, sulphates and tritium. ITER will check the results of these tests before the water is released into the Durance River.

Electrical supply to the ITER site will be guaranteed by an existing network that feeds the Tore Supra Tokamak. A one-kilometre extension will be enough to link the ITER machine into the network without changing the current distribution of electrical lines. Operating the ITER Tokamak will require from 120 MW to up to 620 MW of electricity for peak periods of 30 seconds. No disruption to local users is expected.

- **Fusion products**

The products of the fusion process are helium, which is inert and harmless, and neutrons, which will lodge in the vessel walls and produce heat and activation of materials.

As explained in the previous section of ITER power plant, there is a closed loop fuel cycle where unburned fuel is separated from the different components of the gaseous exhaust produced in the fusion reaction and it is reinjected to the fuel cycle. This system minimizes effluents, the remaining ones will be well below authorized limits: gaseous and liquid tritium releases to the environment from ITER are predicted to have a dosimetry below 10 μSv per year. This is well under ITER's General Safety Objective of 100 μ Sv per year and 100 times lower than the regulatory limit in France of 1,000 μSv per year. Scientists estimate the exposure to natural background radiation to be approximately 2,000 μSv per year.

- **Radioactive products**

The main concern with the waste is radioactive contamination both from tritium and activation products.

During the operational lifetime of ITER, remote handling will be used to refurbish parts of the vacuum vessel. All waste materials will be treated, packaged, and stored on site. The fusion reaction will produce radioactive waste with a life periods equivalent or below 100 years. Once the radioactivity of the materials have diminished in such a significant way the materials can be recycled for use in future fusion plants.

In ITER decommissioning phase, most of the reactor components will be activated, so the necessary measures in the field of radiation protection should be taken for its storage.

- **Social impact**

ITER is an important step on the road to fusion power plants. In fact, success of ITER will give way to DEMO, which would be the first experimental-commercial fusion power plant. The main goal of DEMO is to demonstrate the viability of the commercialization of fusion energy. Therefor, ITER is a big step toward a radically different energy model. So it can be say that ITER is likely to become an important factor of global social change. However, it is a very long project and therefore its consequences on society are still very uncertain.

- **Impact on science and technology**

The ITER project includes studies in many scientific and technological areas. So regardless of the success or failure in its objectives, the progress and contributions in the various fields of technology will probably be very important.

3.4 ITER SAFETY: AINA CODE

ITER has developed simulation software in the area of safety and AINA is one of these codes. AINA is an acronym of *Analyses of IN-vessel Accidents*. It is a code that integrates a global balance plasma dynamics model and a radial and poloidal thermal analysis of in-vessel components, by considering separately first wall and divertor modules and performing a thermal analysis for each one in the depth direction.

AINA is an evolution of the SAFALY code which was an ITER safety code developed by T. Honda (Japan) in the early 90's. SAFALY code was built on the basis of simplified models and it was thought to be fully adaptable to the quantitative analysis of accidental sequences of a *tokamak*. From 2001 it was not implemented any improvement or actualization of the code until EFDA, European Fusion Development Agreement, transferred the code to the Fusion Energy Engineering Laboratory (FEEL) of the *Technical University of Catalonia-BarcelonaTech* by the end of 2004. Since then up to now, big upgrades have been performed over the code, turning it into AINA 1.0 code. Since 2009 a new code was programmed, on the basis of the same 0D plasma algorithms and 1D wall thermal algorithms, receiving the name of AINA 2.0. The current version and used to perform this report,

called AINA 3.0, includes some improvements regarding the configuration management, and new algorithms for plasma, plasma-wall interaction and wall thermal model.

One of AINA functions is to simulate situations of loss of plasma control that allow to know the behaviour of the plasma and the walls of the reactor to unexpected situations, such as the failure of some of the systems that form the ITER machine. So in the following section several loss of plasma control events are investigated with AINA 3.0 code. First the most critical cases are selected based on the plasma behaviour in response to various types of perturbations, be it the effect of a single one or a combination of two. And then a detailed study of selected cases as more dangerous is done.

Furthermore, This report is complemented by *AINA safety code*, a document where physic models and code conventions are described. Hereafter a few physic issues related to AINA operation are described, like energy confinement time or set points for plasma disruptions (see ANNEX A).

4 SIMULATION RESULTS

4.1 SIMULATION SCENARIOS

Three inductive scenarios are considered for the study. First one with a fusion power of 500 MW and Q=10, the second of 400 MW and Q=10 and the last one of 700 MW and Q=20.

The physics parameters and input values used by AINA 3.0 to calculate the initial equilibrium conditions for each scenario have been taken from the *Plasma Performance Assessment* [4] document and are shown in Table 4.1.1.

Variable	Scenario 1	Scenario 2	Scenario 3
	500 MW	**400 MW**	**700 MW**
R (m)/a (m)	6.2/2.0	6.2/2.0	6.2/2.0
κ_{95}/δ_{95}	1.7/0.33	1.7/0.33	1.7/0.33
V_P (m^3)	831	831	831
B_T (T)	5.3	5.3	5.3
I_P (MA)	15.0	15.0	17.0
q_{95}	3.0	3.0	2.7
$\langle n_e \rangle$ ($\cdot 10^{19} m^{-3}$)	11.3	10.1	12.3
$\langle n_e \rangle / n_G$	0.94	0.85	0.91
$\langle T_i \rangle$ (keV)	8.1	8.0	9.1
$\langle T_e \rangle$ (keV)	8.9	8.8	10.0
P_{FUS} (MW)	500	400	700
P_{NB} (MW)	33	33	33
P_{RF} (MW)	17	7	2
P_{OH} (MW)	1	1	1
$Q = P_{FUS}/(P_{NB}+P_{RF})$	10	10	20
P_{BRM} (MW)	26	21	34
P_{SYN} (MW)	8	8	10
P_{LIN} (MW)	27	18	25
P_{RAD} (MW)	61	47	70
P_{SOL} (MW)	104	87	120
P_{L-H} (MW)	51	48	54
$P_{separatrix}$ (MW)	90	75	103
β_T (%)	2.8	2.5	3.5
β_N	2.0	1.8	2.2
β_p	0.72	0.65	0.69
τ_E (s)	3.4	3.7	3.6
W_{th} (MJ)	353	320	434
W_{fast} (MJ)	34	32	41
l_i	0.84	0.84	0.77

[4] ITER JCT: *Plasma Performance Assessment*. 2004, pg. 15-16.

$H_{H98(y,2)}$	1.0	1.0	1.0
I_{BS}/I_P (%)	16	15	17
V_{loop} (mV)	75	75	85
τ_{He}/τ_E	5.0	5.0	5.0
$Z_{eff,ave}$	1.72	1.66	1.69
$f_{He,axis}$ (%)	4.4	4.3	5.2
$f_{He,ave}$ (%)	3.2	3.2	4.4
f_{Be} (%)	2	2	2
f_{Ar} (%)	0.14	0.12	0.12

Table 4.1.1. *Parameters of inductive operation scenarios*

4.2 STEADY STATE

The steady state for each scenario has been simulated with AINA 3.0 and the results obtained has been compared with the previous versions of AINA code (AINA 1.0 and AINA 3.0*) and with the parameters provided by ITER in the *Plasma Performance Assessment* document (PPA).

Table 4.2.1, Table 4.2.2 and Table 4.2.3 shown the results of each version, and the percentage difference existing between the results obtained with AINA 3.0 and the values provided by ITER.

Variable	AINA 1.0	AINA 3.0*	AINA 3.0	PPA	
	Values	Values	Values	Values	%
T_i (keV)	8.96	8.10	**8.10**	8.10	0.00
T_e (keV)	8.99	7.92	**8.17**	8.90	8.87
n_i (/m^3)	8.83E+19	1.18E+20	**9.28E+19**	-	-
n_e (/m^3)	1.08E+20	1.40E+20	**1.12E+20**	1.13E+20	0.86
n_a (/m^3)	4.40E+18	5.39E+18	**3.66E+18**	-	-
V_{loop} (V)	0.10	0.08	**0.11**	0.08	32.61
P_{BRM} (MW)	20.38	38.46	**27.09**	26.00	4.03
P_{OH} (MW)	0.54	0.93	**0.96**	1.00	3.84
P_{SYN} (MW)	3.86	1.95	**3.88**	8.00	106.42
P_{LIN} (MW)	22.12	24.56	**27.18**	27.00	0.66
P_{FUS} (MW)	501.63	500.00	**500.00**	500.00	0.00
$P_{line-edge}$ (MW)	17.73	18.89	**13.59**	-	-
P_{RAD} (MW)	46.35	64.96	**58.15**	61.00	4.91
β_{LIM} (%)	6.37	6.37	**6.36**	-	-
β_T (%)	2.85	3.38	**2.68**	2.80	4.59
β_P (%)	0.78	0.93	**0.74**	0.72	2.20
Z_{eff}	1.44	1.59	**1.78**	1.72	3.59
P_{ext}	49.94	50.00	**52.26**	-	-
P_{ext_i} (MW)	26.05	25.73	**18.83**	-	-
P_{ext_e} (MW)	23.89	24.27	**33.43**	-	-
GRN_{LIM} (/m^3)	2.39E+20	2.39E+20	**2.38E+20**	-	-

n_z (/m^3)	2.19E+18	2.35E+18	**2.38E+18**	-	-
Q	10.04	10.00	**9.57**	10.00	4.30
β_{NORM}	1.39	1.39	**1.39**	-	-
$f_{He,ave}$ (%)	4.07	3.85	**3.27**	3.20	2.11
P_{SOL} (MW)	102.57	127.98	**95.13**	104.00	9.32
n_e/GRN_{LIM}	0.45	0.59	**0.47**	-	-
f_{Be} (%)	1.67	2.00	**2.00**	2.00	0.00
f_{Ar} (%)	0.05	0.12	**0.12**	0.14	16.67
W_{ther} (MJ)	363.59	343.56	**343.10**	353.00	2.89
τ_E (s)	3.55	4.08	**3.61**	3.40	5.73
$f_{bootstrap}$	0.18	0.26	**0.17**	0.16	5.88
$P_{separatrix}$ (MW)	84.83	65.39	**81.54**	90.00	10.37
P_{L-H} (MW)	46.26	43.62	**75.36**	51.00	32.32
I_P (MA)	15	15	**15**	15	0.00
$I_{bootstrap}/I_P$ (%)	17.59	25.96	**16.73**	16.00	4.34

***Table 4.2.1**. AINA: Inductive scenario 1 (500MW)*

Variable	AINA 1.0	AINA 3.0*	AINA 3.0	PPA	
	Value	Value	Value	Value	%
T_i (keV)	9.18	8.00	**8.00**	8.00	0.00
T_e (keV)	9.31	7.84	**8.07**	8.80	9.06
n_i (/m^3)	7.64E+19	1.14E+20	**8.41E+19**	-	-
n_e (/m^3)	9.38E+19	1.39E+20	**1.02E+20**	1.01E+20	0.93
n_a (/m^3)	4.05E+18	6.55E+18	**3.26E+18**	-	-
V_{loop} (V)	0.10	0.09	**0.12**	0.08	37.71
P_{BRM} (MW)	15.72	34.89	**23.04**	21.00	8.86
P_{OH} (MW)	0.52	0.82	**1.02**	1.00	1.88
P_{SYN} (MW)	3.90	2.17	**3.62**	8.00	120.93
P_{LIN} (MW)	15.41	28.55	**25.83**	18.00	30.30
P_{FUS} (MW)	393.17	400.00	**400.00**	400.00	0.00
$P_{line-edge}$ (MW)	17.21	19.58	**12.91**	-	-
P_{RAD} (MW)	35.03	65.61	**52.49**	47.00	10.46
β_{LIM} (%)	6.37	6.37	**6.36**	-	-
β_T (%)	2.55	3.27	**2.40**	2.50	4.36
β_P (%)	0.70	0.90	**0.66**	0.65	1.34
Z_{eff}	1.44	1.59	**1.84**	1.66	10.00
P_{ext}	39.95	40.00	**47.16**	-	-
P_{ext_i} (MW)	16.31	15.68	**15.25**	-	-
P_{ext_e} (MW)	23.64	24.32	**31.91**	-	-
GRN_{LIM} (/m^3)	2.39E+20	2.39E+20	**2.38E+20**	-	-
n_z (/m^3)	1.94E+18	2.28E+18	**2.18E+18**	-	-
Q	9.84	10.00	**8.48**	10.00	15.2
β_{NORM}	1.39	1.39	**1.39**	-	-
$f_{He,ave}$ (%)	4.32	4.71	**3.20**	3.20	0.14
P_{SOL} (MW)	82.58	129.05	**75.74**	87.00	14.87

n_e/GRN_{LIM}	0.39	0.58	**0.43**	-	-
f_{Be} (%)	1.74	2.00	**2.00**	2.00	0.00
f_{Ar} (%)	0.10	0.12	**0.14**	0.12	14.29
W_{ther} (MJ)	325.90	413.96	**307.74**	320.00	3.98
τ_E (s)	3.93	7.69	**4.06**	3.70	8.94
$f_{bootstrap}$	0.15	0.22	**0.14**	0.15	7.14
$P_{separatrix}$ (MW)	65.38	34.29	**62.83**	75.00	19.38
P_{L-H} (MW)	42.62	53.40	**70.34**	48.00	31.76
I_P (MA)	15	15	**15**	15	0.00
$I_{bootstrap}/I_P$ (%)	15.20	21.60	**14.48**	15.00	3.62

Table 4.2.2. *AINA: Inductive scenario 2 (400MW)*

Variable	AINA 1.0	AINA 3.0*	AINA 3.0	PPA	
	Value	Value	Value	Value	%
T_i (keV)	10.18	9.10	**9.10**	9.10	0.00
T_e (keV)	10.34	8.98	**9.19**	10.00	8.86
n_i (/m^3)	8.94E+19	1.31E+20	**9.72E+19**	-	-
n_e (/m^3)	1.13E+20	1.65E+20	**1.20E+20**	1.23E+20	2.12
n_a (/m^3)	6.41E+18	1.04E+19	**5.24E+18**	-	-
V_{loop} (V)	0.09	0.08	**0.10**	0.09	18.46
P_{BRM} (MW)	24.60	53.28	**33.59**	34.00	1.23
P_{OH} (MW)	0.58	0.87	**1.02**	1.00	1.86
P_{SYN} (MW)	5.48	3.27	**5.20**	10.00	92.27
P_{LIN} (MW)	21.76	36.76	**30.11**	25.00	16.97
P_{FUS} (MW)	646.71	700.00	**700.00**	700.00	0.00
$P_{line-edge}$ (MW)	17.23	19.66	**15.05**	-	-
P_{RAD} (MW)	51.84	93.30	**68.90**	70.00	1.60
β_{LIM} (%)	7.22	7.22	**7.07**	-	-
β_T (%)	3.42	4.47	**3.27**	3.50	6.96
β_P (%)	0.73	0.96	**0.73**	0.69	5.33
Z_{eff}	1.47	1.61	**1.81**	1.69	6.40
P_{ext}	34.96	35.00	**41.03**	-	-
P_{ext_i} (MW)	12.16	11.67	**15.65**	-	-
P_{ext_e} (MW)	22.80	23.33	**25.38**	-	-
GRN_{LIM} (/m^3)	2.71E+20	2.71E+20	**2.65E+20**	-	-
n_z (/m^3)	2.26E+18	2.61E+18	**2.56E+18**	-	-
Q	18.50	20.00	**17.06**	20.00	14.69
β_{NORM}	1.57	1.57	**1.57**	-	-
$f_{He,ave}$ (%)	5.67	6.30	**4.35**	4.40	1.22
P_{SOL} (MW)	110.54	183.34	**113.23**	120.00	5.98
n_e/GRN_{LIM}	0.42	0.61	**0.45**	-	-
f_{Be} (%)	1.62	2.00	**2.00**	2.00	0.00
f_{Ar} (%)	0.09	0.12	**0.12**	0.12	0.00
W_{ther} (MJ)	433.31	557.91	**412.04**	434.00	5.33

τ_E (s)	3.92	6.96	**3.64**	3.60	1.07
$f_{bootstrap}$	0.18	0.25	**0.17**	0.17	0.00
$P_{separatrix}$ (MW)	93.31	60.49	**98.18**	103.00	4.91
P_{L-H} (MW)	47.08	58.51	**79.44**	54.00	32.03
I_P (MA)	17.00	17.00	**17.00**	17.00	0.00
$I_{bootstrap}/I_P$ (%)	17.72	24.75	**17.40**	17.00	2.31

Table 4.2.3. *AINA: Inductive scenario 3 (700MW)*

As can be seen in the tables, the most striking result is the synchrotron power (P_{SYN}). For the three scenarios simulated, although obtained results seem more consistent than in the previous version of the code (AINA 3.0*), the values of P_{SYN} are still lower than expected. This may be due to different sources of error. On the one hand, the model used in 2004 for the *Plasma Performance Assessment* document was the Trubnikov model, which is not as accurate as the posterior model of Albajar. On the other hand, the model implemented in AINA 3.0 code is a local variation of the Trubnikov model proposed by Albajar, which is suitable for a 0D code.

In his thesis, Ferran Albajar proposes some results for the ITER case of 410 MW of fusion power. The value of the synchrotron power that he obtained was of 5.32 MW.[5] In our case, the value obtained for 400 MW is of 3.62, which is quite close, so for now the code will no be changed.

Next, the neutronic and electromagnetic loads for the steady state of 500 MW are shown. Table 4.2.4 corresponds to the blanket loads and the Table 4.2.5 to the divertor loads.

Region	Neutronic loads (MW/m^2)	Electromagnetic loads (MW/m^2)
1	1.164	0.527
2	1.315	0.527
3	0.982	0.527
4	0.891	0.527
5	0.488	0.527
6	0.153	0.527
7	0.561	0.527
8	0.697	0.527
9	0.457	0.527

Table 4.2.4. *AINA 3.0: Neutronic and electromagnetic loads at the blanket*

Region	Neutronic loads (MW/m^2)	Electromagnetic loads (MW/m^2)
10	0.169	0.952
11	0.173	7.387
12	0.082	0.423

[5] FERRAN ALBAJAR VIÑAS: *Radiation Tranpsort Modelling in a Tokamak Plasma*, Universitat Politècnica de Barcelona, 2004, pg. 101.

13	0.080	0.423
14	0.315	1.545
15	0.284	7.387
16	0.118	0.656
17	0.113	0.656
18	0.032	1.565
19	0.032	0.127
20	0.032	0.169

Table 4.2.5. *AINA 3.0: Neutronic and electromagnetic loads at the divertor*

As can be seen in Table 4.1.6, the electromagnetic loads do not exceed the satisfying an acceptable steady state power loads (≤ 10 MW/m2) on the divertor's target. And as the neutronic loads are lower than the electromagnetic ones it does not deserve special attention.[6]

Table 4.2.6 shows what is the standard fuelling rate for every scenario and ion temperature. Those standard fuelling rates have been extracted from AINA steady state calculations.

Initial fusion power [MW]	Initial Ti [keV]	Fuelling rate [$\cdot 10^{19}$ / m^3/s]
500	8.1	1.3291
	10.0	1.4263
	12.0	1.5755
	14.0	1.7417
400	8.0	1.0695
700	9.1	1.3946

Table 4.2.6. *AINA 3.0: Fuel injection*

From now overfuelling events will be identified by multiplication factors. Those multiplication factors will refer to standard fuelling rates for every initial temperature and fusion power.

4.3 TRANSIENTS

ITER plasma transients have been studied in the past for safety purposes. The most severe plasma transients expected are disruptions, VDEs and runaway electrons. From the safety studies of these events was concluded that the only consequences affecting the wall integrity would imply the erosion and partial melting of the plasma facing components and, very infrequently, in vessel leaks due to a local perforation of the first wall by runaway electrons.

[6] ITER JCT: *Plasma Performance Assessment*. 2004, pg. 6.

Together with them, the *Loss of Plasma Control transients (LOPC),* which postulate a total failure of the three tiered plasma control system, were also included in the *Design Basis Accident Study*.[7] These postulated transients are the following:

- sudden increase in fuelling rate,
- sudden termination of fuelling and/or auxiliary heating,
- sudden improvement of confinement time,
- sudden increase of auxiliary heating.

4.3.1 Study of plasma transients

These types of studies are focused in finding and studying the most critical situation and, therefore, the most damaging to the reactor. In this study the method of the operating window of the plasma will be used to detect these critical cases. This method determines the effect of the different perturbation using simple calculations. Moreover, the representation of the results plotted on a (n,T) diagram allows to show intuitively the effects of perturbations on the equilibrium plasma.

First, the operation window of the plasma (n,T) implemented in AINA code must be defined. To do this, it has been integrated in code AINA a program that allows calculating it. This program runs some simulations iterating on three parameters of the initial equilibrium: the initial fusion power, the initial ionic temperature and the initial beryllium impurities. Simulations corresponding to equilibrium states form the operation window of the plasma, from which the plasma limits can be represented. These limits indicate when plasma gets a disruption, which is a phenomenon related to plasma instabilities, causing a rapid loss of confinement and consequent termination of the plasma. The lost energy is dissipated in a small area of the wall and can cause serious damage. The four set points that indicate plasma termination are:

- Edge plasma balance: $P_{SOL} \leq 0$
- Density limit: $n_e > 2 \cdot n_{Greenwald}$
- Beta limit: $\beta > \beta_{LIMIT}$
- Locked modes limit: $n_e < 2 \cdot 10^{19} m^{-3}$

On the other hand, H-L limit transition indicates when plasma pass from H-mode confinement to L-mode confinement.

In Figure 4.3.1.1 the plasma operation window and the different limits are represented.

[7] N. TAYLOR: *Preliminary safety analysis of ITER Fusion Sci. Technol. 56*, 2009, pp. 573–580.

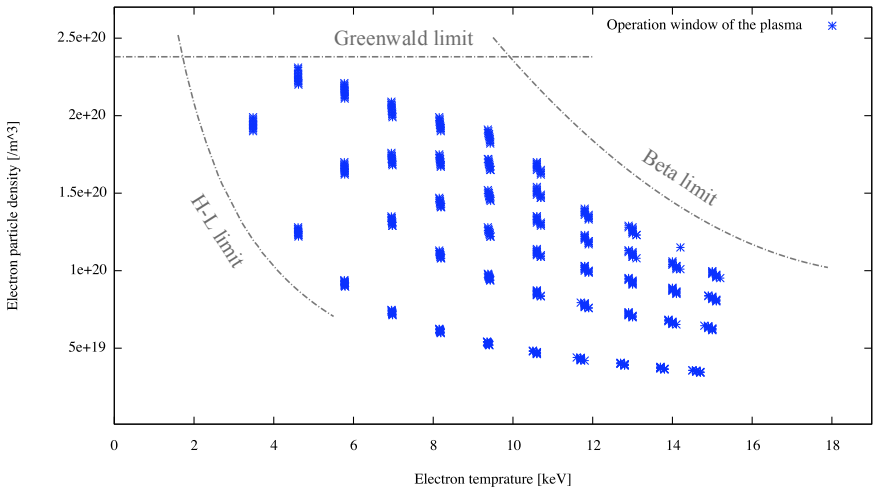

Figure 4.3.1.1. *Operation window of the plasma*

As can be seen, the Greenwald limit is not well defined by the plasma operation window calculated with AINA and therefore in future code improvements would be interesting to fix this.

Once the operation window of the plasma is defined, the behaviour of the different variables inside the window must be known. As this is a study of the blanket and divertor's critical scenarios, the most representative parameters are the fusion power achieved by the plasma and the scrape-off power, since the latter determines the loads on the divertor.

To understand the behaviour of these two parameters two 3D graphs have been done with the results of the simulations that pertain to the operation window of the plasma, that is, with the results of the steady states. The first one has been done with T_e, n_e and P_{FUS}, and the second one with T_e, n_e and P_{SOL}. In both cases, the power has been projected to the (n_e,T_e) plane according to a colour palette as can be seen in Figure 4.3.1.2 and Figure 4.3.1.3.

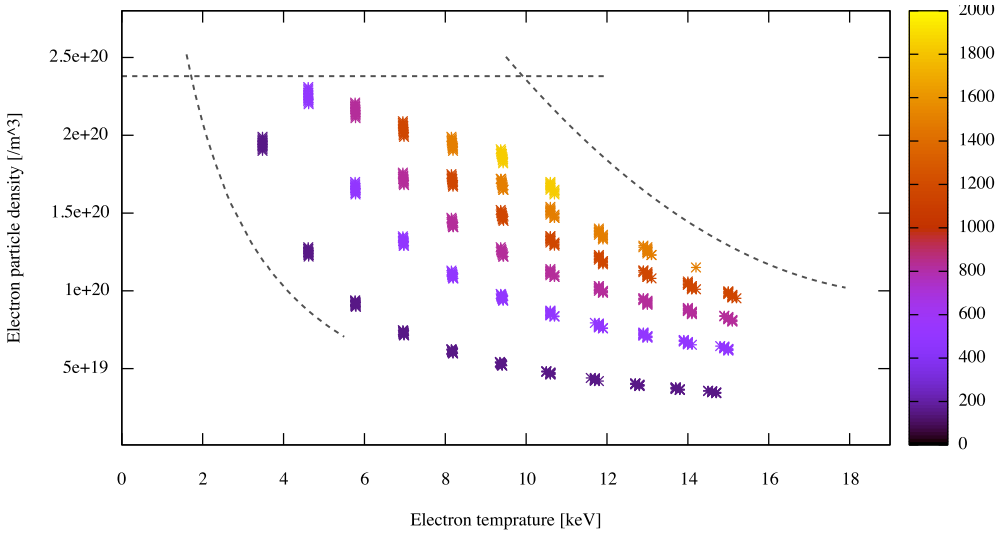

Figure 4.3.1.2. *Behaviour of the fusion power in MW within the operation window of the plasma*

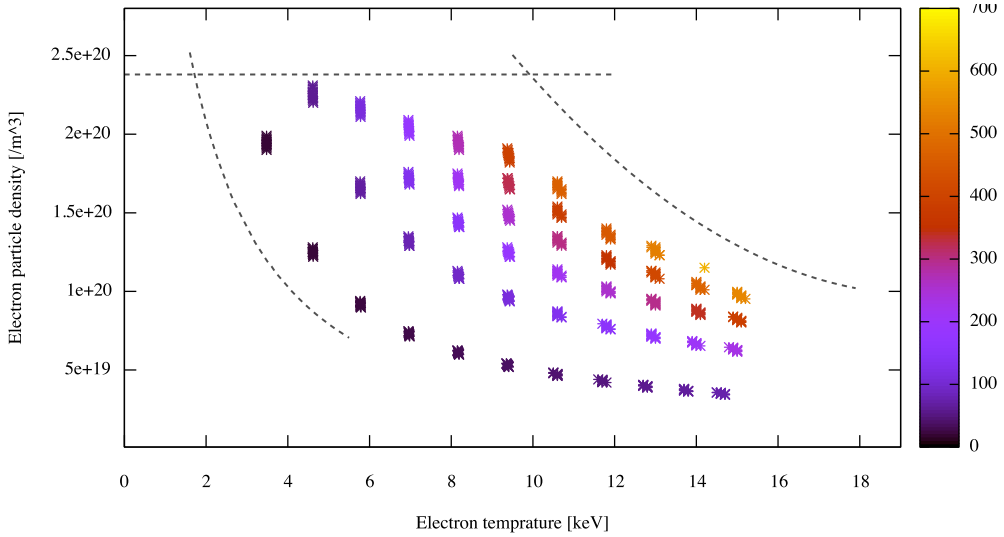

Figure 4.3.1.3. *Behaviour of the scrape-off power in MW within the operation window of the plasma*

The fusion power and the scrape-off power have not the same behaviour. While fusion power, which determines the temperature on blankets, increase when it moves to the top right side of the plasma operation window, the scarpe-off power, related to the divertor's temperatures, increase while moving to the right of the window.

The next step is to perform several simulations by introducing various perturbations and to show the results over the plasma operating window. The different transients are plotted over the n,T diagram, starting from the equilibrium point (500 MW and T_i=8.1 keV) and ending in a disruption or in a new steady state. As seen above, the new steady states which are situated to the top right corner of the window are the most dangerous to the integrity of the blankets while those ones situated at the right are the most critical for the divertor, so a complete analysis of the wall thermal equilibrium will be done for this critical cases, to detect possible risks for the wall integrity (melting) during the transient. The study have been done for a single type of perturbation, for example, pure overfuelling, pure overheating or pure confinement time improvement; also for a combination of two different types, that is, for cases in which two unexpected events coincide in time; and finally, it has also been studied the case of two consecutive perturbations, that is, one after the other.

- **Pure overfuelling, pure overheating and pure confinement time improvement perturbations**

First of all, the study of pure overfuelling, pure overheating and pure confinement time improvement perturbation is done. The results obtained have been plotted in Figure 4.3.1.4, where the limits of the operation window and the fusion power curves of 400, 500 and 700 MW are also represented.

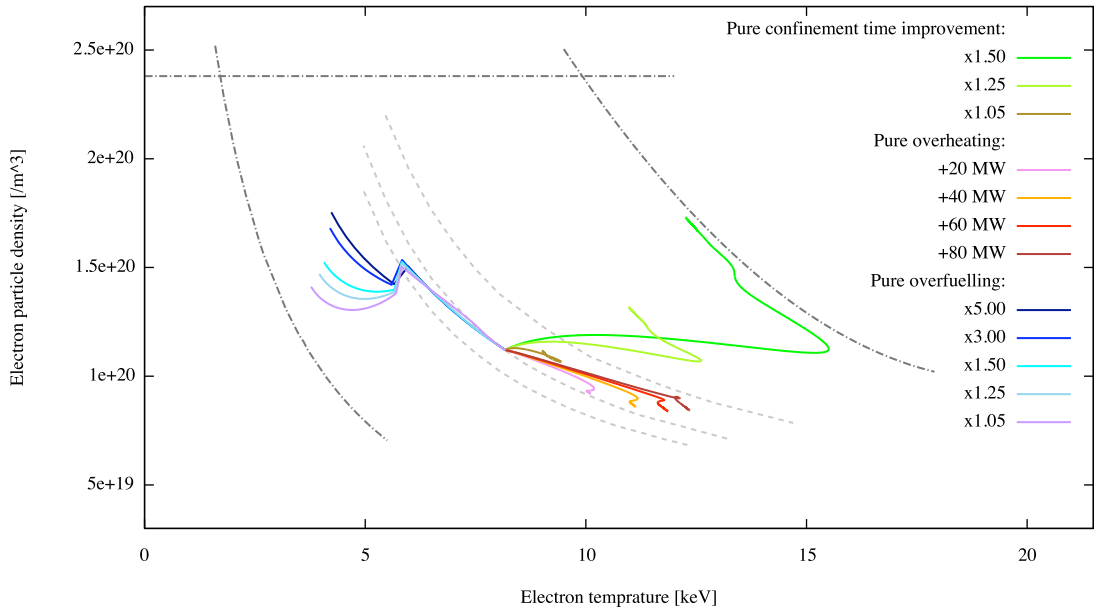

Figure 4.3.1.4. *Pure overfuelling, pure overheating and pure improvement of confinement time perturbations, T_i = 8.1 keV, P_{FUS} = 500 MW*

As can be observed in the graph, assuming that there is only a failure in the fuel injection system, that is, a pure overfuelling case, all the transients move to the left, crossing the limit of the H-L transition, where there is a discontinuity in the derivative of the transient line, and finally the plasma collapses by P_{SOL}. So, in either of the studied cases a new H-mode steady state is achieved.

Something that can draw the attention is the fact that the H-L limit represented at the chart does not match with the H-L transition suffered by the transients. The limit shown is further to the left. As explained above, the represented limits have been calculated from the values that form the operation window of the plasma, that is, from steady states. The results obtained during the transient are not entirely accurate, since the program tries to adjust the various variables to find an equilibrium state. That's why the fact that the transient's H-L transition does not match with the represented curve must not be considered as a miscalculation.

It also draws the attention that despite being transients that do not reach a new H-mode equilibrium state, they end within the operation window of the plasma displayed. This is because the equilibrium state depends on many variables, and in this type of graphs are only considered two of them (n, T). So it may be that a non-balance state ends inside the window, since although the density and the temperature take equilibrium values, other variables do not.

In the *Loss of Plasma Control Transients* study done in 2007, the method followed to find critical situations was to perform parametric sweeps by running multiple simulations.[8] This method allows to represent the maximum fusion power achieved in each transient from a parametric sweep of a perturbation, for example, an overfuelling or an improvement of the confinement time perturbation. So this report has complemented the study of plasma operating window with some parametric sweeps, to allow comparison with *Loss of Plasma Control Transients* (2007) report and to better illustrate the behavior of various perturbations.

In Figure 4.3.1.5 the parametric sweep of the fuelling rate multiplication factor (overfuelling event) obtained this time with AINA 3.0 is shown.

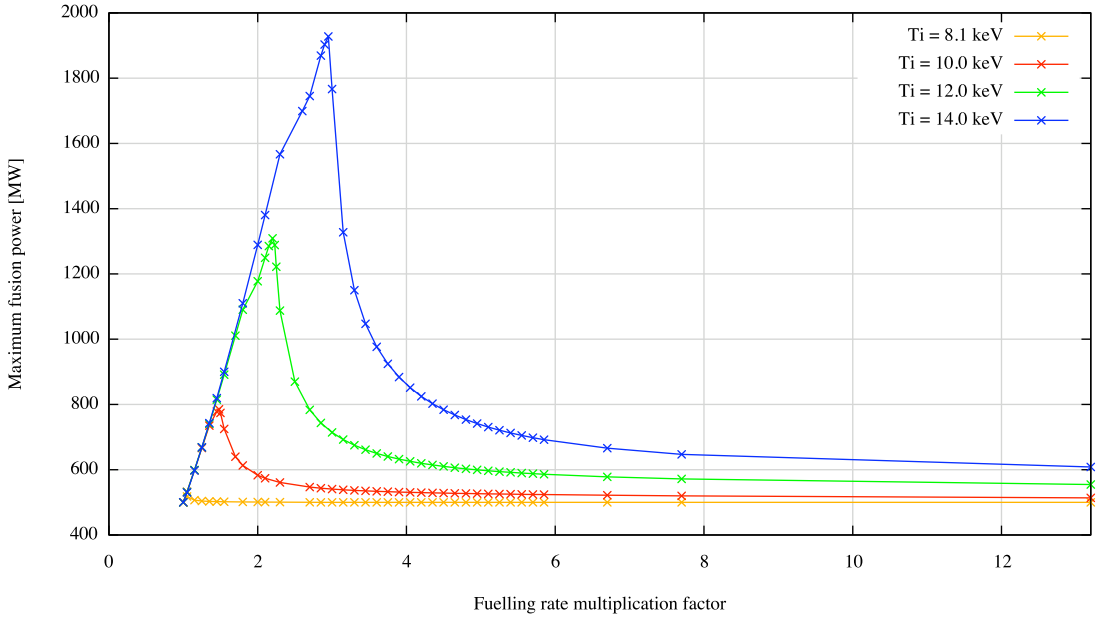

Figure 4.3.1.5. *Maximum fusion power in case of increase of fuelling rate for different initial T_i*

Figure 4.3.1.5 shows the maximum fusion power in case of increase of fuelling rate multiplication factor for different initial T_i and for an initial fusion power of 500 MW. It can be seen that maximum fusion power achieved is higher for higher initial ion temperatures.

As written in *PID* [9], the fuelling system of ITER has a limited capacity. Assuming this limitation of 240 Pa·m3/s (~7.8x1019 /m3/s) of fuelling rate, the maximum fuelling rate multiplication factor that can be given from the equilibrium point (500 MW and Ti=8.1 keV) is 5.87. However, by safety margins issues to study cases with higher overfuellings is better.

[8] J. DIES, M. DAPENA, M. RAMÓN, R. LÓPEZ, J. GARCÍA: *Review of Loss of Plasma Control Transients in ITER*. FEEL-UPC, 2007, pg. 51.
[9] ITER JCT: *Project Integration Document (PIC)*. January 2007, 151 [Table 4.5-1].

The variation of the initial ionic temperature is equivalent to an external power perturbation combined with an overfuelling from the equilibrium point of 500 MW and T_i=8.1 keV, achieving a new steady state.

As T_i varies, the equilibrium point moves along the constant fusion power curve of 500 MW, reaching equilibrium points in which the gain (Q) is not maximum, that is, in which it is not equivalent to 10. In this situation, the plasma requires an external power variation to maintain a constant fusion power of 500 MW (see Eq. 4.1). By increasing T_i, different equilibriums are reached in which Q<10, and therefore the external heating must increase too.

$$Q = \frac{Fusion\ power}{Total\ external\ power} \qquad \textbf{\textit{Eq. 4.1}}$$

As regards to the fuel injection, in Table 4.2.6 the standard fuelling rate for each initial ionic temperature is shown. It can be seen that the higher the T_i, higher the fuelling rate.

Thus, in the parametric sweep showed in Figure 4.3.1.1 is not only analysed the effect of an overfuelling, but the effect of various combined and consecutive perturbations. In particular, the variation of T_i corresponds to an overheating combined with an overfuelling that moves the plasma to a new steady state, and then an overfuelling perturbation is introduced.

In Table 4.3.1.1 it can be seen the transients with the higher maximum fusion power obtained from the parametric sweep, the fuelling rate multiplication factor in which it takes place, the fuel injection and also the external power needed for each T_i.

	T_i = 8.1 keV	T_i = 10.0 keV	T_i = 12.0 keV	T_i = 14.0 keV
Plasma termination	$P_{SOL} \leq 0$	$P_{SOL} \leq 0$	Greenwald	Greenwald
External power [MW]	52.26	67.30	101.72	145.99
Higher maximum fusion power [MW]	518.02	785.03	1309.16	1927.79
Fuelling rate multiplication factor	1.05	1.48	2.20	2.95
Fuel injection [$\cdot 10^{19}$ / m^3/s]	1.3956	2.1109	3.4661	5.1380

Table 4.3.1.1. *Most critical cases of overfuelling for different initial T_i*

Indeed, and as shown in the Table 4.3.1.1, for higher values of T_i higher is the external power needed. However, the plasma heating system of ITER has an installed capacity up to 130 MW but it can provide up to 110 MW at a time.[10] The maximum initial T_i that can be achieved, considering the limit of the heating system, is around 13 keV. For higher values it would be necessary an extra

[10] ITER JCT: *Plasma Performance Assessment*. 2004, pg. 63.

heating. However in order to perform conservative analyses, that is, for safety margins, it is suitable to study higher values.

In order to know how each simulation scenario affects to maximum achievable fusion power, transients with different multiplication factors and standard T_i have been simulated. Output values are shown in Figure 4.3.1.6.

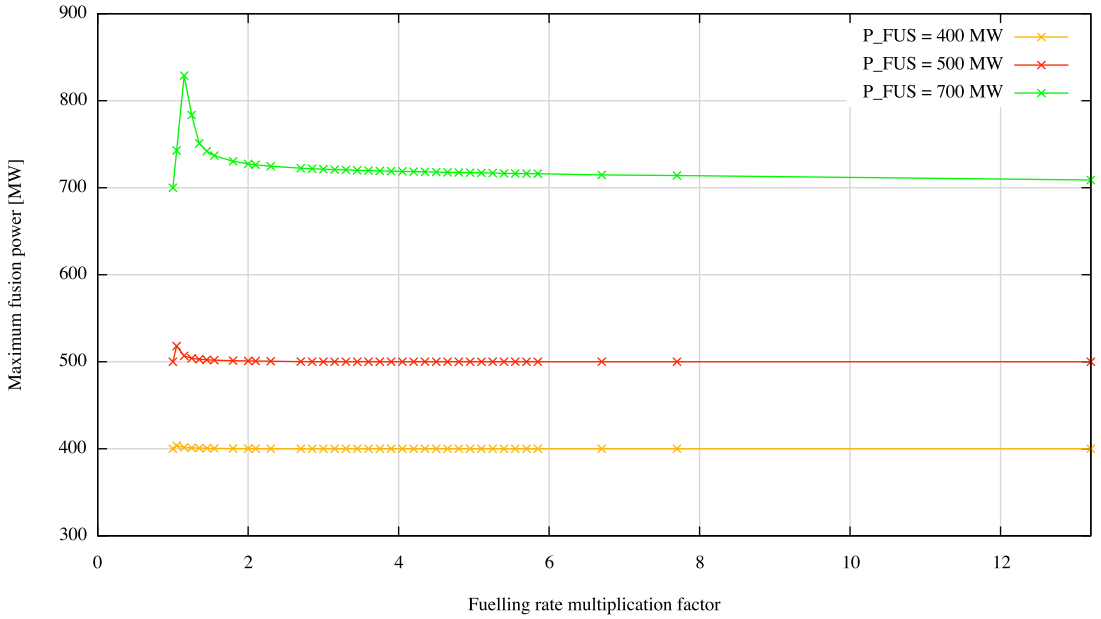

Figure 4.3.1.6. *Maximum fusion power in case of increase of fuelling rate for different initial* P_{FUS}

As expected, the higher the fusion power of the initial equilibrium the greater the maximum fusion power achieved in the transients.

In Table 4.3.1.2 it can be seen the transients with the higher maximum fusion power for each T_i and the fuelling rate multiplication factor in which it takes place.

	P_{FUS} = 400 MW	P_{FUS} = 500 MW	P_{FUS} = 700 MW
Plasma termination	$P_{SOL} \leq 0$	$P_{SOL} \leq 0$	$P_{SOL} \leq 0$
Higher maximum fusion power [MW]	403.55	518.02	828.94
Fuelling rate multiplication factor	1.05	1.05	1.15

Table 4.3.1.2. *Most critical cases of overfuelling for different initial* P_{FUS}

As it can be seen in Table 4.3.1.2, maximum fusion power strongly depends on initial fusion power. So as the 700 MW scenario implies higher initial ion temperature, it is easier to achieve higher fusion power.

Pure overheating cases has been also studied. According to *ITER Physics Guidelines*, 130 MW of heating power will be installed on ITER, although only 110 MW will be available to be working

simultaneously.[11] In order to perform conservative analyses, up to 130 MW of additional heating power has been studied, that is an overheating up to 80 MW.

As can be seen in Figure 4.3.1.4, all the studied overheating transients move to the right to reach a new steady state very close to the constant fusion power curve of 500 MW. However, although the achieved fusion power do not imply a danger to the blanket, the new steady states are situated in higher P_{SOL} points within the operation window of the plasma, which may involve a danger to the divertor. In Table 4.3.1.3 the P_{SOL} of the overheating events new steady states is shown.

Overheating	+20 MW	+40 MW	+60 MW	+ 80 MW
Plasma termination	stabilized	stabilized	stabilized	stabilized
New steady state P_{SOL} [MW]	120.71	137.46	152.62	166.68

Table 4.3.1.3. *Summary of pure overheating results*

As can be seen, the higher the external heating the higher the scrape-off power, which means that an overheating event can damage the divertor.

Finally, it has been studied the pure confinement time improvement events. In Table 4.3.1.4 a summary of the results obtained is shown.

Confinement time multiplication factor	1.05	1.25	1.50	> 1.50
Plasma termination	stabilized	stabilized	stabilized	β
New steady state P_{FUS} [MW]	576.21	938.43	1526.69	-
New steady state P_{SOL} [MW]	106.70	139.20	167.38	-

Table 4.3.1.4. *Summary of pure confinement time improvement results*

It is observed that increasing the multiplication factor of the confinement time the fusion power and the scrape-off power of the new steady states increases too, up to a multiplication factor of 1.50 from which the transients do not achieve a new equilibrium state, but cross the beta limit to end in disruption. Therefore it can be concluded that for this type of event, the most critical new steady state corresponds to a multiplication factor of 1.50. The transient that cross the beta limit are also dangerous because they reach very high powers, both fusion as scarpe-off, before ending in disruption.

The study of the pure confinement time improvement has also been complemented by parametric sweeps, the results are shown in Figure 4.3.1.7 and Figure 4.3.1.8.

[11] ITER: *ITER Physics Guidelines*. July 2013, pg. 98.

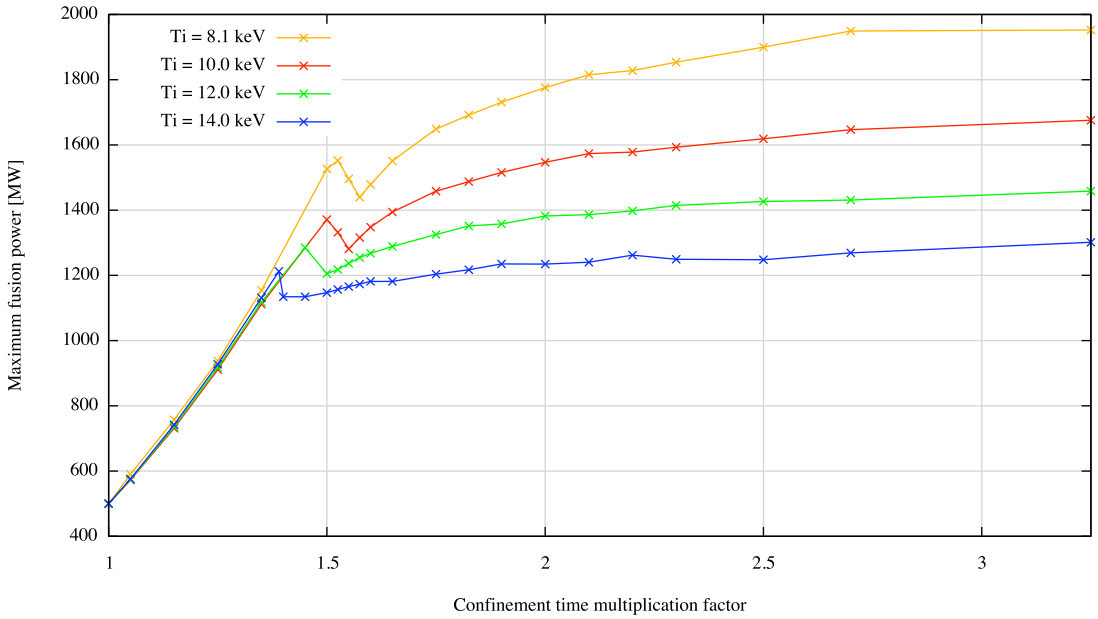

Figure 4.3.1.7. *Maximum fusion power in case of increase of confinement time for different initial T_i*

In Figure 4.3.1.7 different initial ion temperatures are scanned in order to find maximum achievable fusion power. As can be seen, for any improvement of confinement time low Ti produce higher fusion power. The discontinuity in the derivative of the parametric sweep lines determines the point from which the transients do not get a new steady state. In case of high ion temperature, beta limit terminations can be observed with lower multiplication factors. Also, for high confinement time multiplication factors, plasma experiences fast terminations by beta limit. In Table 4.3.1.5 the most critical cases for different initial T_i are shown.

	T_i = 8.1 keV	T_i = 10.0 keV	T_i = 12.0 keV	T_i = 14.0 keV
Plasma termination	β	β	β	β
External power [MW]	52.26	67.30	101.72	145.99
Fuel injection [$\cdot 10^{19}$ / m^3/s]	1.3956	2.1109	3.4661	5.1380
Higher maximum fusion power [MW]	1952.32	1675.61	1458.38	1301.54
Fuelling rate multiplication factor	3.25	3.25	3.25	3.25

Table 4.3.1.5. *Most critical cases of confinement time improvement for different initial T_i*

Figure 4.3.1.8 shows the maximum fusion power as function of confinement time improvement in different simulation scenarios. Scenarios with higher initial P_{FUS} bring higher final fusion power. Plasma collapses by beta limit. Table 4.3.1.6 shows those values.

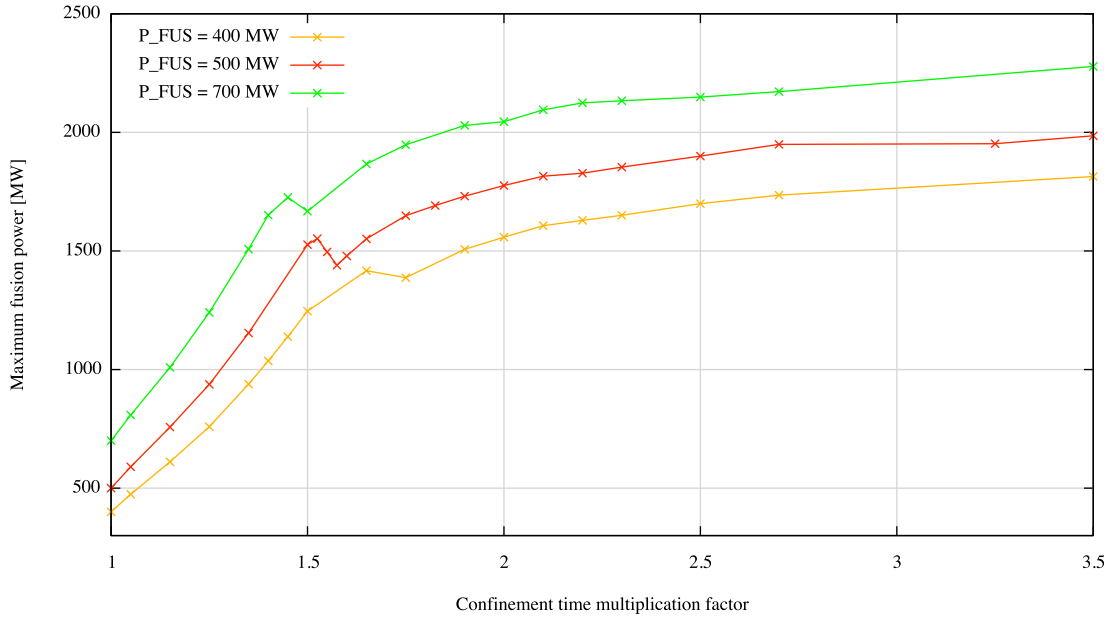

Figure 4.3.1.8. *Maximum fusion power in case of increase of confinement time for different initial* P_{FUS}

	P_{FUS} = 400 MW	P_{FUS} = 500 MW	P_{FUS} = 700 MW
Plasma termination	β	β	β
Higher maximum fusion power [MW]	1813.93	1985.73	2277.86
Fuelling rate multiplication factor	3.5	3.5	3.5

Table 4.3.1.6. *Most critical cases of confinement time improvement for different initial* P_{FUS}

- **Combination of overfuelling and overheating perturbations**

Once studied the pure overheating and the pure overfuelling, different combinations of the two perturbations have been explored. In Figure 4.3.1.9 the results of this case are shown.

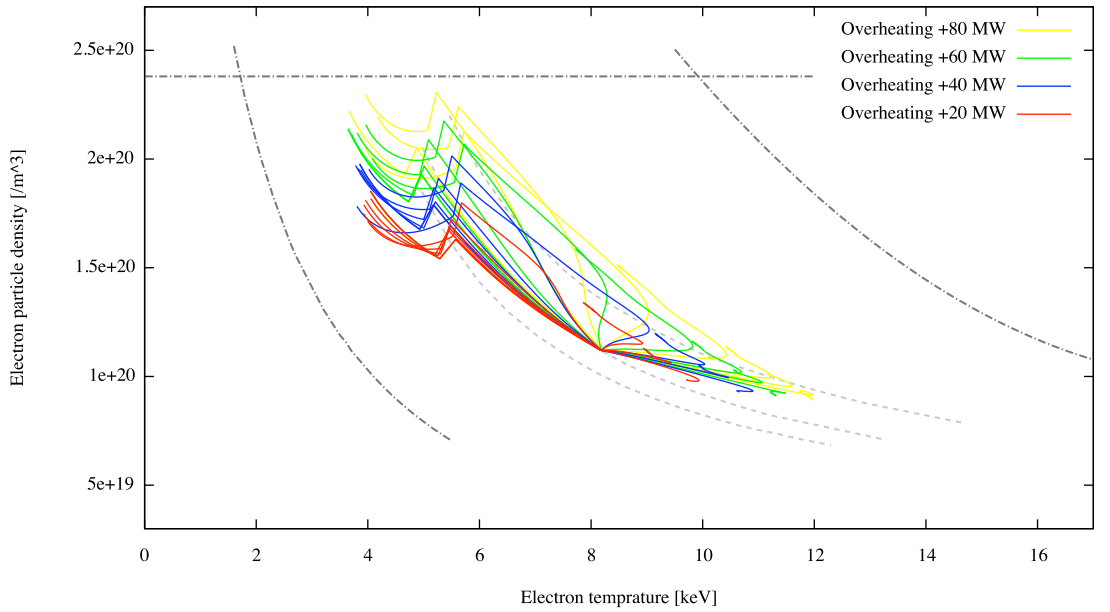

Figure 4.3.1.9. *Combination of overheating and overfuelling perturbations,* T_i *= 8.1 keV,* P_{FUS} *= 500 MW*

In Figure 4.3.1.8 have been considered four overheatings (+20 MW, +40 MW, +60 MW and +80 MW) and each of them have been combined with different values of the fuelling rate multiplication factor between 1.05 and 5. It can be seen that increasing the overheating the transients move to the left. And therefore, the steady states with the highest fusion and scrape-off powers correspond to the largest overheating. So it will focus on the study of the case of higher possible overheating, that is, the case of +80 MW.

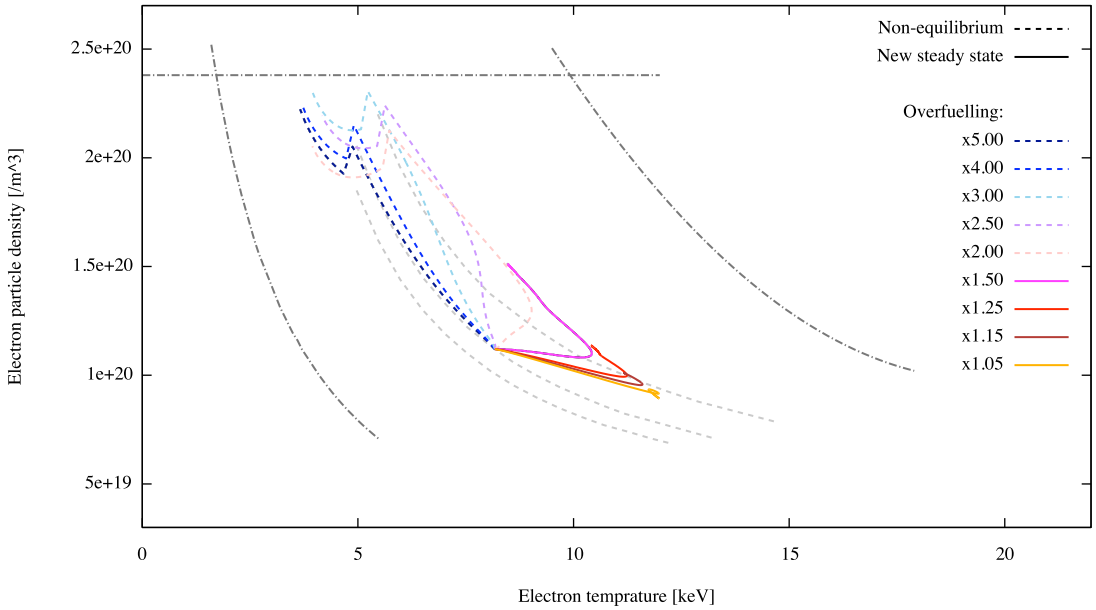

***Figure 4.3.1.10**. Combination of an overheating of +80 MW and different overfuellings between 1.05 and 5, T_i = 8.1 keV, P_{FUS} = 500 MW*

Figure 4.3.1.10 shows that for an overheating of +80 MW new steady states are achieved for fuelling rates multiplication factor between 1.05 and 1.5. In Figure 4.3.1.7 a summary of results is shown.

Fuelling rate multiplication factor	1.05	1.15	1.25	1.50	> 1.50
Plasma termination	stabilized	stabilized	stabilized	stabilized	$P_{SOL} \leq 0$
New steady state P_{FUS} [MW]	475.57	543.83	614.32	789.28	-
New steady state P_{SOL} [MW]	168.63	170.71	171.05	160.99	-

***Table 4.3.1.7.** Summary of obtained results for a combination of +80 MW of overheating and overfuelling*

It can be concluded that for these type of combination of perturbations, the most dangerous event to the blanket corresponds to a multiplication factor of 1.5, at which a new steady state of 789.28 MW of fusion power is achieved. While the most critical case for divertor corresponds to a multiplication factor of the fuelling rate of 1.25, with which a P_{SOL} of 171.05 is achieved. For fuelling rates multiplication factors up to 1.5 the transients end in plasma collapse by P_{SOL} after crossing the H-L limit.

Until now, the cases in which the two perturbations happen simultaneously have been studied, but can also be the case that these are consecutives, ie, one after the other. The behaviour of the plasma if there is first an increase of the external heating and after getting a new steady state it is introduced an overfuelling is shown in the Figure 4.3.1.11. In Table 4.3.1.8 a comparison between the results obtained with simultaneous perturbations and those obtained in the case in which are consecutive is shown.

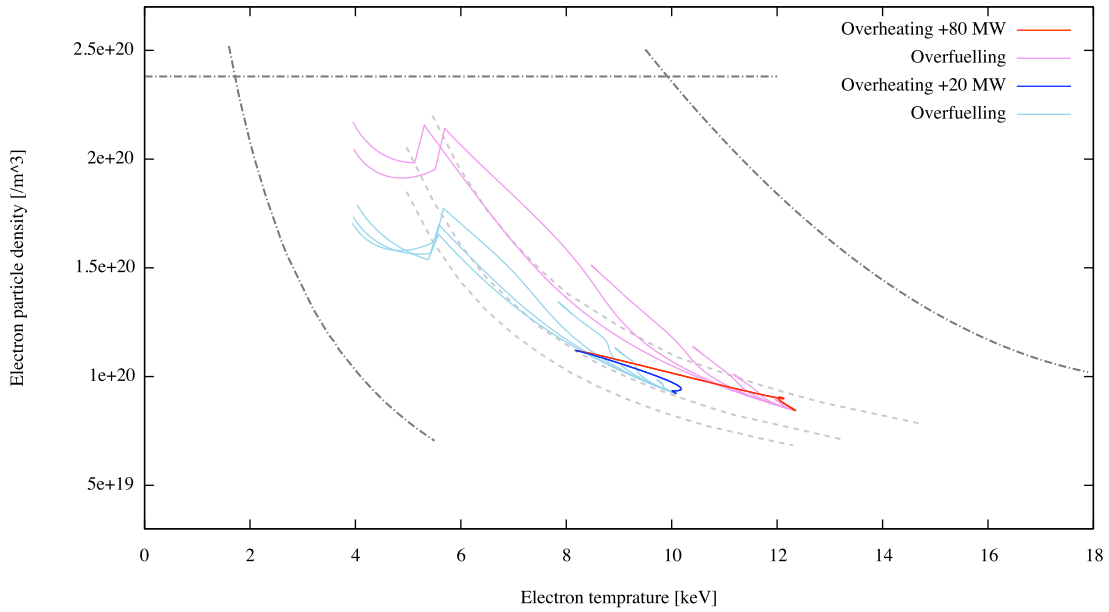

***Figure 4.3.1.11**. Consecutive perturbations: overheating followed by overfuelling, T_i = 8.1 keV, P_{FUS} = 500 MW*

Fuelling rate multiplication factor	1.05	1.15	1.25	1.50	> 1.50
Plasma termination	stabilized	stabilized	stabilized	stabilized	$P_{SOL} \leq 0$
Final fusion power [MW] **Simultaneous perturbations**	475.57	543.83	614.32	789.28	-
Final fusion power [MW] **Consecutive perturbations**	476.47	544.47	614.74	789.30	-

***Table 4.3.1.8.** Simultaneous perturbations vs. consecutive perturbations (overheating +80 MW)*

It is observed that the behaviour of the plasma facing simultaneous or consecutive perturbations is very similar.

Other cases in which the overfuelling is introduced at different times of the transient caused by the external heating increase have been studied, and there has not been any situation that can be considered more harmful than previously studied in this section.

- **Combination of overheating and confinement time perturbations**

In Figure 4.3.1.12 and Table 4.3.1.9 the results obtained by combining an overheating and an improvement of the confinement time are shown.

Four different overheatings (+20 MW, +40 MW, +60 MW and +80 MW) have been studied, each of them have been combined with various values of the confinement time multiplication factor between 1.05 and 3.

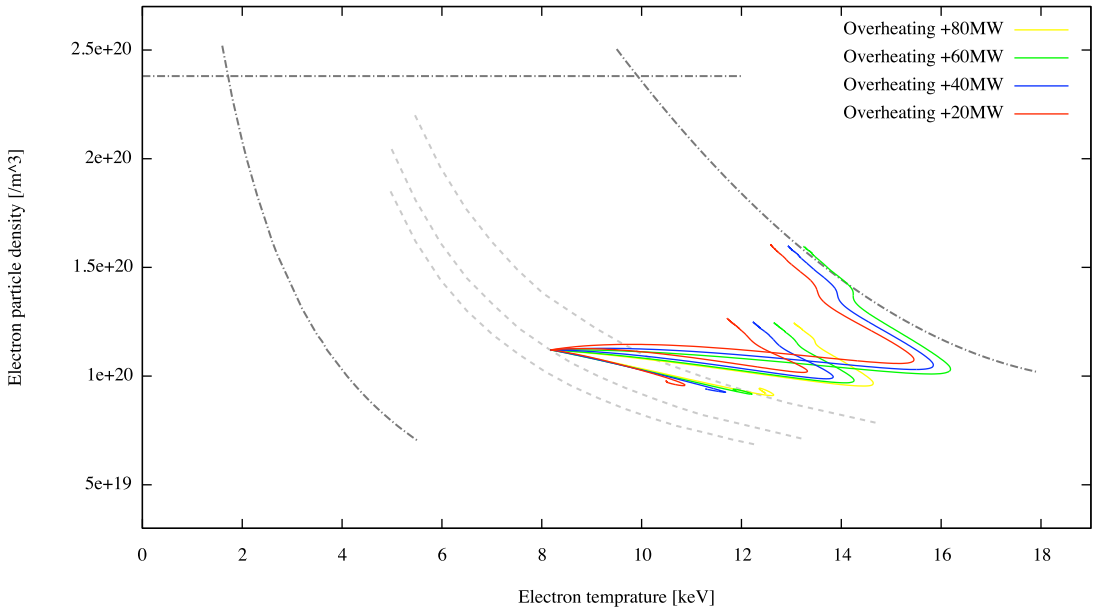

Figure 4.3.1.12. *Combination of overheating and improvement confinement time perturbations, T_i = 8.1 keV, P_{FUS} = 500 MW*

Overheating +20 MW				
Confinement time multiplication factor	1.05	1.25	1.45	> 1.45
Plasma termination	stabilized	stabilized	stabilized	β
New steady state P_{FUS} [MW]	549.28	912.40	1368.22	-
New steady state P_{SOL} [MW]	127.56	153.07	174.02	-

Overheating + 40 MW				
Confinement time multiplication factor	1.05	1.25	1.45	> 1.45
Plasma termination	stabilized	stabilized	stabilized	β
New steady state P_{FUS} [MW]	537.77	897.32	1351.97	-
New steady state P_{SOL} [MW]	143.04	165.21	183.25	-

Overheating + 60 MW				
Confinement time multiplication factor	1.05	1.25	1.45	> 1.45
Plasma termination	stabilized	stabilized	stabilized	β
New steady state P_{FUS} [MW]	529.33	885.27	1335.88	-
New steady state P_{SOL} [MW]	157.34	176.57	192.47	-

Overheating + 80 MW				
Confinement time multiplication factor	1.05	1.25	1.40	> 1.40
Plasma termination	stabilized	stabilized	stabilized	β
New steady state P_{FUS} [MW]	516.74	870.76	1198.79	-
New steady state P_{SOL} [MW]	171.04	187.68	198.38	-

Table 4.3.1.9. *Summary of obtained results for a combination of overheating and improvement of the confinement time*

This is a good example to illustrate the differet behavior between fusion power and scrape-off power. While lower overheatings achieve new steady states with a higher fusion power, higher overheatings gets higher scrape-off powers. This means that lower overheatings are most critical to blanket, and the higher ones are more damaging to the divertor.

However, there do not exist big differences by varying the external power, that is, for a same value of the confinement time multiplication factor the obtained results for the different overheatings are close.

By increasing the confinement time multiplication factor the new steady states moves to the top right side of the operation window of the plasma, up to a multiplication factor from which transients cross the beta limit to end in disruption. Those transients, despite they get the disruption soon, reach even higher fusion and scrape-off powers.

In these cases of combination the behaviour of the plasma is quite similar to the pure confinement time improvement studied in one of the previous sections (see Figure 4.3.1.4). Furthermore, in the case of combined perturbations transients cross before the beta limit, that is, for lower confinement time multiplication factors.

However, the pure improvement of confinement time is more critical to the blanket than the combination with an overheating, since in the pure perturbation event a new steady state is achieved with a fusion power of 1526.69 MW for a multiplication factor of the confinement time of 1.5 (see Table 4.3.1.4). But scrape-off powers are higher in case of combined overheating and improvement of confinement time, in particular, the most critical case correspond to an overheating of +80 MW and a confinement time multiplication factor of 1.45, in which the scrape-off power achieved for the new steady state is 198.38 MW.

Next, a study of consecutive perturbations is done. The plasma behaviour assuming a failure in the external heating system in first place, which would cause an overheating event, and secondly, once reached a new steady state, an improvement of the confinement time of the plasma is shown in Figure 4.3.1.13. In Figure 4.3.1.14 the same situation is shown, but exchanging the perturbations

order, ie, first occurs the confinement time improvement and after reaching equilibrium an overheating is introduced.

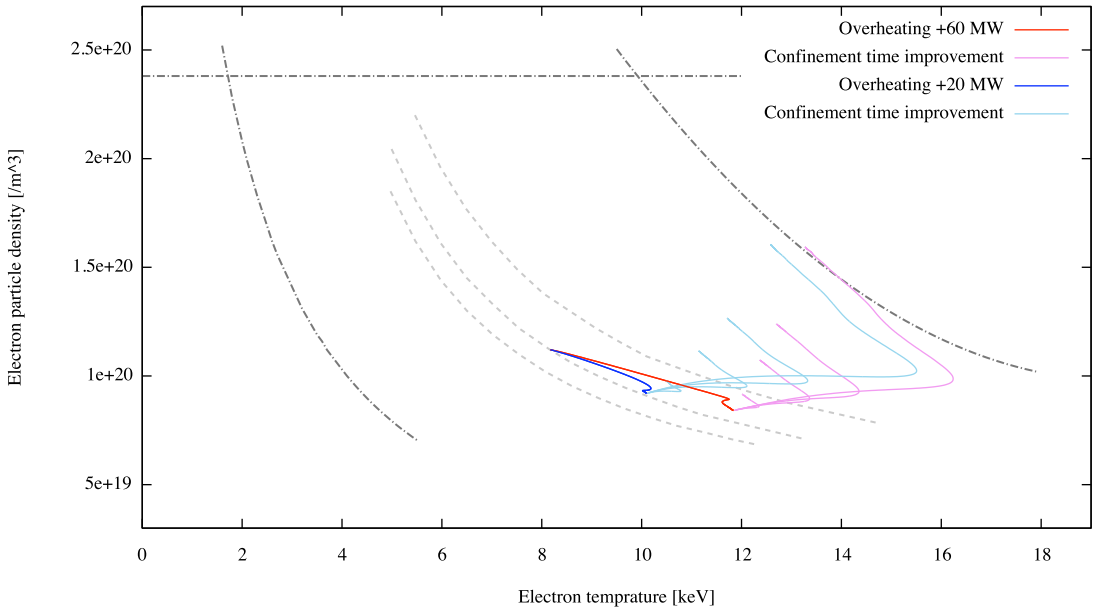

Figure 4.3.1.13. *Consecutive perturbation: overheating followed by confinement time improvement, T_i = 8.1 keV, P_{FUS} = 500 MW*

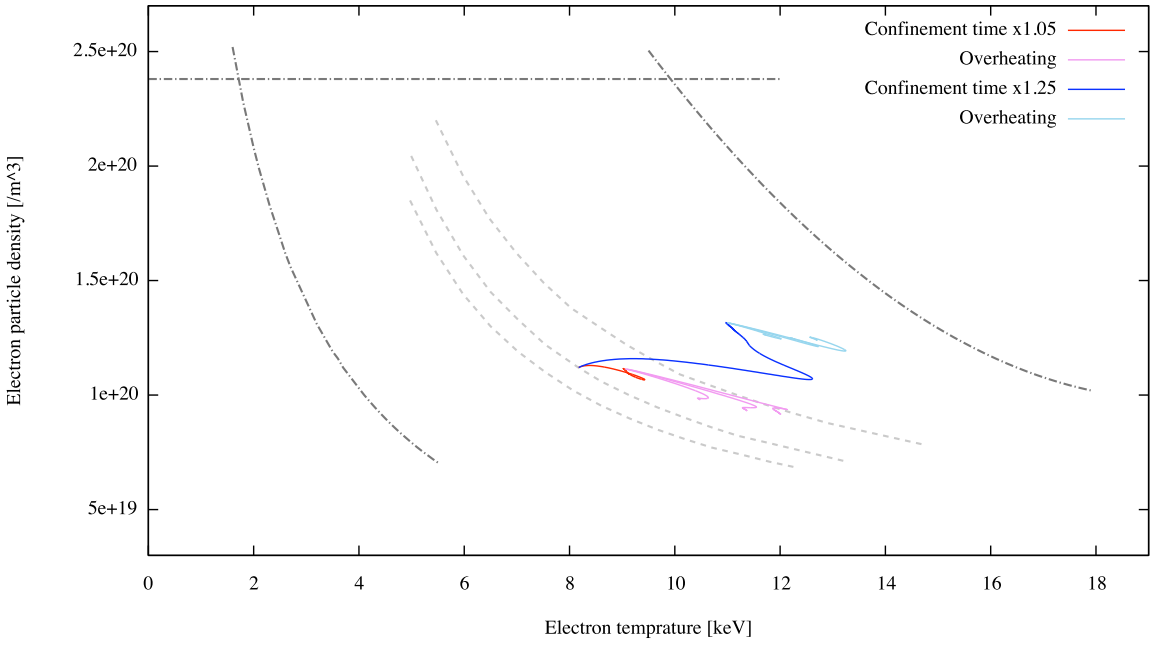

Figure 4.3.1.14. *Consecutive perturbation: confinement time improvement followed by overheating, T_i = 8.1 keV, P_{FUS} = 500 MW*

The fusion powers of the new steady states achieved in each case for the particular case of an overheating of +20 MW are shown in Table 4.3.1.10.

As can be observed, the results of the simultaneous and the two types of consecutive events are quite similar.

Simultaneous perturbations				
Confinement time multiplication factor	1.05	1.25	1.45	> 1.45
Plasma termination	stabilized	stabilized	stabilized	β
New steady state P_{FUS} [MW]	549.28	912.40	1368.22	-
New steady state P_{SOL} [MW]	127.56	153.07	174.02	-

Consecutive perturbations Overheating followed by confinement time improvement				
Confinement time multiplication factor	1.05	1.25	1.45	> 1.45
Plasma termination	stabilized	stabilized	stabilized	β
New steady state P_{FUS} [MW]	549.28	912.40	1368.01	-
New steady state P_{SOL} [MW]	127.56	153.07	173.99	

Consecutive perturbations Confinement time improvement followed by overheating				
Confinement time multiplication factor	1.05	1.25	1.45	> 1.45
Plasma termination	stabilized	stabilized	stabilized	β
New steady state P_{FUS} [MW]	549.28	912.40	1370.76	-
New steady state P_{SOL} [MW]	127.56	153.07	174.06	

Table 4.3.1.10. *Simultaneous perturbations vs. consecutive perturbations (overheating +20 MW)*

- **Combination of overfuelling and confinement time perturbations**

In Figure 4.3.1.15 and Table 4.3.1.11 the results of combining improvement of confinement time and overfuelling perturbations are shown.

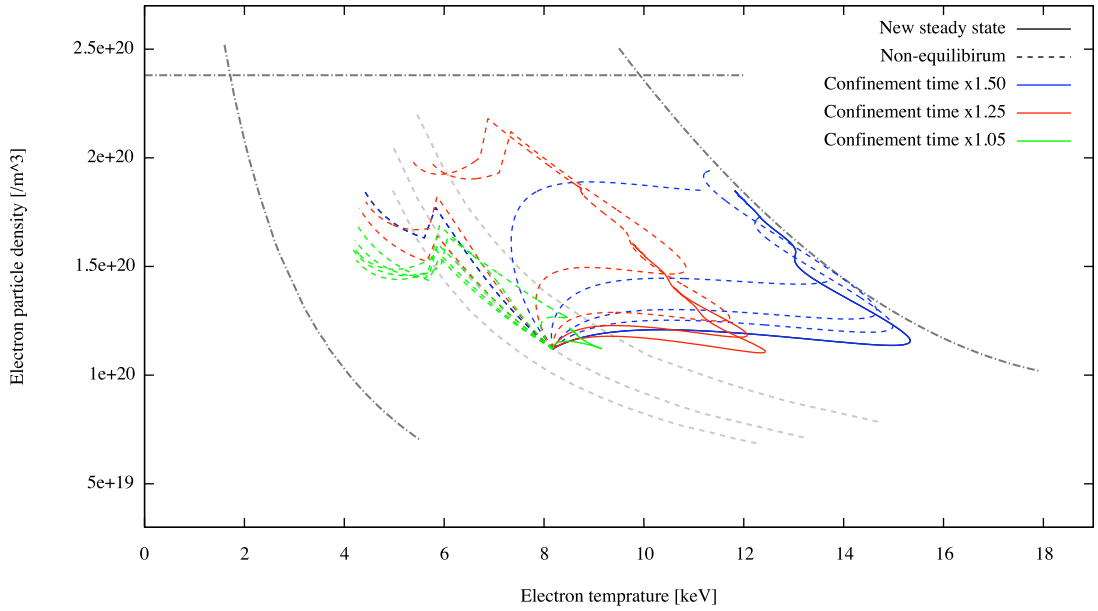

Figure 4.3.1.15. *Combination of improvement confinement time and overfuelling perturbations, T_i = 8.1 keV, P_{FUS} = 500 MW*

Confinement time x1.05		
Fuelling rate multiplication factor (f_s)	1.05	> 1.05
Plasma termination	stabilized	$P_{SOL} \leq 0$
New steady state P_{FUS} [MW]	614.22	-
New steady state P_{SOL} [MW]	105.36	-

Confinement time x1.25			
Fuelling rate multiplication factor	1.05	1.15	> 1.15
Plasma termination	stabilized	stabilized	$P_{SOL} \leq 0$
New steady state P_{FUS} [MW]	1003.80	1141.07	-
New steady state P_{SOL} [MW]	140.93	141.40	-

Confinement time x1.50			
Fuelling rate multiplication factor (f_s)	1.05	$1.05 < f_s < 2.50$	≥ 2.50
Plasma termination	stabilized	β	$P_{SOL} \leq 0$
New steady state P_{FUS} [MW]	1640.76	-	-
New steady state P_{SOL} [MW]	168.77	-	-

Confinement time x1.75			
Fuelling rate multiplication factor (f_s)	$1.05 \leq fs < 2.5$	2.50	> 2.50
Plasma termination	β	Greenwald	$P_{SOL} \leq 0$

Table 4.3.1.11. *Summary of obtained results for a combination of overfuelling and improvement of the confinement time*

Four values of the multiplication factor of the confinement time have been studied: 1.05, 1.25, 1.50 and 1.75, each of them has been combined with different values of the fuelling rate multiplication factor between 1.05 and 3.

As indicated in Table 4.3.1.10, the most critical new steady state is given for a multiplication factor of the confinement time of 1.5 and a fuelling rate multiplication factor of 1.05. Those transients that cross the beta limit, despite they get the disruption soon, reach even higher fusion and scrape-off powers.

As in the previous sections, it has also made a study of consecutive perturbations of confinement time and overfuelling. The behaviour of the plasma in case of an improvement of the confinement time followed by an overfuelling once the equilibrium is get is shown in Figure 4.3.1.16. And in Table 4.3.1.11 a comparison between the results of the simultaneous events and the consecutive events is done.

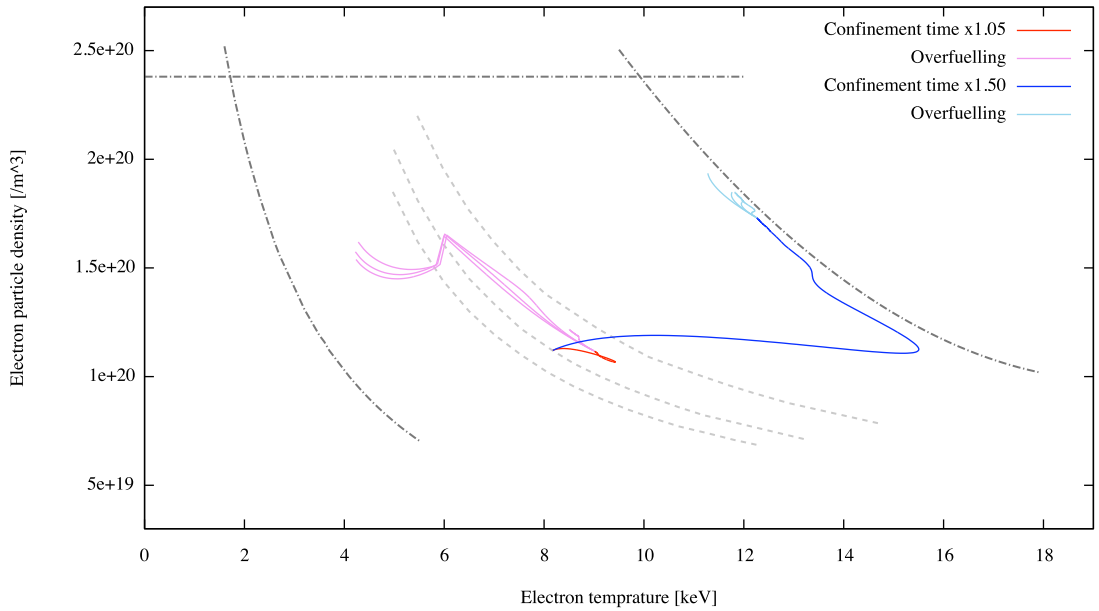

Figure 4.3.1.16. *Consecutive perturbations: improvement of the confinement time followed by overfuelling, T_i = 8.1 keV, P_{FUS} = 500 MW*

Simultaneous perturbations			
Fuelling rate multiplication factor (f_s)	1.05	1.05 < f_s <2.50	≥ 2.50
Plasma termination	stabilized	β	$P_{SOL} \leq 0$
New steady state P_{FUS} [MW]	1640.76	-	-
New steady state P_{SOL} [MW]	168.77	-	-

Consecutive perturbations		
Fuelling rate multiplication factor (f_s)	1.05	≥ 1.05
Plasma termination	stabilized	β
New steady state P_{FUS} [MW]	1640.35	-
New steady state P_{SOL} [MW]	168.77	-

Table 4.3.1.12. *Simultaneous perturbations vs. consecutive perturbations (particular case of a confinement time multiplication factor of 1.5)*

As can be seen in Table 4.3.1.12 the fusion power of the new steady state achieved with consecutive perturbation is quite similar to the simultaneous ones. In the same manner as in the previous sections in which it has not been observed significant difference in the comparison between simultaneous and consecutive events. However, a different plasma termination is observed.

Until now, there have only been studied those cases in which there was an increase in the fuel injection or in external heating. However, it may also be interesting to study cases where the external

heating or the fuelling is insufficient or even stop working altogether, as contemplated in the *Design Basis Accident Study*.[12]

Following, the situations in which an underfuelling or an underheating event occurs have been studied, both pure cases as combination with other types of perturbations.

- **Pure underheating and pure underfuelling**

First of all, the study of pure underfuelling and pure underheating is done. The results obtained have been plotted in Figure 4.3.1.17.

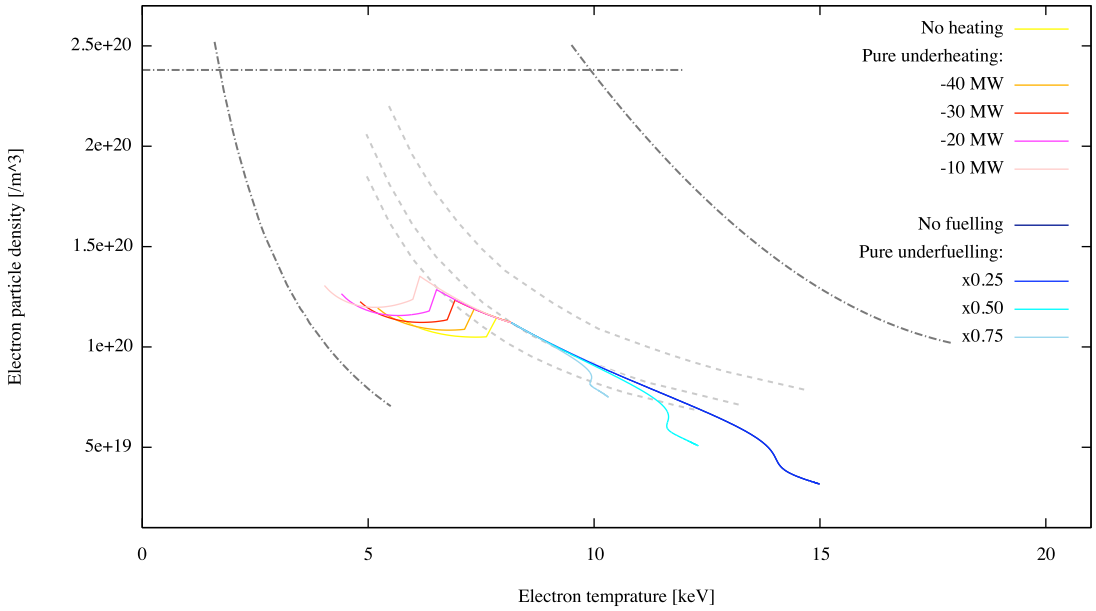

Figure 4.3.1.17. *Pure underheating and no heating and pure underfuelling and no fuelling, T_i = 8.1 keV, P_{FUS} = 500 MW*

As can be observed in Figure 4.3.1.17 in case of a pure underheating the transients move to the left of the operation window of the plasma, crossing the H-L transition limit and ending in disruption by plasma collapse (P_{SOL}<0).

The underfuelling events move the transients to new low fusion power steady states. However, the case in which there is no fuel injection the transient crosses the locked modes limit, it is recalled that for values $n_e \leq 2 \cdot 10^{19}$ m^{-3} there are instabilities susceptible to drive the plasma to a sudden disruption. They are very likely to appear during the low density phase required for H-mode access, although the might also be present in other transients. In Table 4.3.1.13 a summary of the obtained results for this type of events is done.

[12] N. TAYLOR: *Preliminary safety analysis of ITER Fusion Sci. Technol. 56*, 2009, pp. 573–580.

Fuelling rate multiplication factor (f_s)	0.00	0.25	0.50	0.75
Plasma termination	Locked modes	stabilized	stabilized	stabilized
New steady state P_{FUS} [MW]	-	89.66	206.40	344.15
New steady state P_{SOL} [MW]	-	54.73	74.35	90.78

Table 4.3.1.13. *Summary of pure underfuelling and pure underheating results*

- **Combination of underheating and overfuelling**

In Figure 4.3.1.18 the results of combining underheating and overfuelling are shown. Two values of underheating (-10 and -30 MW) and the no heating case have been studied; each of them has been combined with different values of the fuelling rate multiplication factor between 1.05 and 5.

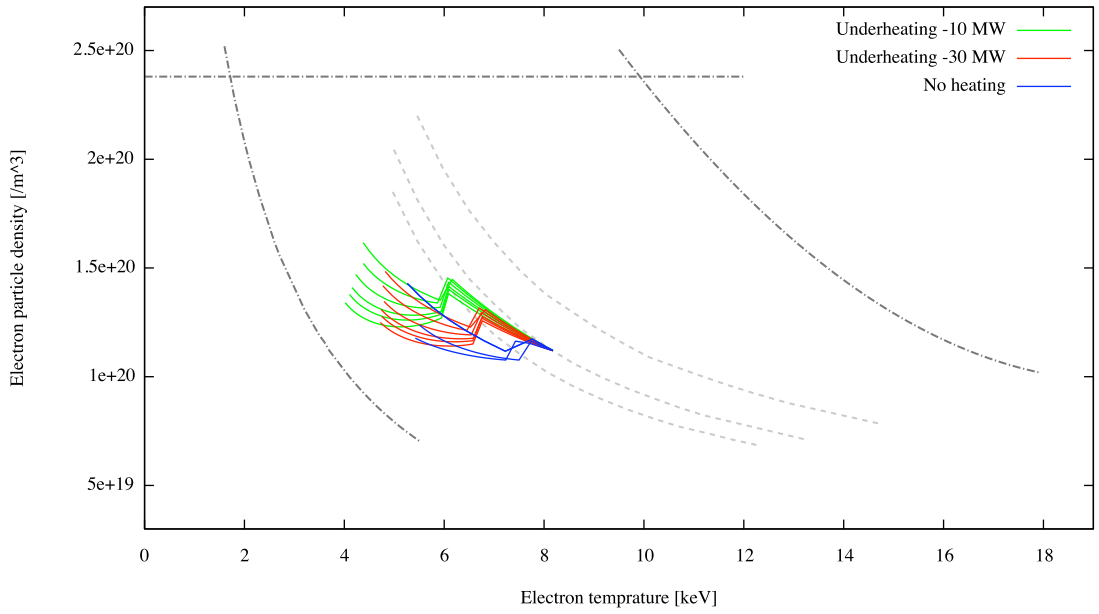

Figure 4.3.1.18. *Combination of underheating and overfuelling, T_i = 8.1 keV, P_{FUS} = 500 MW*

As can be observed in all the cases the transients move to the left and cross the H-L transition limit and end in disruption by plasma collapse by P_{SOL}.

- **Combination of underheating and improvement of the confinement time**

In this section those cases in which a failure in the heating system, which would provide a lower external heating than required, and an improvement of the confinement time coincide are studied.

In Figure 4.3.1.19 the behaviour of the plasma in front of this type of perturbations can be seen, it is the particular case of an underheating of -30 MW. In Table 4.3.1.14 a summary of the results obtained from the different combinations of underheating and confinement time perturbations is shown.

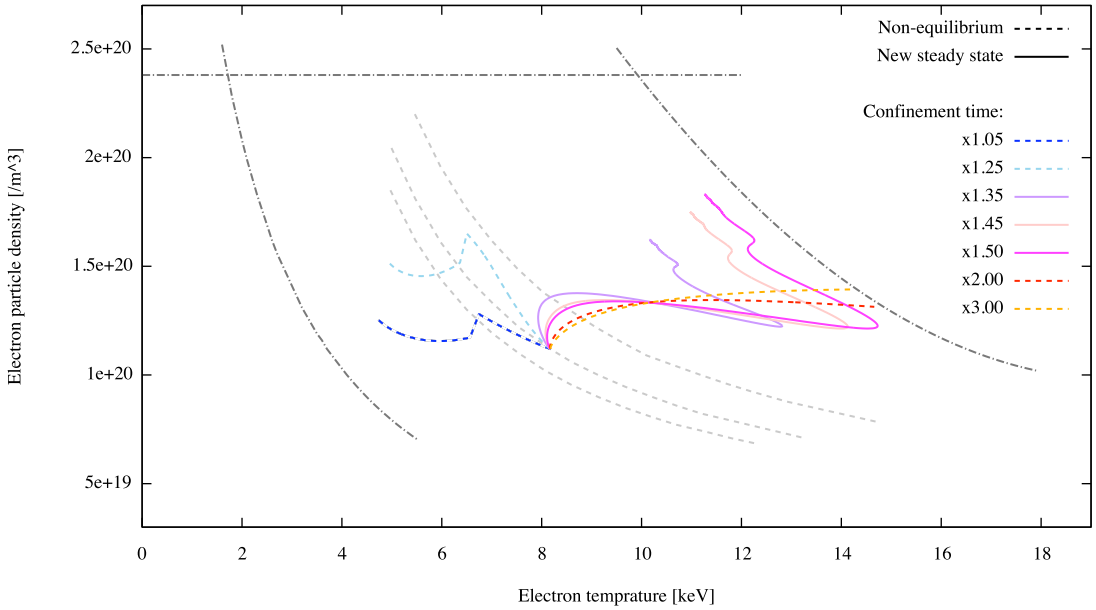

Figure 4.3.1.19. *Combination of an underheating of -30 MW and different confinement time perturbations, T_i = 8.1 keV, P_{FUS} = 500 MW*

Underheating -10 MW					
Confinement time multiplication factor	1< tau < 1.15	1.15	1.25	1.50	tau > 1.50
Plasma termination	$P_{SOL} \leq 0$	stabilized	stabilized	stabilized	β
New steady state P_{FUS} [MW]	-	762.49	953.68	1543.17	-
New steady state P_{SOL} [MW]	-	113.42	131.95	161.72	-

Underheating -30 MW					
Confinement time multiplication factor	1< tau < 1.35	1.35	1.45	1.50	tau > 1.50
Plasma termination	$P_{SOL} \leq 0$	stabilized	stabilized	stabilized	β
New steady state P_{FUS} [MW]	-	1217.28	1457.01	1586.88	-
New steady state P_{SOL} [MW]	-	128.00	142.62	148.43	-

Underheating -40 MW			
Confinement time multiplication factor	1< tau < 1.50	1.50	tau > 1.50
Plasma termination	$P_{SOL} \leq 0$	stabilized	β
New steady state P_{FUS} [MW]	-	1619.36	-
New steady state P_{SOL} [MW]	-	139.52	-

No heating		
Confinement time multiplication factor	1< tau < 1.50	tau > 1.50
Plasma termination	$P_{SOL} \leq 0$	β

Table 4.3.1.14. *Obtained results of combining underheating and confinement time perturbations*

As can be seen for each value of undeheating exists a range of values of the confinement time multiplication factor for which new steady states are achieved. For this type of perturbation combination, the higher the underheating the higher fusion power achieved by the new steady states.

While the highest scrape-off powers are achieved for lower underheating. For the case of no heating new equilibrium is not obtained.

- **Combination of underfuelling and improvement of the confinement time**

In Figure 4.3.1.20 the behaviour of the plasma in front of a combination of underfuelling and improvement of the confinement time can be seen. In Table 4.3.1.14 a summary of the results obtained is shown.

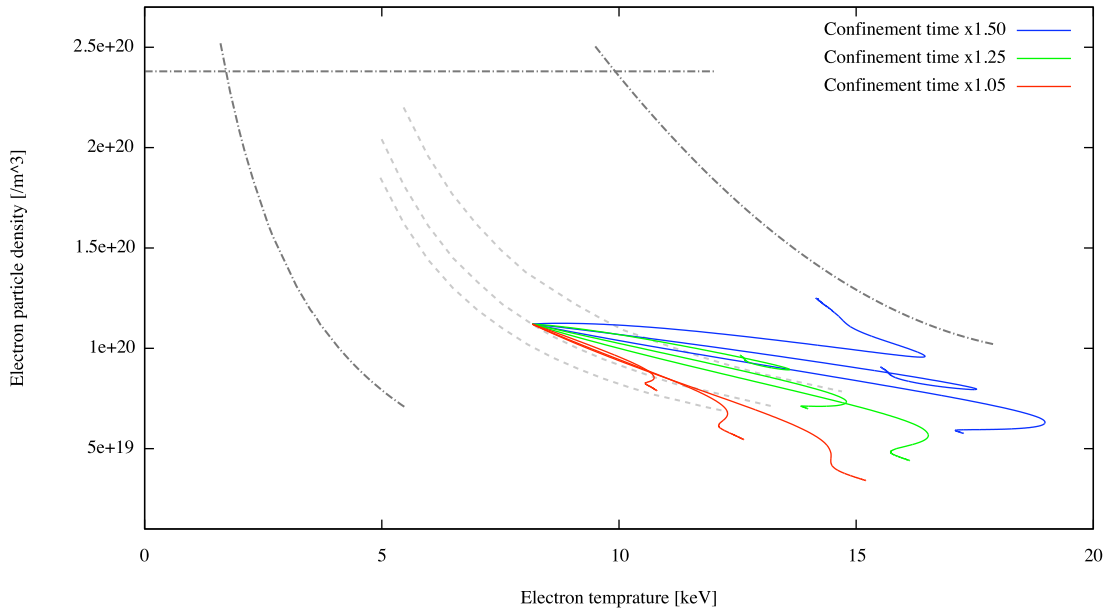

Figure 4.3.1.20. *Combination of underfuelling and confinement time improvement, T_i = 8.1 keV, P_{FUS} = 500 MW*

Confinement time multiplication factor		1.05	1.25	1.50	> 1.50
Plasma termination		stabilized	stabilized	stabilized	β
Underfuelling x0.25	New steady state P_{FUS} [MW]	103.33	168.58	272.34	-
	New steady state P_{SOL} [MW]	55.71	60.17	66.23	-
Undefuelling x0.50	New steady state P_{FUS} [MW]	238.62	389.12	621.06	-
	New steady state P_{SOL} [MW]	77.67	91.72	108.89	-
Underfuelling x0.75	New steady state P_{FUS} [MW]	396.47	639.96	1023.25	-
	New steady state P_{SOL} [MW]	96.55	120.08	146.03	-

Table 4.3.1.14. *Summary of obtained results of combining undefuelling and confinement time perturbations*

As can be seen, for values of underfuelling closer to the unity the new steady states achieved have a higher fusion and scrape-off power. Also, the higher the confinement time multiplication factor the

higher the fusion and scrape-off powers of the equilibrium. However, for values above 1.5 the transients do not get a new equilibrium.

- **Combination of underfuelling and overheating**

In Figure 4.3.1.21 the behaviour of the plasma in front of a combination of underfuelling and overheating can be seen. In Table 4.3.1.15 a summary of the results obtained is shown.

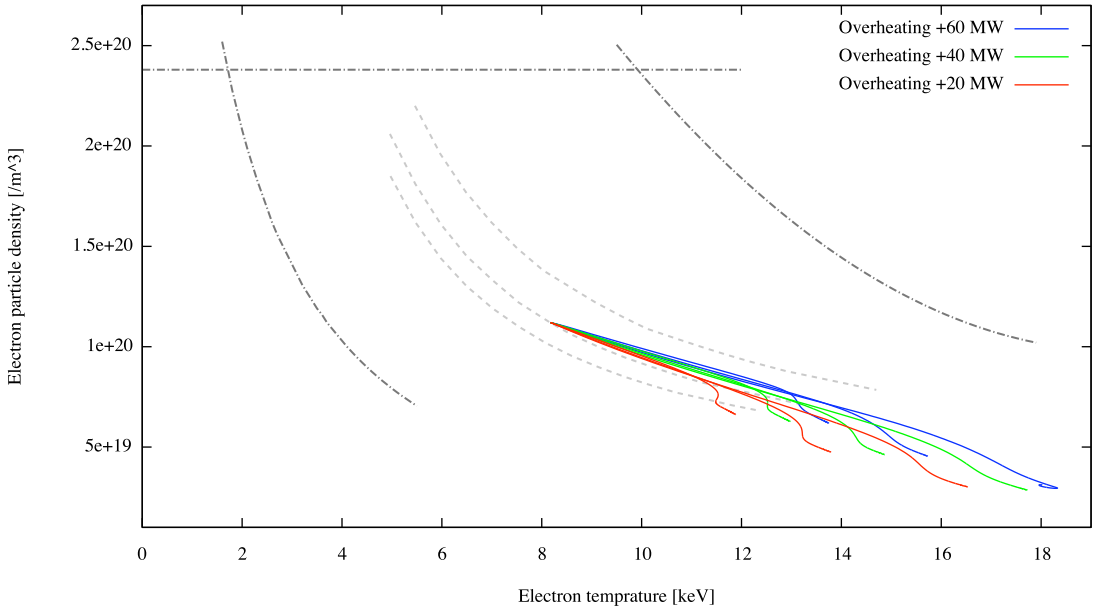

Figure 4.3.1.21. *Combination of underfuelling and overheating, T_i = 8.1 keV, P_{FUS} = 500 MW*

Fuelling rate multiplication factor		0.25	0.50	0.75	> 1.50
Plasma termination		stabilized	stabilized	stabilized	$P_{SOL} < 0$
Overheating +20 MW	New steady state P_{FUS} [MW]	80.31	194.49	322.88	-
	New steady state P_{SOL} [MW]	70.16	89.65	107.81	-
Overheating + 40 MW	New steady state P_{FUS} [MW]	70.35	185.73	309.71	-
	New steady state P_{SOL} [MW]	86.27	105.04	123.40	-
Overheating + 60 MW	New steady state P_{FUS} [MW]	66.69	177.33	301.67	-
	New steady state P_{SOL} [MW]	102.10	120.69	138.58	-

Table 4.3.1.15. *Summary of obtained results of combining undefuelling and overheating*

As can be seen, for values of underfuelling closer to the unity the new steady states achieved have a higher fusion and scrape-off power. Also, the higher the overheating the lower the fusion power achieved by the new equilibrium but the higher the scrape-off power, and the higher the fuelling rate multiplication factor the higher the fusion and the scrape-off power. However, for values above 1.5 the transients do not get a new equilibrium.

After the study of plasma behaviour in response to various types of perturbations the following cases have been selected for doing a complete analysis of the wall thermal equilibrium, to detect possible risks for the wall integrity (melting) during the transient:

- sudden increase of fuelling rate by factor 1.05, Ti = 8.1 keV, P_{FUS} = 500 MW;
- sudden energy confinement time improvement by factor 1.5, Ti = 8.1 keV, P_{FUS} = 500 MW;
- sudden increase of external heating up to 130 MW, Ti = 8.1 keV, P_{FUS} = 500 MW;
- fuelling and external heating cut-off, Ti = 8.1 keV, P_{FUS} = 500 MW;
- combination of an underheating of -40 MW and an increase of confinement time multiplication factor of 1.50;
- combination of sudden increase of external heating up to 110 MW and a fuelling rate multiplication factor of 0.75, Ti = 8.1 keV, P_{FUS} = 500 MW;

4.3.2 Sudden increase of fuelling rate

As can be observed in the Figure 4.3.1.4 of the previous section, assuming that there is a pure overfuelling event in the P_{FUS} = 500 MW and T_i = 8.1 keV scenario, all the plasma transients move to the left, crossing the limit of the H-L transition.

In order to show the behaviour of the plasma and the wall in case of a sudden increase of fuelling rate, a 1.05 multiplication factor has been applied to the standard fuelling rate of 500 MW normal operation scenario. This case has been selected because it is the overfuelling event that gets the highest fusion power during the transient in the 500 MW scenario. The results are shown in Figure 4.3.2.1.

The fuelling increase is introduced at second 0. Fusion power increase slightly up to 518.02 MW and then starts decreasing until the plasma collapses by P_{SOL} at 70.5 seconds. The confinement mode transition takes place after 66.7 seconds from the start of the perturbation.

Ion and electron temperatures decrease while their densities increase. The radiated power also increases. It can be observed that when the confinement mode transition takes place a sudden drop appears in densities and radiated power; this drop is caused by the bremsstrahlung losses and it does not has any consequence from the point of view of a safety analysis.

Beta parameter gives information about the pressure of the plasma, since it is the relation between plasma pressure and magnetic field pressure. For values below the beta limit plasma is confined, that is why beta parameter is considered a good indicator of the plasma confinement. In this case, it can be observed that at any time the beta limit is exceeded, so there is no beta limit disruption.

The evolution of the temperature and heat loads on the mid-high outer blanket and lower inner vertical target are shown in the Figure 4.3.2. These two regions has been chosen for this study because they are the ones that support the higher heat loads and temperatures throughout the wall, that is, the most stressed parts.

As can be seen, heat fluxes on blanket and divertor regions are not a big concern, they decrease in value over the transient, least at the end, where they suffer a peak and, as usual, highest loads are sustained by the lower vertical target.

Temperatures on first node of the tungsten PFC of lower inner VT decrease during the transient, however the temperature of the mid-high outer blanket increase reaching almost 480 ºC.

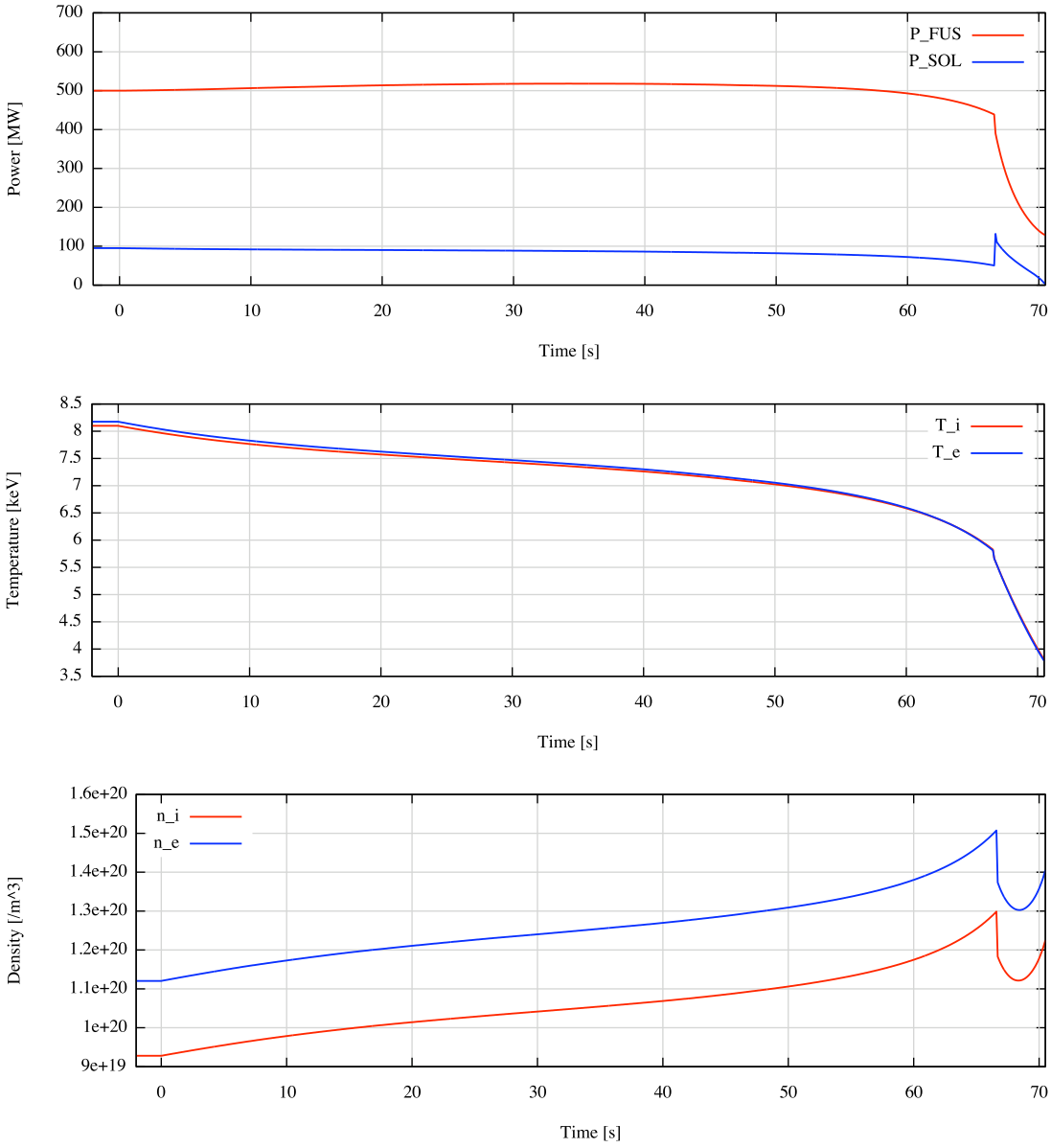

Figure 4.3.2.a. *Sudden increase of fuelling rate by factor 1.05, T_i = 8.1 keV, P_{FUS} = 500 MW*

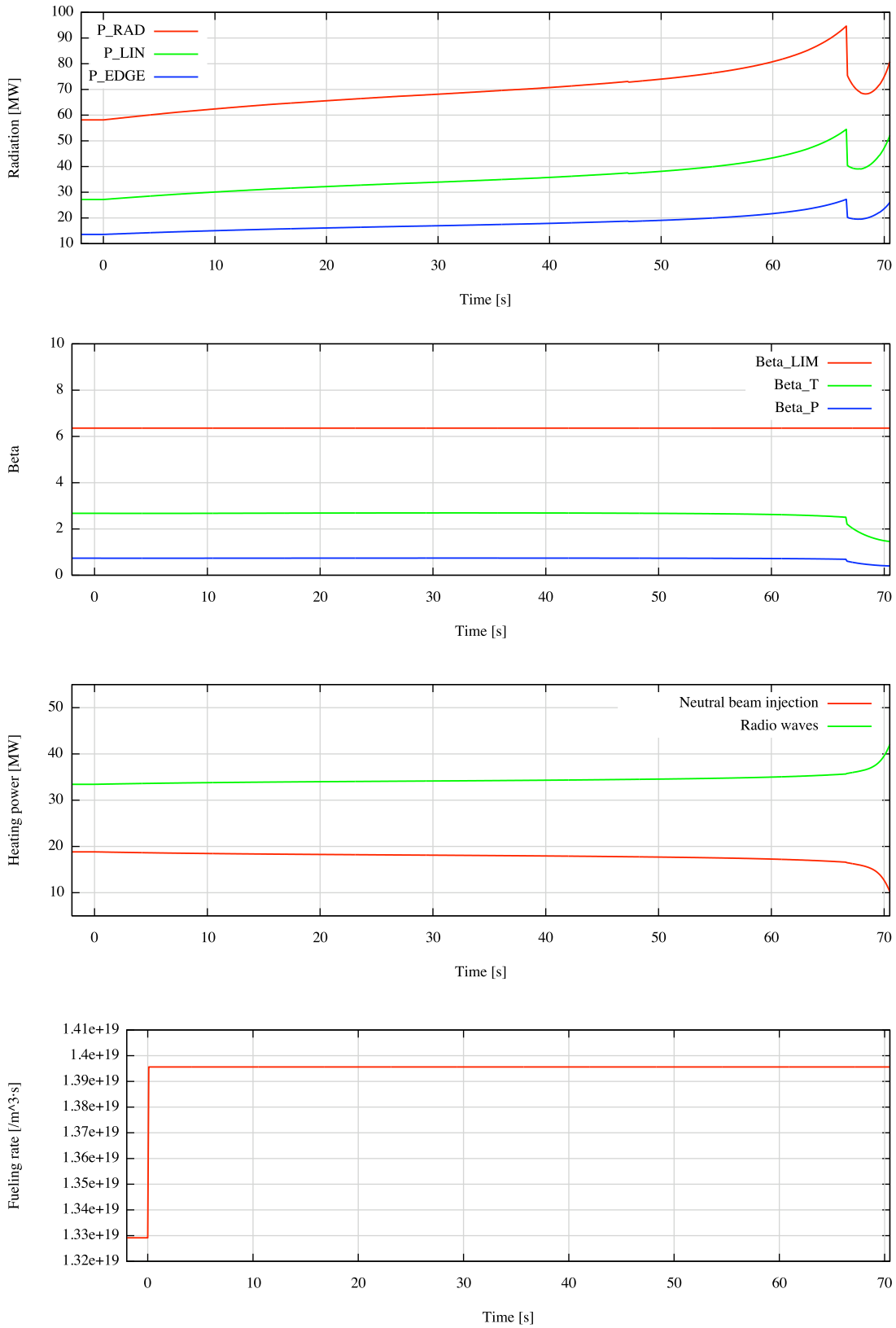

Figure 4.3.2.b. *Sudden increase of fuelling rate by factor 1.05, T_i = 8.1 keV, P_{FUS} = 500 MW*

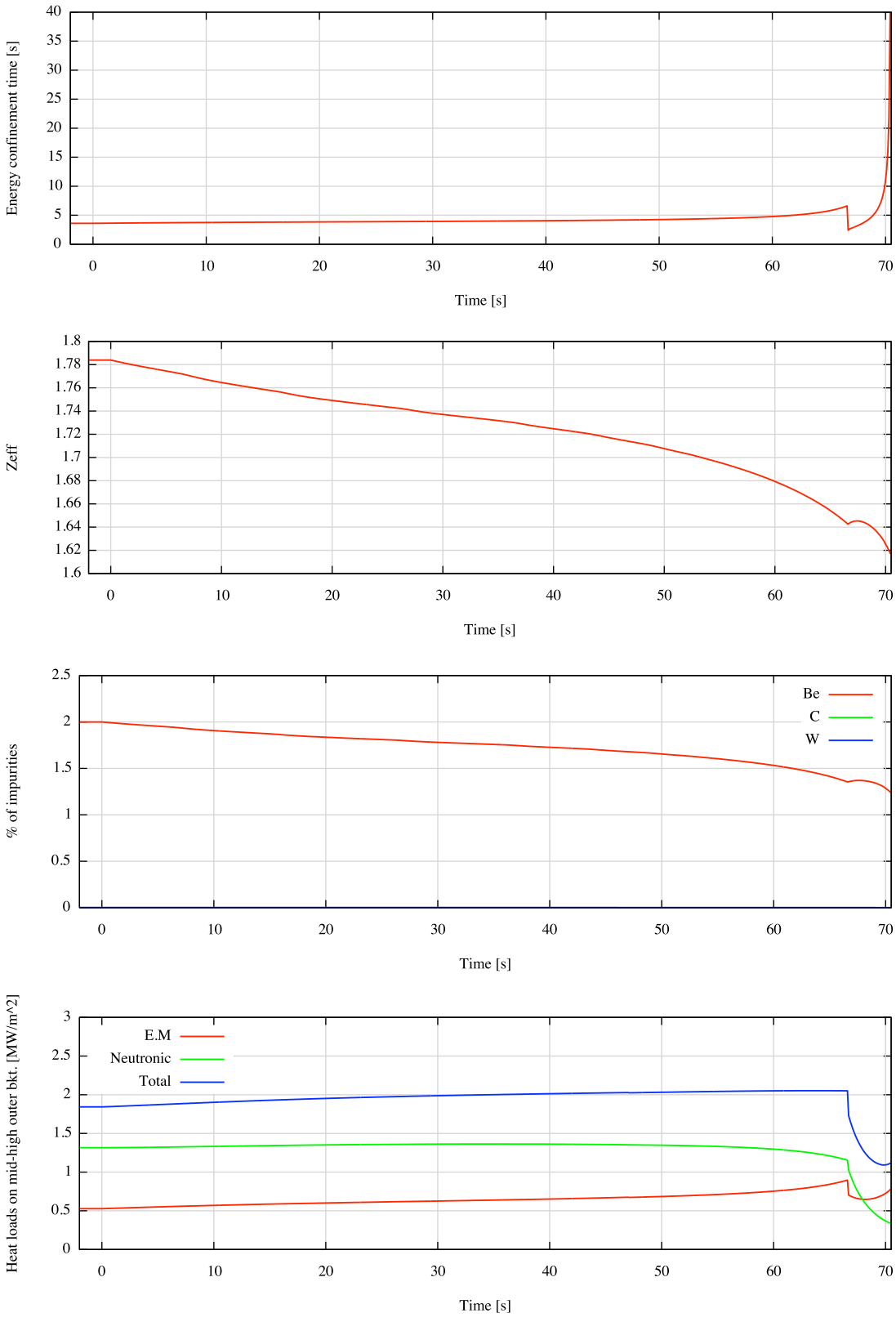

Figure 4.3.2.c. *Sudden increase of fuelling rate by factor 1.05, T_i = 8.1 keV, P_{FUS} = 500 MW*

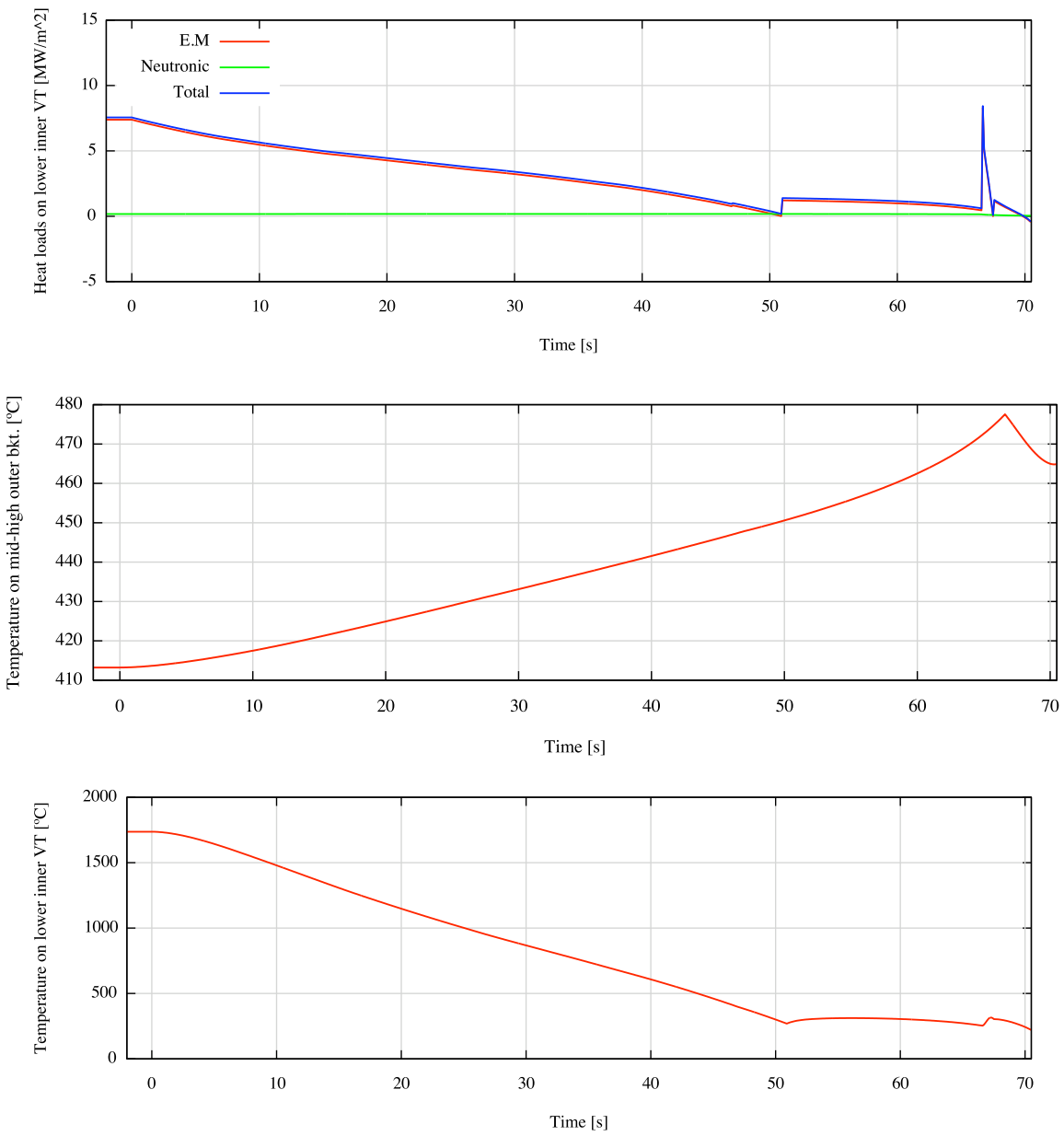

Figure 4.3.2.d. *Sudden increase of fuelling rate by factor 1.05, T_i = 8.1 keV, P_{FUS} = 500 MW*

This report has focused on the study of the scenario of 500 MW and T_i=8.1 keV. However, the figures of the case of 700 MW, in which higher fusion powers are reached, has been included in the Annex A (see section A.1).

4.3.3 Sudden improvement of energy confinement time

In order to illustrate the behaviour of plasma parameters in case of a sudden increase of confinement time, an event with multiplication factor 1.5 in 500 MW scenario has been simulated. The results are shown in Figure 4.3.3.

As it can be seen the confinement time improvement produces a fast increase of temperatures and

densities, which drives to an overall raise of fusion power reaching almost 1300 MW. Heat fluxes into the most stressed divertor part grow significantly from the steady state: the lower inner VT heat loads pass from around 7 to almost 35 MW/m^2.

In Table 4.3.3.1 the evolution of the temperatures reached by in-vessel components and their safety margins are shown. Both temperatures of the blanket as the divertor increase along the transient. It has been found that lower inner vertical target's cooling pipe would melt after 7.1 seconds and water vapour would be poured into the vacuum vessel terminating the plasma. Most of the graphs in Figure 4.3.3 are shown up to 7.1 seconds, so the evolution of the different variables until the moment of the divertor melting can be seen clearly.

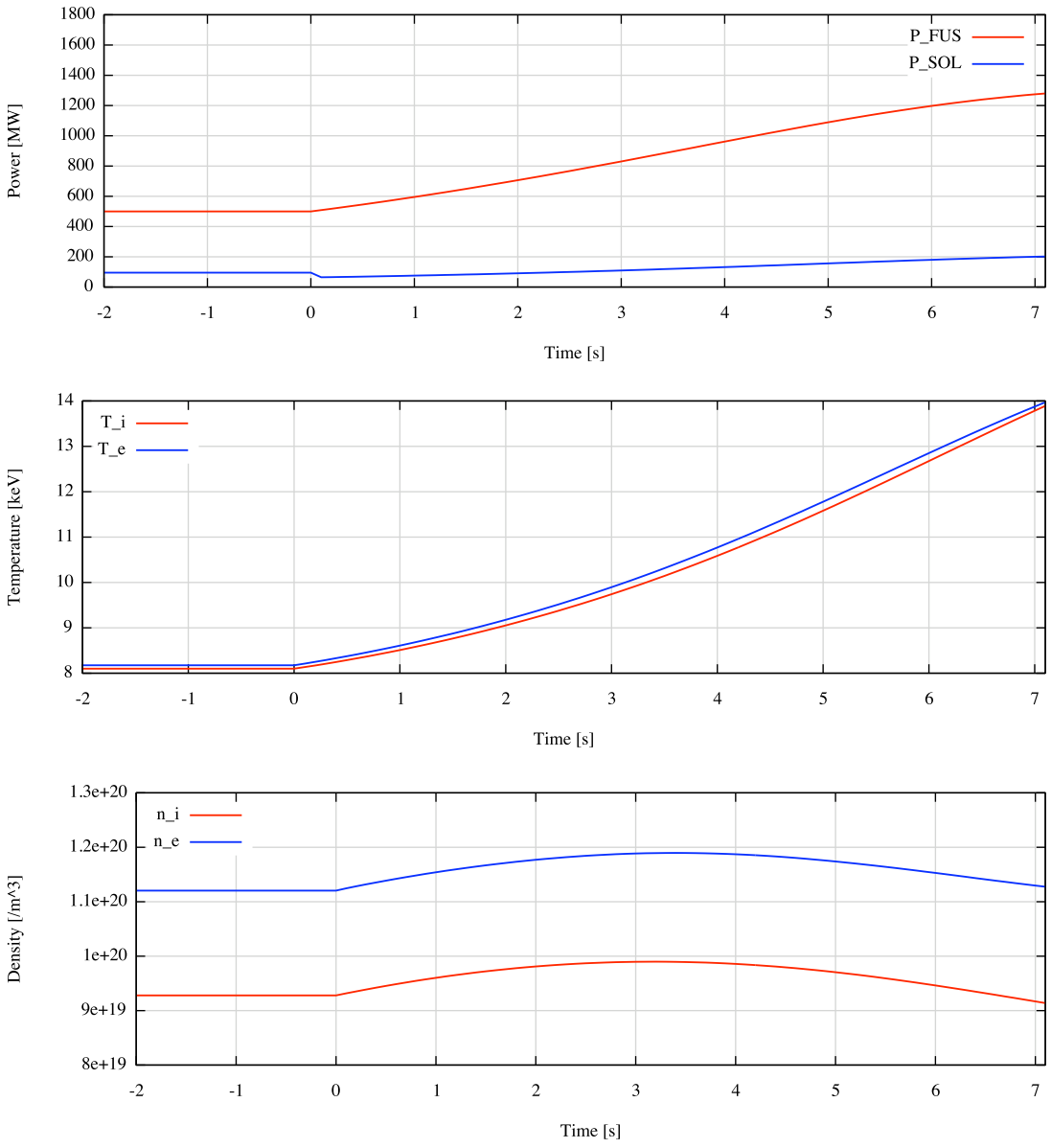

Figure 4.3.3.a. *Sudden energy confinement time improvement by factor 1.5, T_i = 8.1 keV, P_{FUS} = 500 MW*

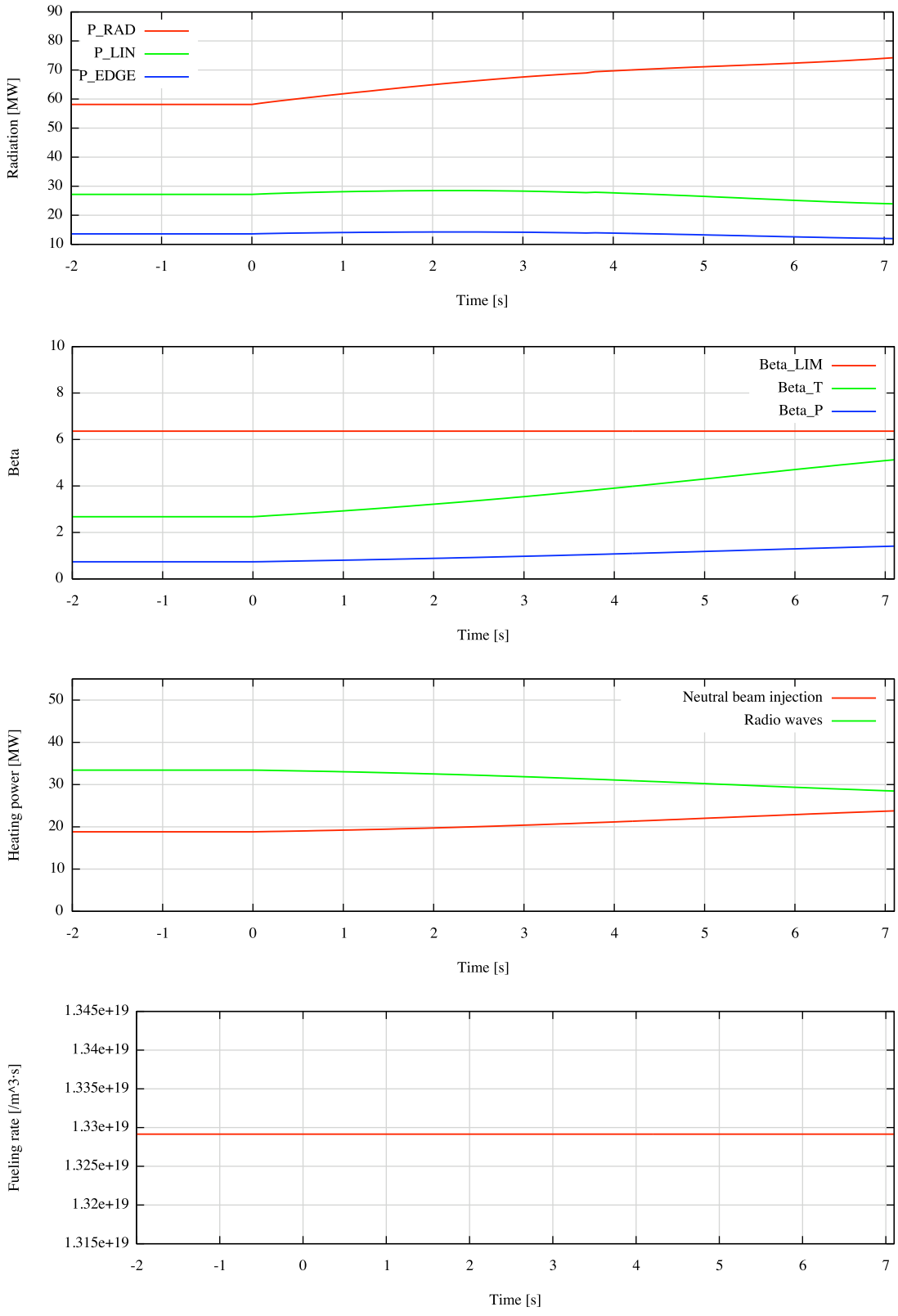

Figure 4.3.3.b. *Sudden energy confinement time improvement by factor 1.5, T_i = 8.1 keV, P_{FUS} = 500 MW*

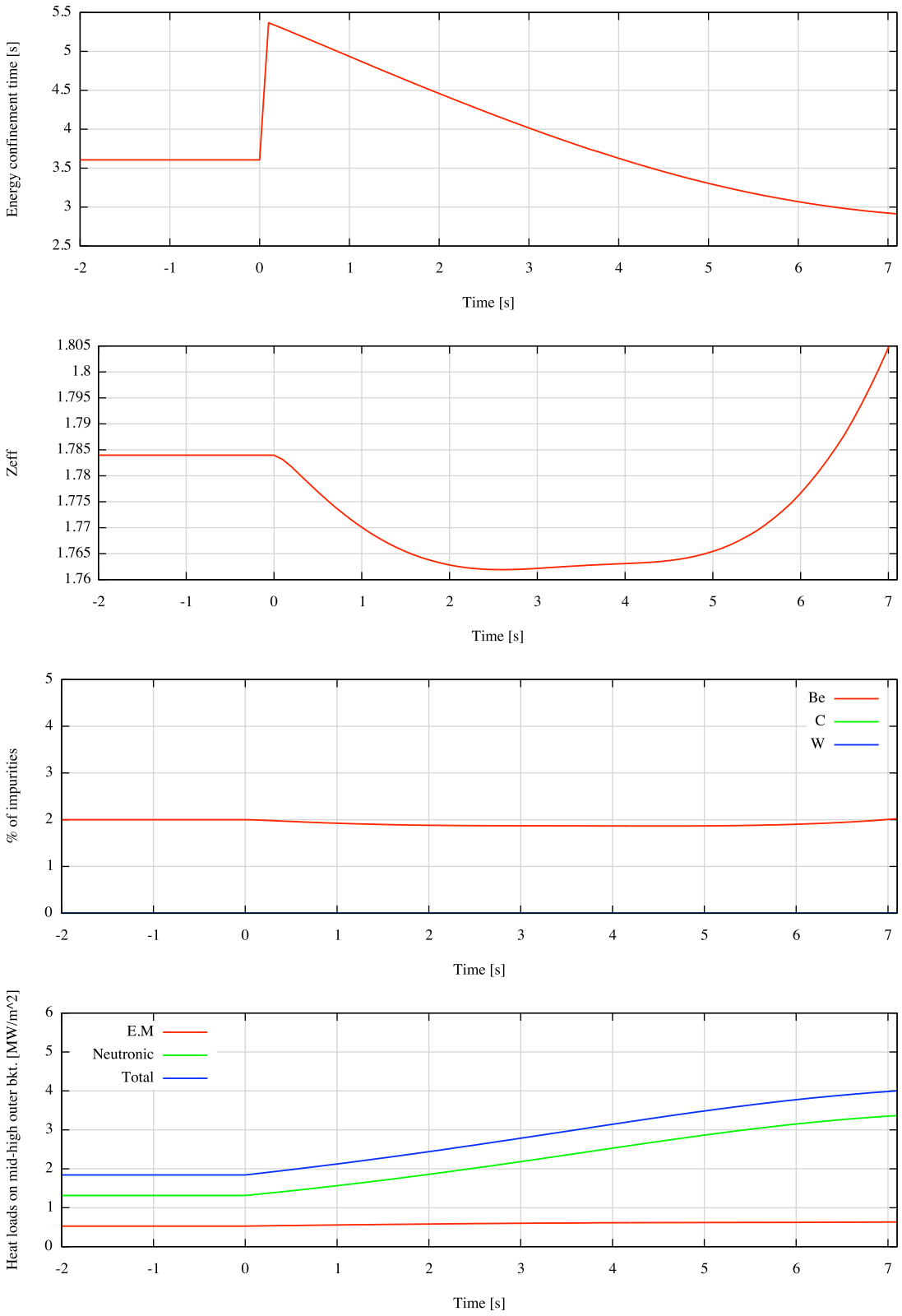

Figure 4.3.3.c. *Sudden energy confinement time improvement by factor 1.5, T_i = 8.1 keV, P_{FUS} = 500 MW*

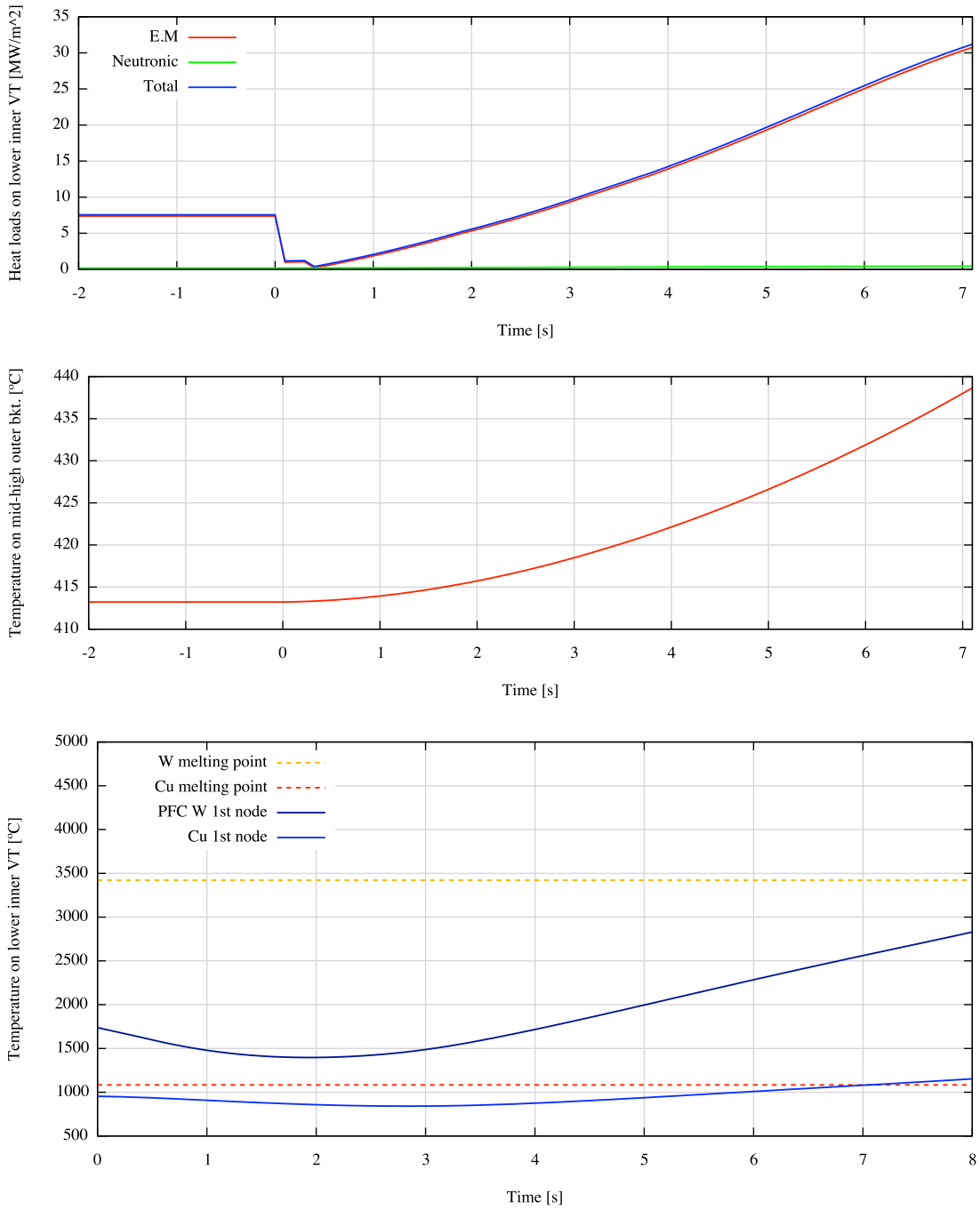

Figure 4.3.3.d. *Sudden energy confinement time improvement by factor 1.5, T_i = 8.1 keV, P_{FUS} = 500 MW*

	Layer	Depth	Material Melting point		t = 0.0 s	t = 5.0 s	t = 7.1 s
Mid-high outer blanket	PFC	0.0 cm	Be 1287 ºC	**Temperature [ºC]**	413.23	426.61	438.65
				Safety margin over melting point	67.89 %	66.85	65.92 %
	Cooling pipe	1.0 cm	Cu Alloy 1083 ºC	**Temperature [ºC]**	371.76	386.47	400.40
				Safety margin over melting point	65.67 %	65.67	63.03 %
Lower inner VT	PFC	0 cm	W 3422 ºC	**Temperature [ºC]**	1736.79	1996.02	2587.09
				Safety margin over melting point	49.25 %	41.67	24.40 %
	Cooling pipe	1.2 cm	Cu Alloy 1083 ºC	**Temperature [ºC]**	953.72	937.65	1086.63
				Safety margin over melting point	11.94 %	13.42	-0.34 %

Table 4.3.3.1. Comparison between blanket region 2 and divertor regions 11 temperatures

Figures of the study for the scenario of 700 MW can be found in the Annex A (see section A.2).

4.3.4 Sudden increase of external heating

In one of the previous sections, the behaviour of the plasma in front of different pure overheating events has been studied (see Figure 4.3.1.4). It can be observed that the plasma gets a new steady state after introducing and extra external heating.

Now, to illustrate the behaviour of plasma and wall parameters in the event of a sudden increase of auxiliary power, a 500 MW scenario with full heating power injection event has been simulated. According to *ITER Physics Guidelines* 130 MW of heating power will be installed on ITER, although only 110 MW will be available to be working simultaneously.[13] However, in order to perform conservative analyses, an additional external heating power of 80 MW has been studied.

As can be seen, ion and electron temperatures begin raising, which makes fusion power to increase up to 604.83 MW at 2.6 seconds. During the increase of temperatures, densities diminish.

At second 8.5 the temperature achieved in the cooling pipe of the lower inner vertical target get up to 1087.45 ºC, this means that the lower inner vertical target Cu first node would melt after 8.5 seconds and water vapour would be poured into the vacuum vessel terminating the plasma. Most of the graphs are shown up to 8.5 seconds, so the evolution of the different variables until the moment of the divertor melting can be seen clearly.

In Table 4.3.4.1 the evolution of the temperature in the PFC of the most stressed parts of the wall is shown.

[13] ITER: *ITER Physics Guidelines*. July 2013, pg. 98.

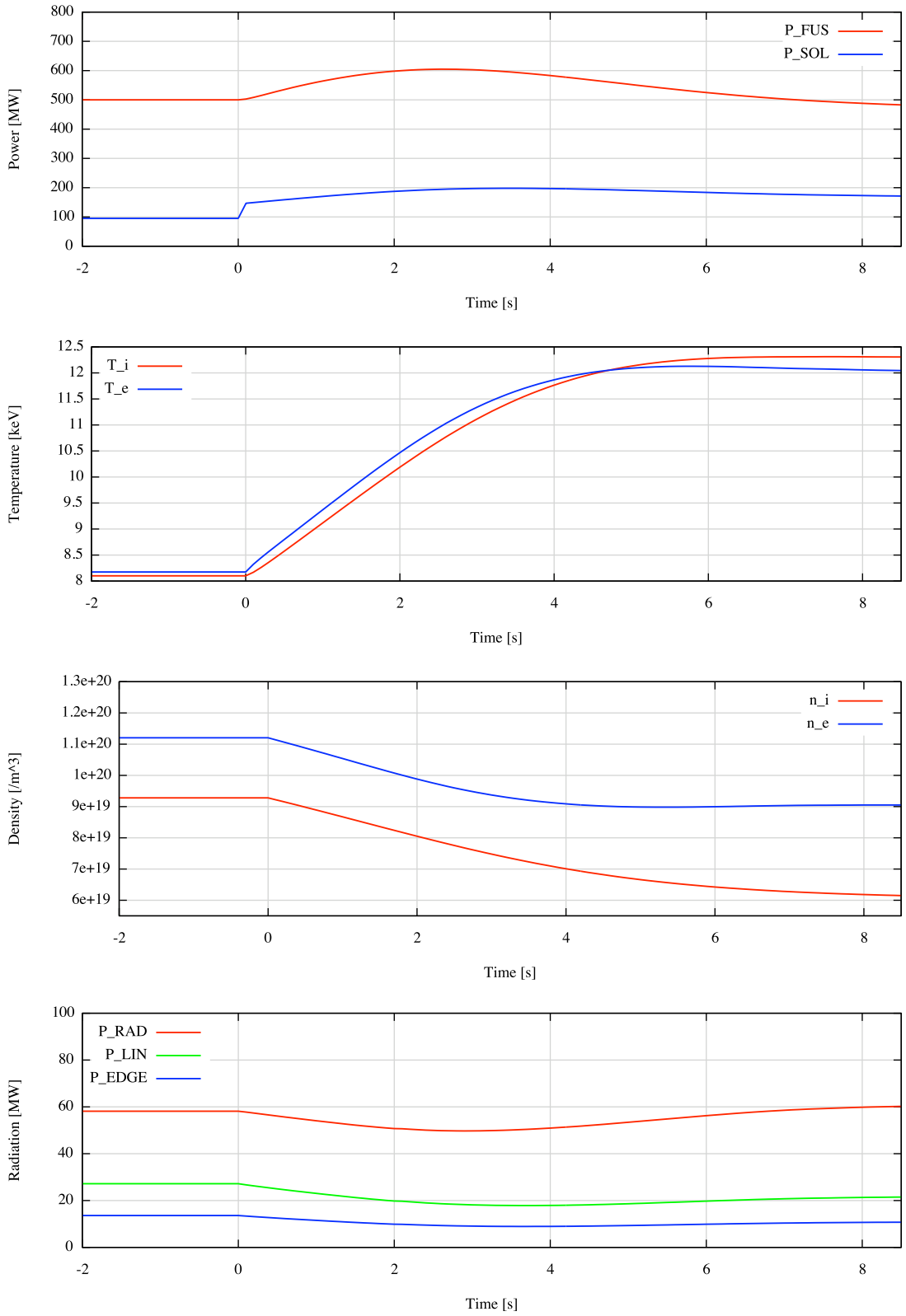

Figure 4.3.4.a. *Sudden increase of external heating up to 130 MW, T_i = 8.1 keV, P_{FUS} = 500 MW*

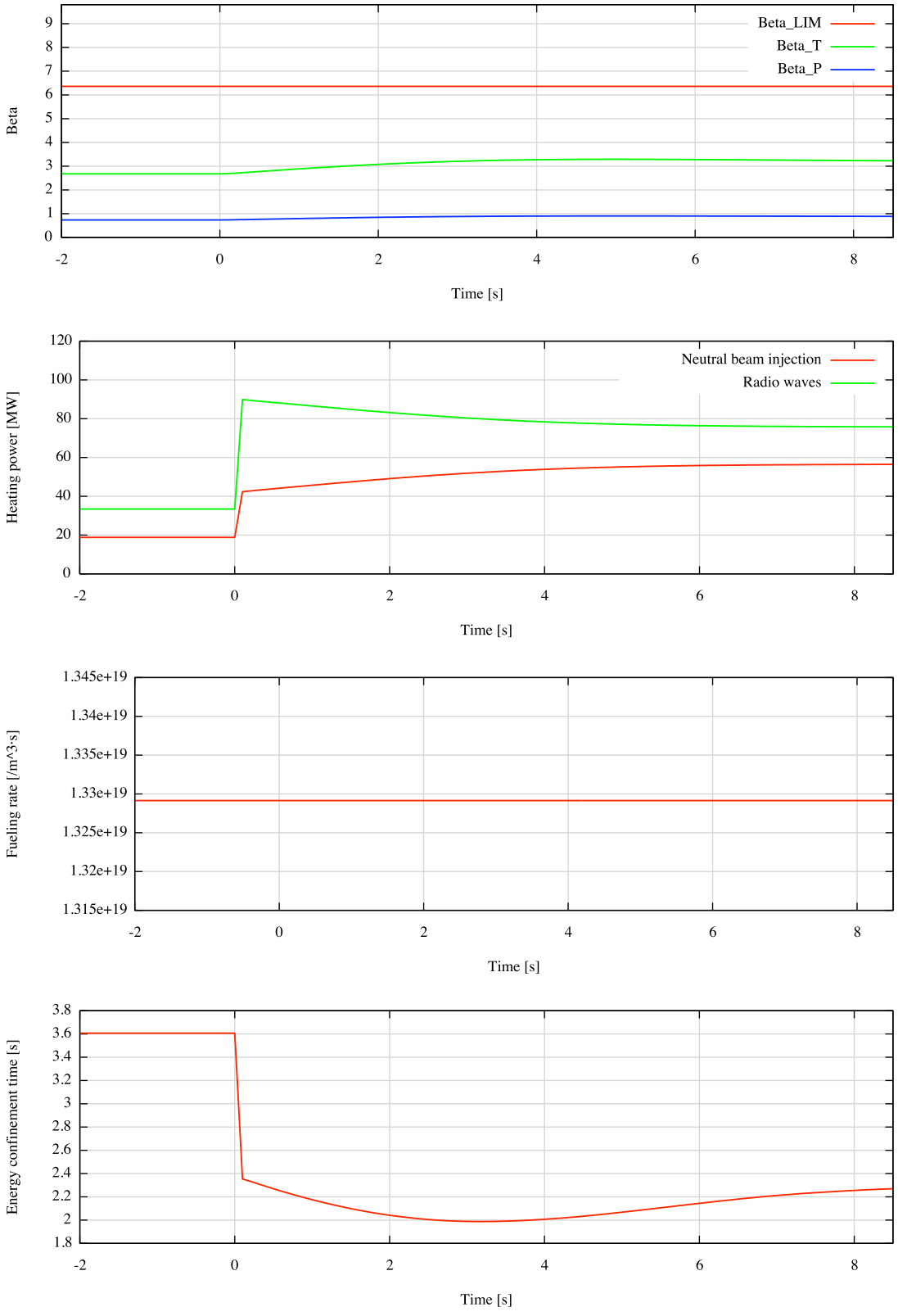

Figure 4.3.4.b. *Sudden increase of external heating up to 130 MW, T_i = 8.1 keV, P_{FUS} = 500 MW*

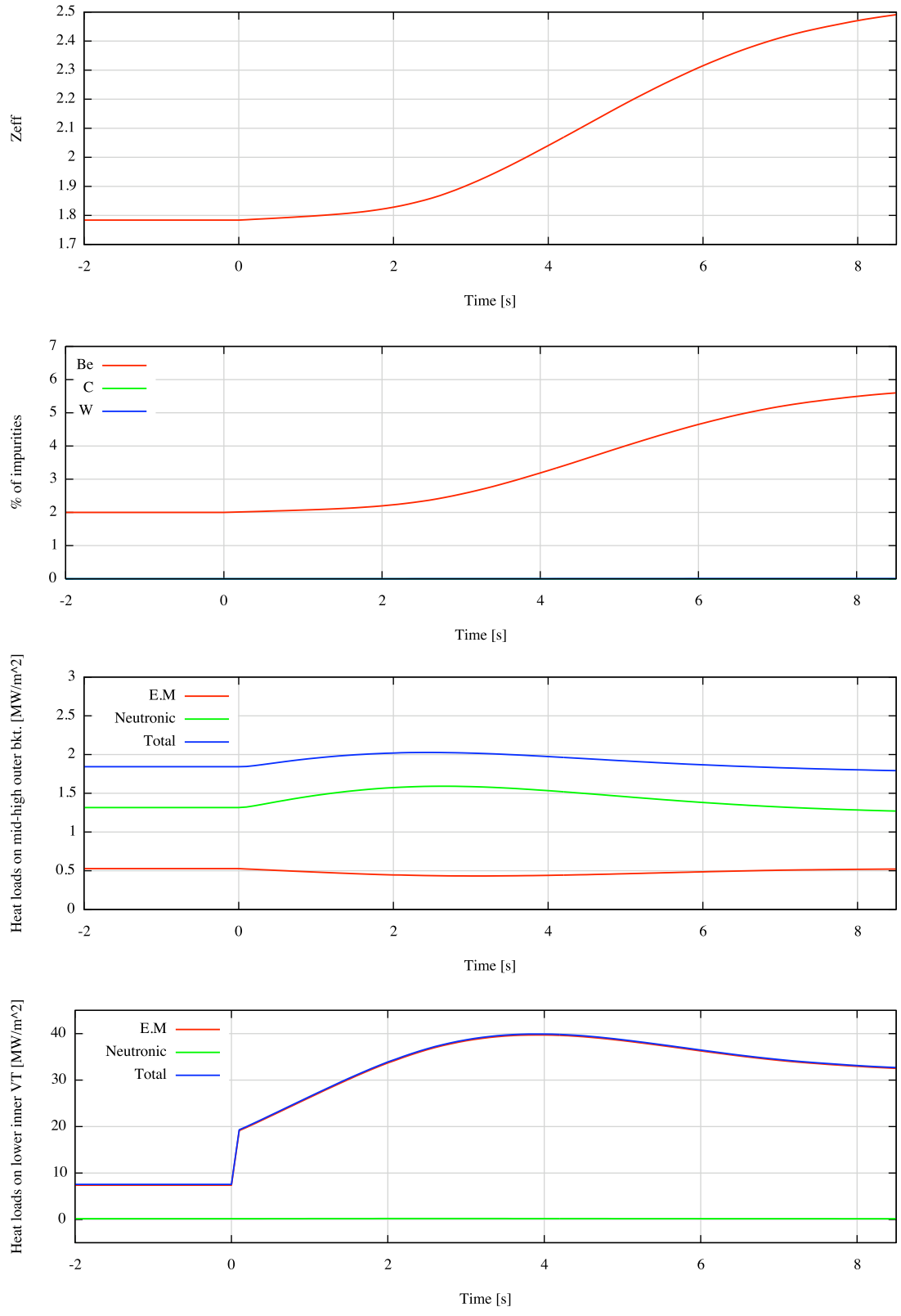

Figure 4.3.4.c. *Sudden increase of external heating up to 130 MW, T_i = 8.1 keV, P_{FUS} = 500 MW*

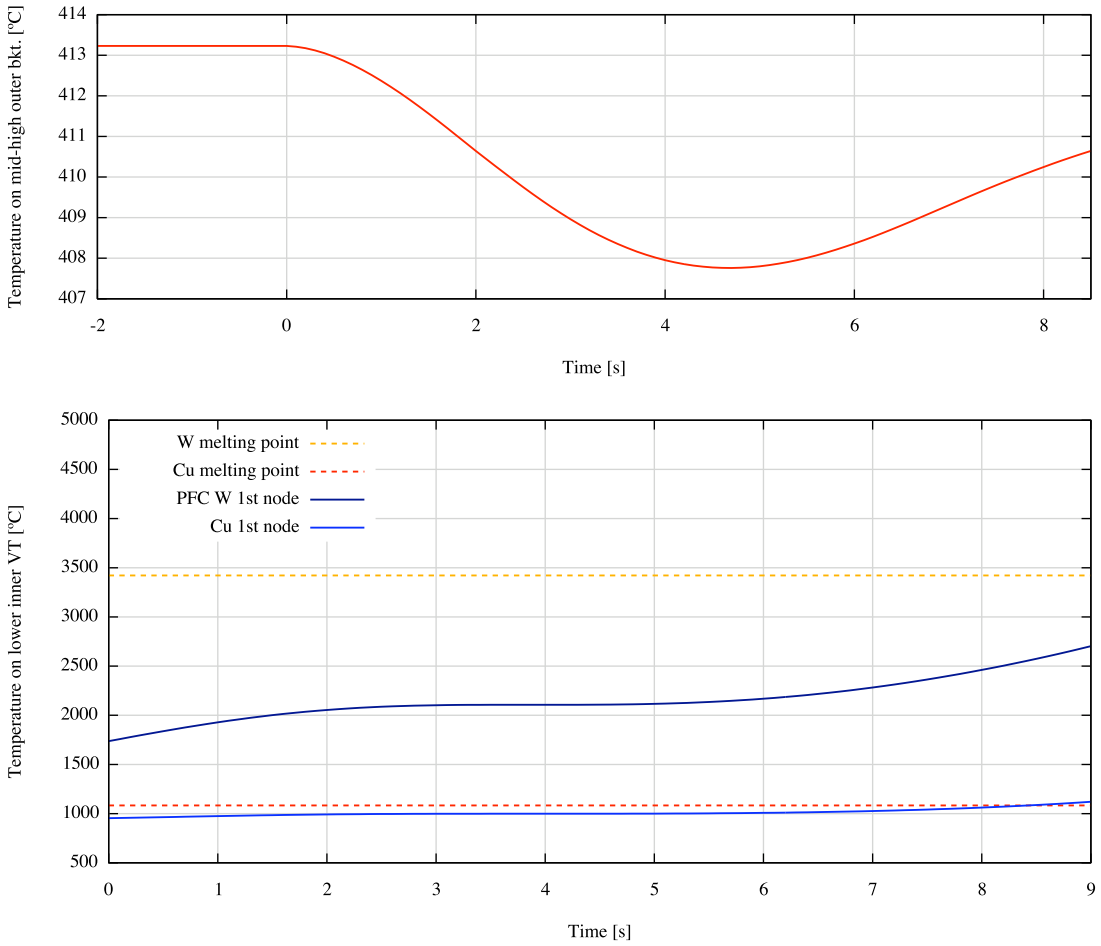

Figure 4.3.4.d. *Sudden increase of external heating up to 130 MW, T_i = 8.1 keV, P_{FUS} = 500 MW*

	Layer	Depth	Material Melting point		t = 0.0 s	t = 4.0 s	t = 8.5 s
Mid-high outer blanket	PFC	0.0 cm	Be 1287 ºC	**Temperature [ºC]**	413.23	407.95	410.64
				Safety margin over melting point	67.89 %	68.30 %	68.09 %
	Cooling pipe	1.0 cm	Cu Alloy 1083 ºC	**Temperature [ºC]**	371.76	372.24	371.02
				Safety margin over melting point	65.67 %	65.63 %	65.74 %
Lower inner VT	PFC	0 cm	W 3422 ºC	**Temperature [ºC]**	1736.79	2106.77	2574.20
				Safety margin over melting point	49.25 %	38.43 %	24.77 %
	Cooling pipe	1.2 cm	Cu Alloy 1083 ºC	**Temperature [ºC]**	953.72	998.88	1087.45
				Safety margin over melting point	11.94 %	7.77 %	-0.41 %

Table 4.3.4.1. Comparison between blanket region 2 and divertor region 11 temperatures

Figures of the study for the scenario of 700 MW can be found in the Annex A (see section A.3).

4.3.5 Fuelling and external heating cut-off

In case of fuelling and auxiliary heating cut-off in a 500 MW scenario P_{FUS} and P_{SOL} decrease, as can be seen in Figure 4.3.5. Transition from H-mode to L-mode takes place after 5.3 seconds from the beginning of the event. Plasma finally terminates after 15.4 seconds by edge energy collapse ($P_{SOL} \leq 0$).

Fuelling cut-off makes ion and electrons densities to decrease, while temperature increases until the mode transition. After that, both temperatures start decreasing. Radiated power is related to the density, so it increases too.

The decrease of the power crossing scrape-off layer makes PFC temperatures to decrease, since incoming heat loads decrease with P_{SOL}.

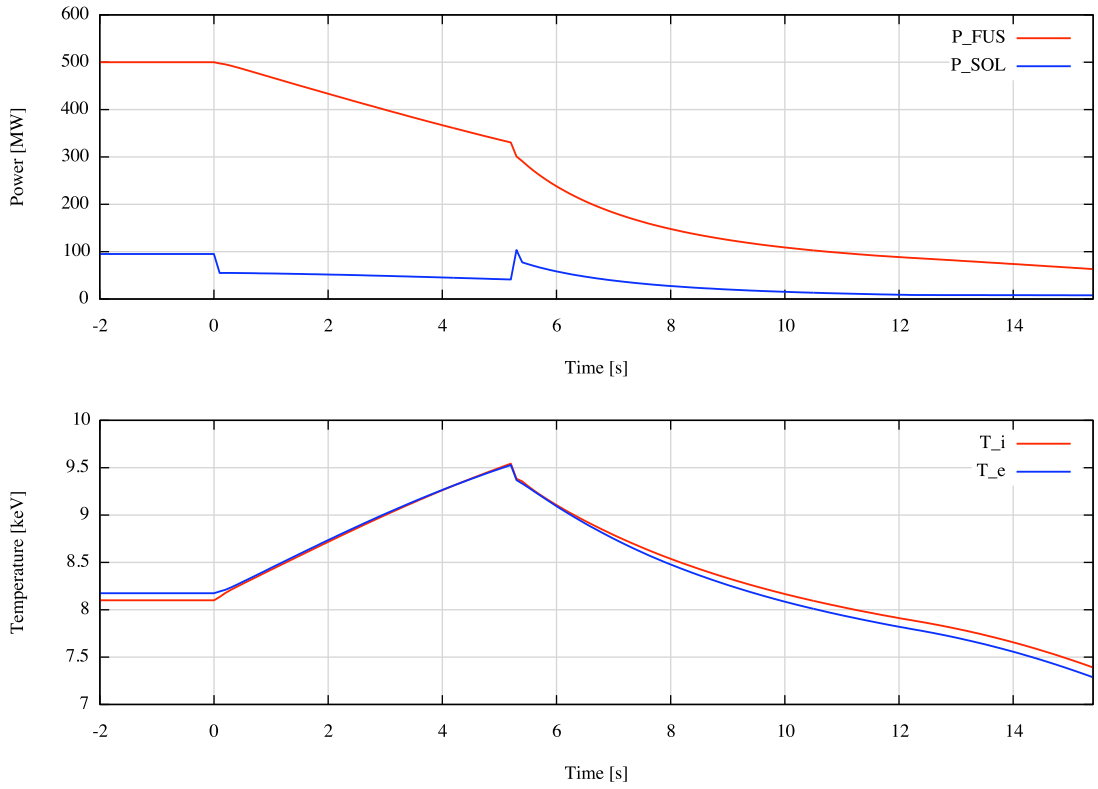

Figure 4.3.5.a. *Sudden fuelling and external heating cut-off, T_i = 8.1 keV, P_{FUS} = 500 MW*

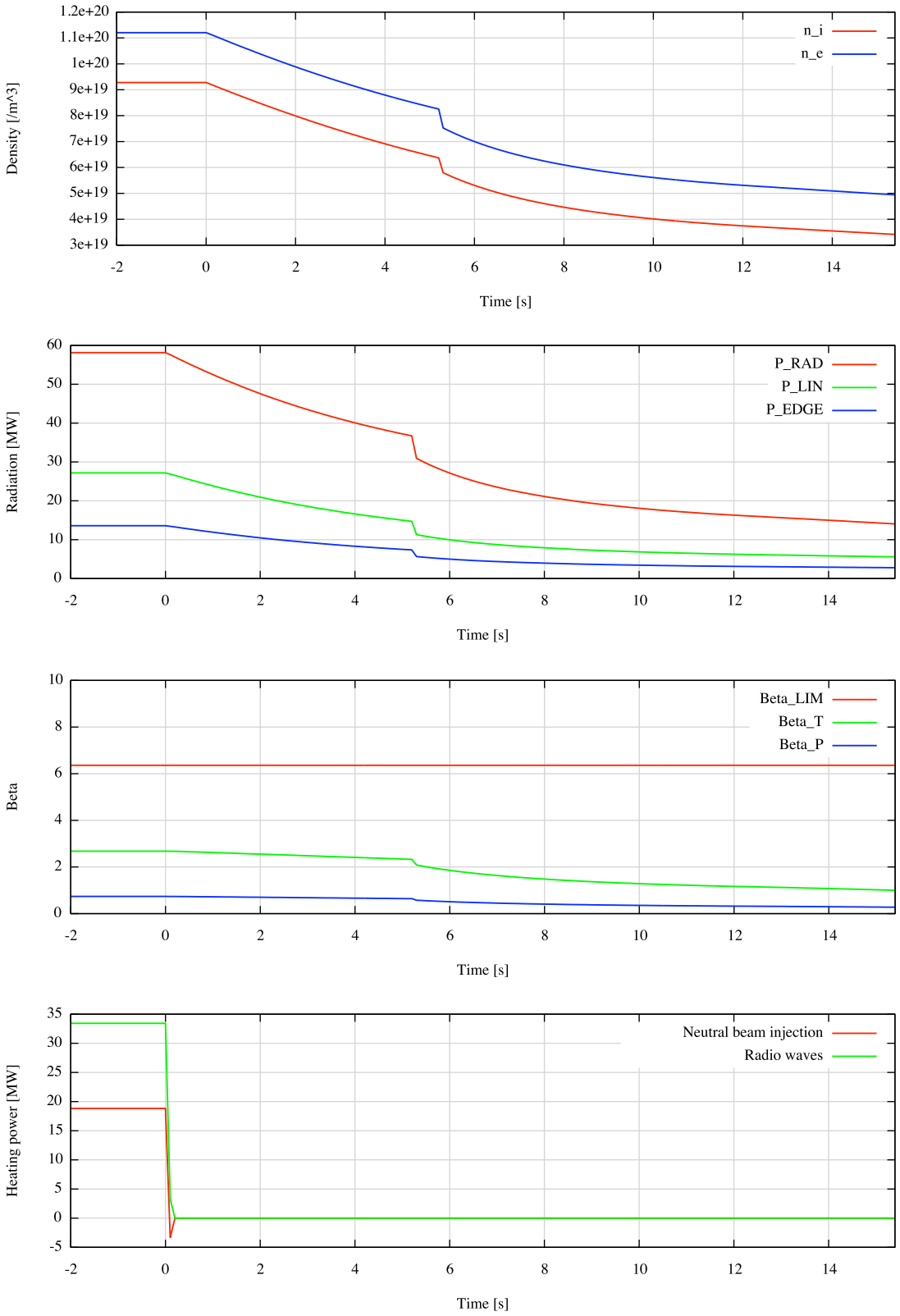

Figure 4.3.5.b. *Sudden fuelling and external heating cut-off, T_i = 8.1 keV, P_{FUS} = 500 MW*

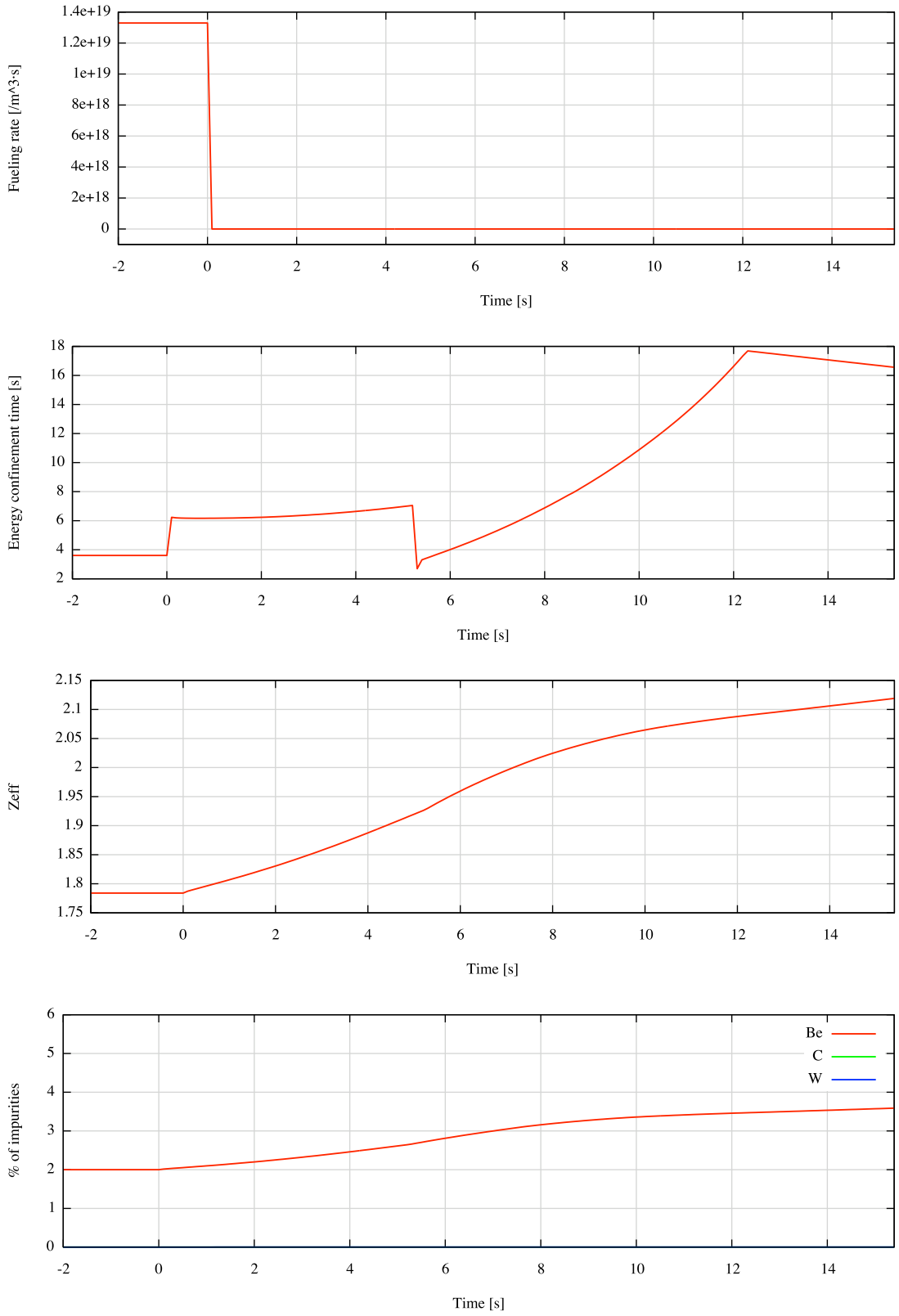

Figure 4.3.5.c. *Sudden fuelling and external heating cut-off, T_i = 8.1 keV, P_{FUS} = 500 MW*

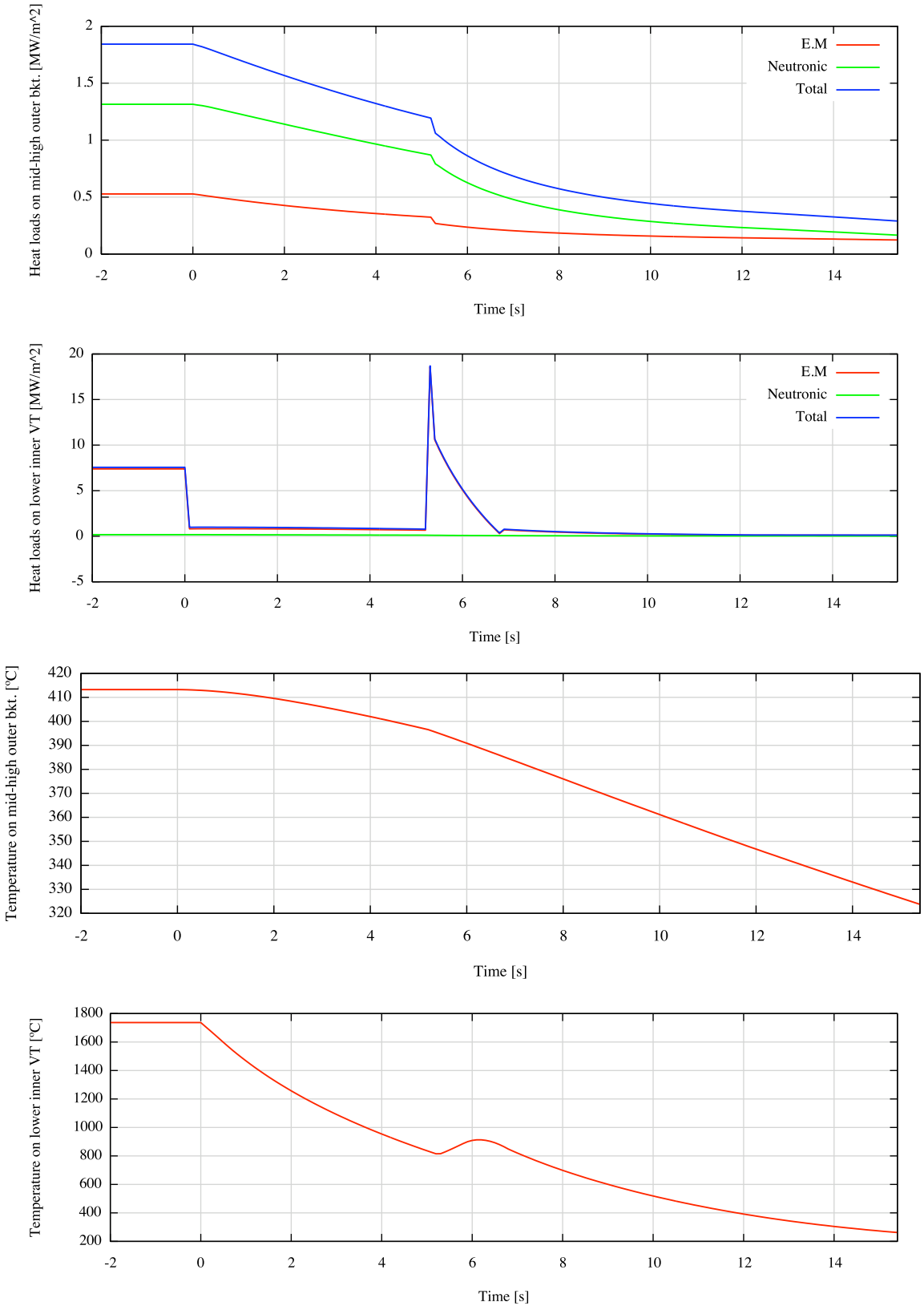

Figure 4.3.5.d. *Sudden fuelling and external heating cut-off, T_i = 8.1 keV, P_{FUS} = 500 MW*

4.3.6 Combination of sudden improvement of confinement time and underheating

This case has been selected to illustrate some of the combined perturbation cases studied on the previous section. The combination of an underheating of -40 MW and an improvement of the confinement time by factor 1.50 has been the case, for all studied, which has achieved a new steady state with the higher fusion power (see Table 4.3.1.14). In Figure 4.3.6 the results for this event are shown.

Blanket temperature increase along transient, while the divertor temperature decrease first to start increasing from second 10 until the melting of the cooling pipe at second 19.6, moment at which water vapour would be poured into the vacuum vessel terminating the plasma. So most of the graphs in Figure 4.3.6 are shown up to 19.6 seconds.

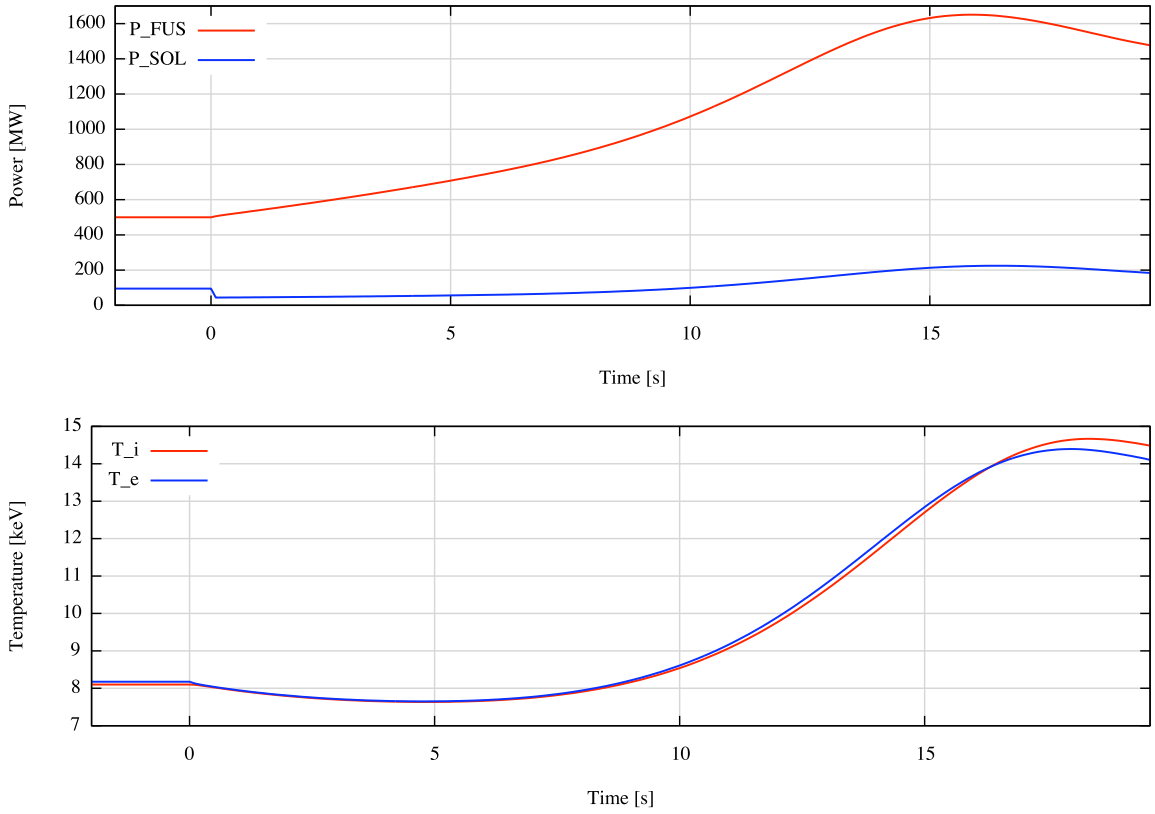

Figure 4.3.6.a. *Combination of an underheating of -40 MW and a confinement time improvement by factor 1.5, T_i = 8.1 keV, P_{FUS} = 500 MW*

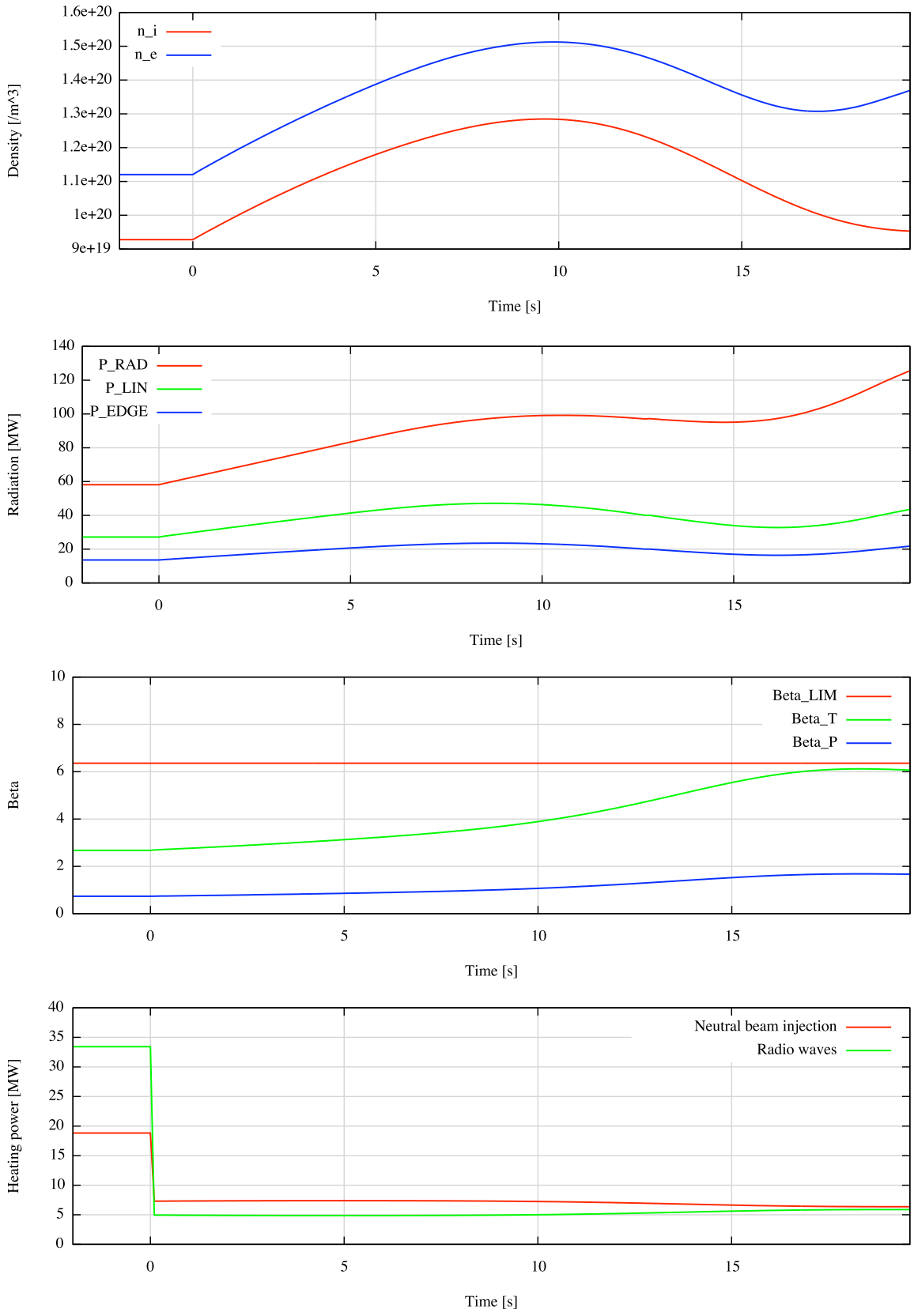

Figure 4.3.6.b. *Combination of an underheating of -40 MW and a confinement time improvement by factor 1.5, T_i = 8.1 keV, P_{FUS} = 500 MW*

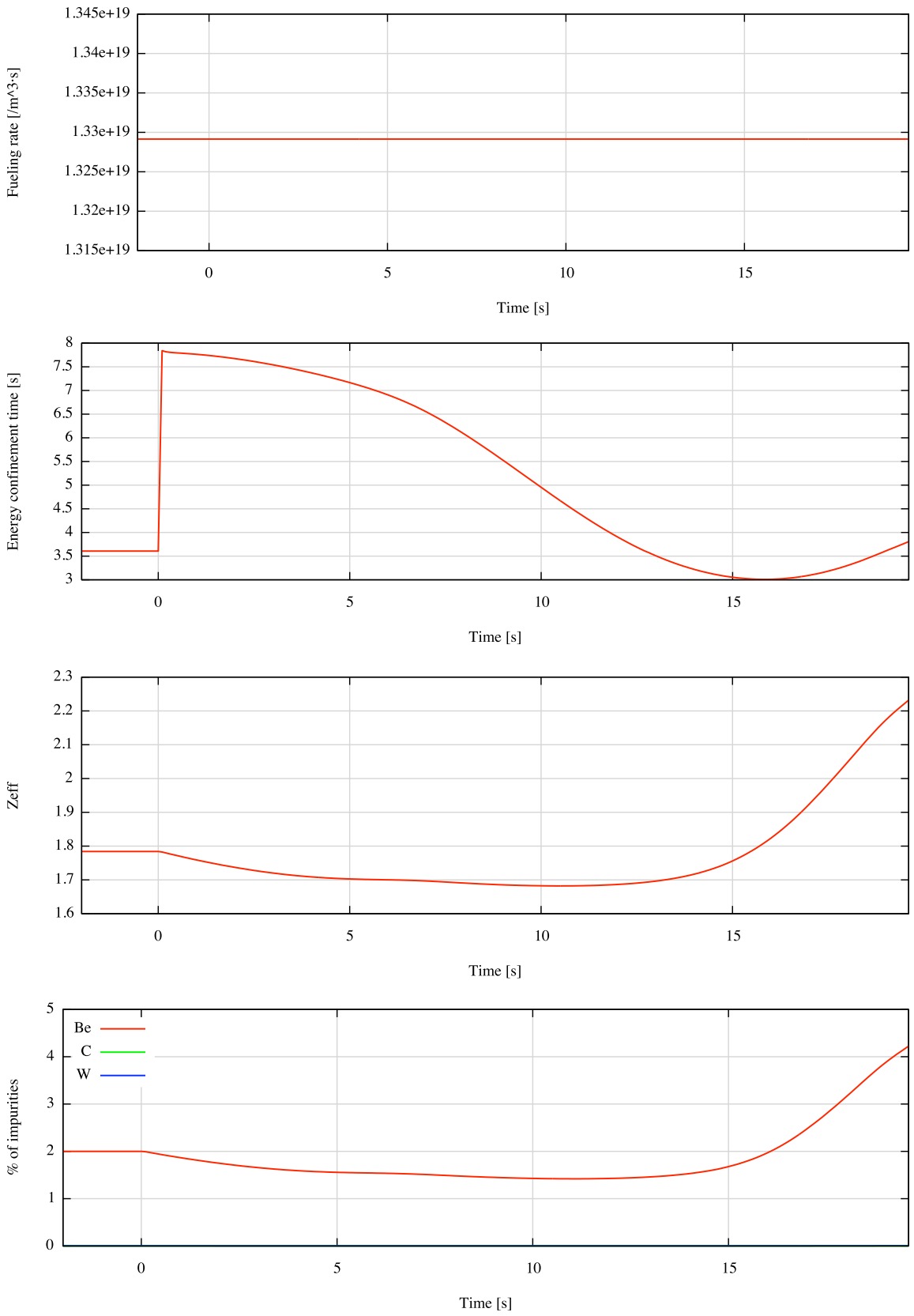

Figure 4.3.6.c. *Combination of an underheating of -40 MW and a confinement time improvement by factor 1.5, T_i = 8.1 keV, P_{FUS} = 500 MW*

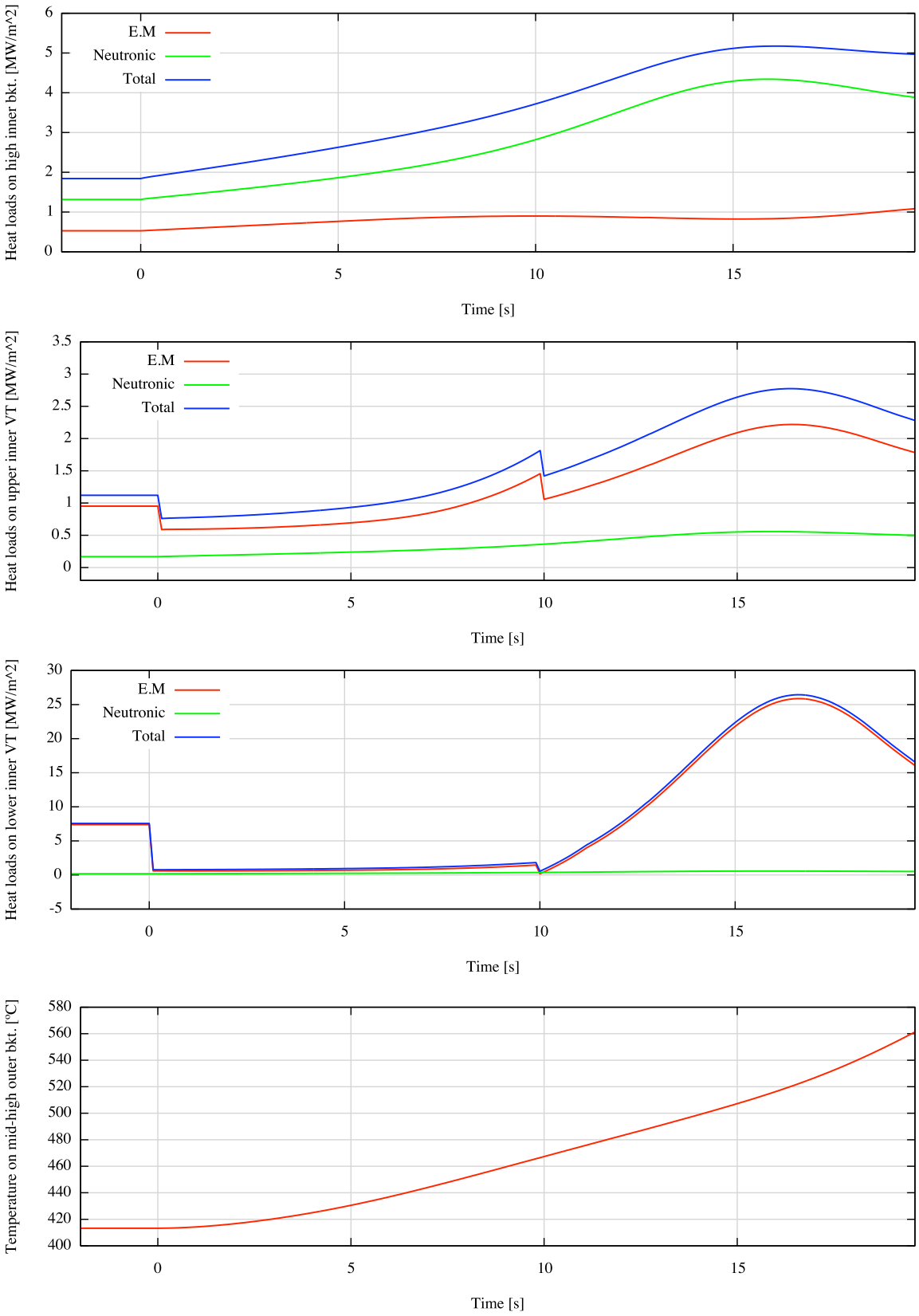

Figure 4.3.6.d. *Combination of an underheating of -40 MW and a confinement time improvement by factor 1.5, T_i = 8.1 keV, P_{FUS} = 500 MW*

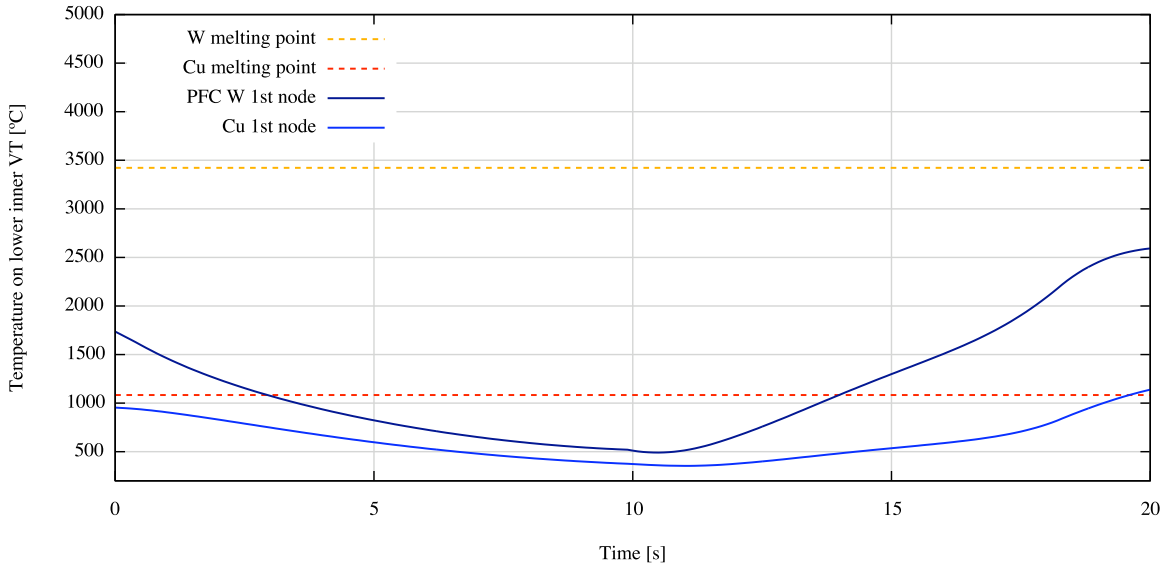

Figure 4.3.6.e. *Combination of an underheating of -40 MW and a confinement time improvement by factor 1.5, T_i = 8.1 keV, P_{FUS} = 500 MW*

4.3.7 Combination of sudden increase of external heating and underfuelling

This case has been selected to illustrate the difference between P_{SOL} and P_{FUS} behaviour. As seen in one of the previous sections (see Table 4.3.1.15) when overheating and underfuelling perturbation are combined the higher the overheating the lower the fusion power achieved by the new equilibrium but the higher the scrape-off power, and the higher the fuelling rate multiplication factor the higher the fusion and the scrape-off power. So an event of +60 MW of overheating and 0.75 of underfuelling has been selected. The results are shown in Figure 4.3.7.

As can be seen, when the two perturbations are introduced at second 0 the fusion power and the scarpe-off power start increasing, at second 2.3 fusion power reaches 560.24 MW and from then it decreases. However P_{SOL} continues increasing until second 4.6 when the cooling pipe of the lower inner vertical target of the divertor melts, which eventually leads to plasma termination. However Figure 4.3.7 is represented until the moment of the melting.

Mid-high outer blanket temperature decreases from the beginning, while lower inner vertical target increases until the melting of the cooling pipe at second 4.6.

While heat loads on mid-high outer blanket stay practically constant during the transient, on lower inner vertical target it reaches almost 40 MW/m^2, which means that they multiplied by 5 with respect to the 500 MW reference scenario.

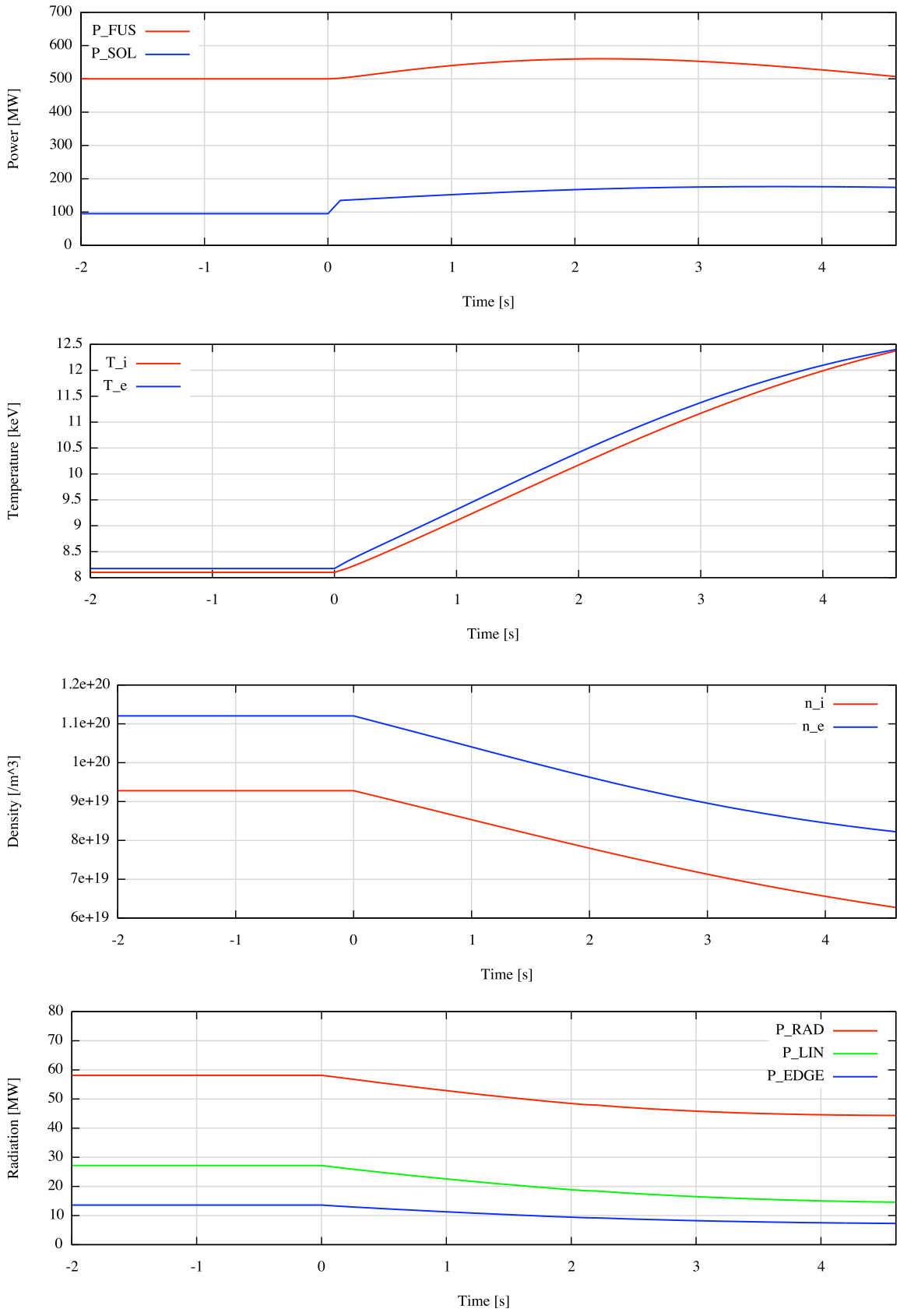

Figure 4.3.7.a. *Combination of increase of external heating up to 110 MW and fuelling rate multiplication factor of 0.75, T_i = 8.1 keV, P_{FUS} = 500 MW*

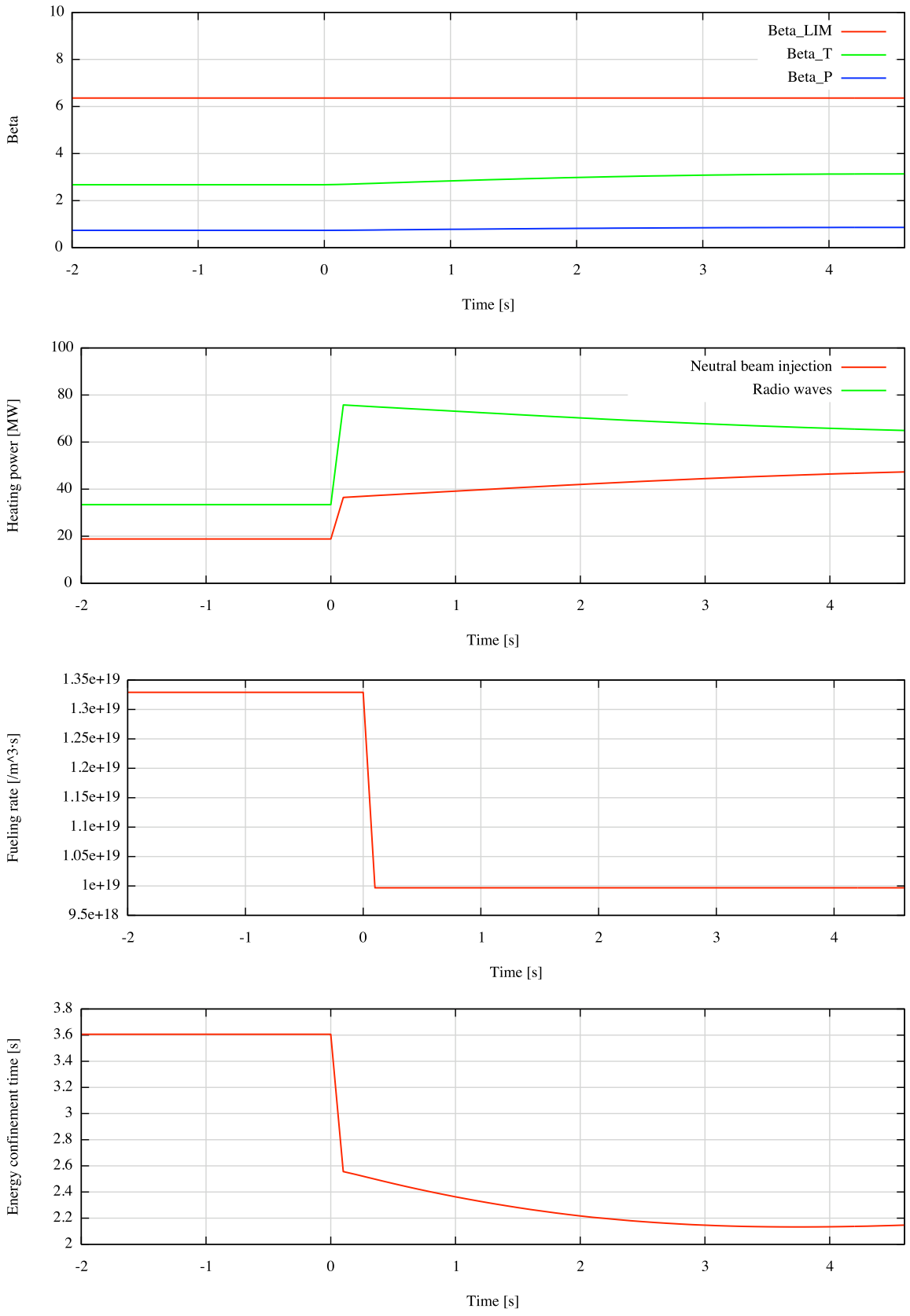

Figure 4.3.7.b. *Combination of increase of external heating up to 110 MW and fuelling rate multiplication factor of 0.75, T_i = 8.1 keV, P_{FUS} = 500 MW*

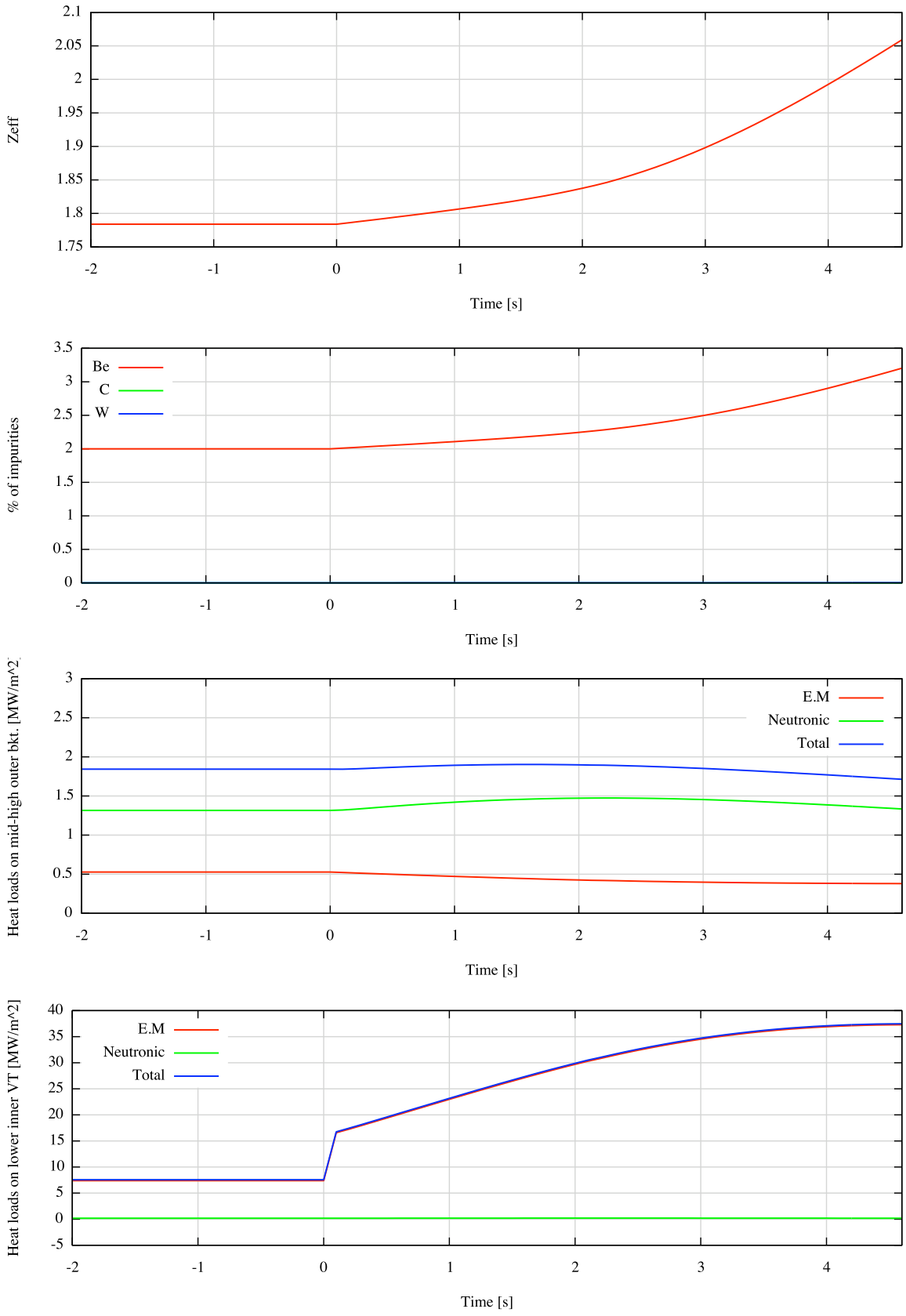

Figure 4.3.7.c. *Combination of increase of external heating up to 110 MW and fuelling rate multiplication factor of 0.75, T_i = 8.1 keV, P_{FUS} = 500 MW*

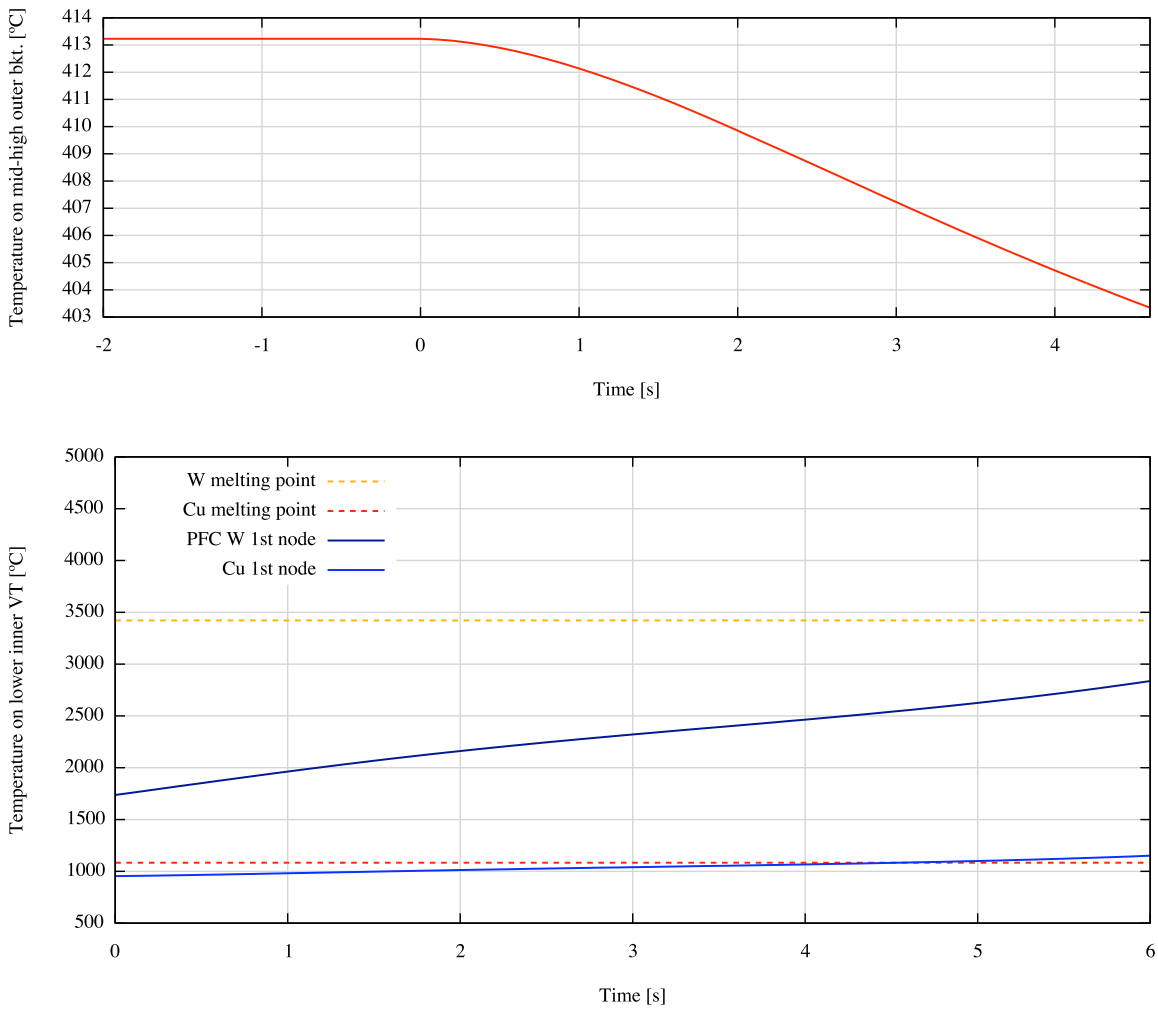

Figure 4.3.7.d. *Combination of increase of external heating up to 110 MW and fuelling rate multiplication factor of 0.75, T_i = 8.1 keV, P_{FUS} = 500 MW*

5 PROJECT COST

5.1 ITER PROJECT COST

In Table 5.1.1 the ITER project cost by phase is shown. As can be seen, ITER has a really high cost. The initial estimation was 5000 M€ for the construction phase, but today the budget has increased to more than double.

Construction phase	13000 M€	2007-2019 (12 years)
Operation phase	5200 M€	2019-2037 (18 years)
Deactivation phase	281 M€	2037-2042 (5 years)
Decommissioning phase	530 M€	After 2042

Table 5.1.1. *ITER project cost by phase*

5.2 PROJECT COST

- **Staff cost**

It has been working on the project for seven month, from October of 2013 to April of 2014, part-time, that is four hours per day. A net salary of 1000 €/month has been considered, since it is a salary of a junior engineer. In Eq. 5.1 and Eq. 5.2 calculation of total staff cost is done considering the different taxes to which salary is subject in Spain:

$$NS = GS - IRPF = GS - 0.21 \cdot GS \rightarrow GS = \frac{1000\ €/month}{0.79} = 1265.82\ €/month \qquad \textbf{Eq. 5.1}$$

$$Staff\ cost = GS + taxes = GS * 1.35 = \ 1708.86\ €/month \qquad \textbf{Eq. 5.2}$$

where *GS* is gross salary and *NS* is net salary.

So considering the seven month of work, the total staff cost of the project rises to 11962.02 €.

- **Depreciation of equipment and licenses**

A service time of 5 years has been considered both equipment and licenses.

The only equipment depreciation considered is the computer, because it is the only one used during the project. A cost of 1000 € has been considered for the computer amortized over 5 years, which rises the cost of equipment depreciation to 116.67 €.

The considered licenses are Microsoft Windows 7 Professional with a cost of 3.08 €/month and Microsoft Office Small Business with a cost of 4.1 €/month per user, which raises the licenses cost of the seven month of work to 50.26.

The total depreciation of equipment and licenses rises to 166.93 €.

- **Overhead cost**

Finally an overhead with a value of the 5% of the total of other costs has been considered, which rises to 606.48 €. In this overhead the cost of office supplies, office rent, print and photocopies, etc. are included.

- **Total cost of the project**

Total cost of the project rises to 12735.40 €.

CONCLUSIONS

In the *Loss of Plasma Control Transients* document made in 2007, the method followed to find critical situations was some parametric sweeps by running multiple simulations. This method allows representing the maximum fusion power achieved in each transient from a parametric sweep of a perturbation. However, this method gives little information about the behaviour of the transients. So in this study the method of the operating window of the plasma has also been used. This method determines the effect of the different perturbations, included combined perturbations, using simple calculations and without the need of a parametric sweep, which is very laborious, as it requires performing many simulations. Moreover, the representation of the results plotted on a (n,T) diagram allows to show more intuitively the effects of perturbations on the equilibrium plasma. And even, through an exhaustive study of different plasma transients, it could be possible to predict the various perturbations that must be introduced to bring the plasma to a desired equilibrium state within the window. It would be also interesting to use operation window method with the scenarios of 700 MW and 400 MW to compare plasma transients in each case.

However, it has been found that the limits of the operating window of the plasma are not entirely well defined in AINA code, especially Greenwald limit, so it would be suitable to find the reason why this happens and try to fix it.

From the study completed it can also be concluded that the behaviour of the fusion power (P_{FUS}) is different to the scrape-off power (P_{SOL}). P_{FUS} is maximum in the top-right corner of the operation window of the plasma, while P_{SOL} is maximum at its right. Thus two separated studies must be done to find the most critical cases: in one hand the most dangerous cases to the blankets, which are related to P_{FUS}, and by the other hand the critical events to the divertor, related with P_{SOL}.

It has also been found that, in case of two combined perturbations, the obtained results of new steady states either if the perturbations are simultaneous or consecutive are practically equal.

According to AINA results the most critical divertor PFCs would not melt even if the worst LOPC event should happen. Nevertheless, simulations performed show that copper cooling pipes of the divertors would exceed their melting temperature; it is specially true for the lower inner VT. Therefore it is an issue of the utmost importance to validate the thermal behaviour of the walls.

REFERENCES

BIBLIOGRAPHY

[1] JOSÉ CARLOS RIVAS, JAVIER DIES: *AINA safety code: User's Manual and Code Description (Release 3.0)*. FEEL-UPC, 2013.

[2] ITER – The way to new energy.
[http://www.iter.org, March, 3rd 2014]*. *[URL, date of consultation].

[3] JOHN WESSON: *Tokamaks*. Oxford, Third Edition, 2004, pg. 24-25.

[4] ITER JCT: *Plasma Performance Assessment*. 2004, pg. 15-16.

[5] FERRAN ALBAJAR VIÑAS: *Radiation Tranpsort Modelling in a Tokamak Plasma*, Universitat Politècnica de Barcelona, 2004, pg. 101.

[6] ITER JCT: *Plasma Performance Assessment*. 2004, pg. 6.

[7] N. TAYLOR: *Preliminary safety analysis of ITER Fusion Sci. Technol. 56*, 2009, pp. 573–580.

[8] J. DIES, M. DAPENA, M. RAMÓN, R. LÓPEZ, J. GARCÍA: *Review of Loss of Plasma Control Transients in ITER*. FEEL-UPC, 2007, pg. 51.

[9] ITER JCT: *Project Integration Document (PIC)*. January 2007, 151 [Table 4.5-1].

[10] ITER JCT: *Plasma Performance Assessment*. 2004, pg. 63.

[11] ITER: *ITER Physics Guidelines*. July 2013, pg. 98.

[12] N. TAYLOR: *Preliminary safety analysis of ITER Fusion Sci. Technol. 56*, 2009, pp. 573–580.

[13] ITER: *ITER Physics Guidelines*. July 2013, pg. 98.

OTHER REFERENCES

JEFFREY P. FREIDBERG: *Plasma Phyysics and Fusion Energy*. Cambridge University Press, 1st edition, August 2008.